

# The Use of Visual Comfort Metrics in the Design of Daylit Spaces

by

John Alstan Jakubiec

*Bachelor of Science in Architecture  
Georgia Institute of Technology, 2008*

*Master of Architecture  
University of Pennsylvania, 2010*



Submitted to the Department of Architecture  
In Partial Fulfillment of the Requirements for the Degree of

Doctor of Philosophy in Architecture: Building Technology

at the

Massachusetts Institute of Technology

June 2014

© 2014 Massachusetts Institute of Technology.  
All rights reserved.

**Signature redacted**

Signature of Author: \_\_\_\_\_

\_\_\_\_\_  
Department of Architecture  
May 2, 2014

**Signature redacted**

Certified by: \_\_\_\_\_

\_\_\_\_\_  
Christoph F. Reinhart  
Associate Professor of Building Technology  
Thesis Supervisor

**Signature redacted**

Accepted by: \_\_\_\_\_

\_\_\_\_\_  
Takehiko Nagakura  
Associate Professor of Design and Computation  
Chair, Departmental Committee on Graduate Studies



Thesis Committee:

Christoph F. Reinhart  
Assistant Professor of Building Technology  
Massachusetts Institute of Technology  
*Thesis Supervisor*

Mehlika N. Inanici  
Associate Professor of Architecture  
University of Washington  
*Thesis Reader*

Leslie K. Norford  
Professor of Building Technology  
Massachusetts Institute of Technology  
*Thesis Reader*





# The Use of Visual Comfort Metrics in the Design of Daylit Spaces

by

John Alstan Jakubiec

Submitted to the Department of Architecture  
on May 2, 2014 in Partial Fulfillment of the Requirements  
for the Degree of Doctor of Philosophy in Architecture: Building Technology

## Abstract

It is desirable to design buildings with natural daylight and views to the outside, which can maximize passive solar heating, minimize electric lighting use and contribute to feelings of well-being and awareness. Unfortunately, the presence of daylight is not always a positive one. Excessive brightness, strong contrast or intense reflections from daylight can cause visual discomfort or the inability to perform tasks. Typically, the total amount of luminous flux incident upon a surface per unit area – illuminance – present is used to predict visual discomfort due to questions about the benefit and validity of luminance-based analysis measures that are more related to the way the human visual system perceives light. This thesis aims to advance the understanding and usefulness of visual comfort prediction to the point that it can become commonly used in architectural design processes.

One method through which this is achieved is by testing the ability of visual comfort analysis to resolve subjective occupant comfort. It was found that of existing discomfort glare metrics, daylight glare probability (DGP) was the most likely to perform well in a variety of daylight conditions and space types. Furthermore, a long-term simulation and survey study found that between 53.7% and 70.1% of an occupant's visual satisfaction could be resolved by analyzing DGP, the presence of direct sunlight and predicted monitor contrast ratio. This choice of metrics was reinforced by a separate laboratory study, which found that 74.4% of subjective comfort could be resolved and identified new subjective luminance thresholds that identify likely discomfort. A new adaptive visual comfort model, the 'adaptive zone,' is proposed in this thesis to deal with spatiality and view in visual discomfort analysis. Finally, ways of applying these verified and new measures in design processes are tackled in this work by producing new temporal maps, spatial discomfort analysis, and plan-based mappings of visual satisfaction.

Thesis supervisor: Christoph F. Reinhart  
Title: Associate Professor of Building Technology



# Acknowledgments

First I extend my sincere gratitude to my advisor, Prof. Christoph Reinhart. During my PhD studies, Christoph was overwhelmingly supportive of the many tasks I put my energies towards, introduced me to the mysterious arts of research and always inspired me to produce high quality work. Beyond nurturing my development as a researcher, he has aided my ascent into the professional world and become a good friend. I hope our collaboration continues beyond that of the past four years.

I would also like to thank the members of my thesis committee. Prof. Mehlika Inanici provided valuable insights into luminance measurements, photometric accuracy and visual comfort evaluations. Prof. Les Norford's feedback on my research was also incredibly valuable and his expertise appreciated.

I extend a special thank you to Prof. Kevin Van Den Wymelenberg from the University of Idaho for graciously allowing me to analyze the dataset he collected during his own PhD work.

Jan Wienold deserves recognition for his assistance in evaluating high dynamic range photographs and early comments on many of the research projects in this thesis.

Adam Klauber and Brian Hanley from the US Department of Transportation's John A. Volpe National Transportation Systems Center were instrumental in the organization and fruitful nature of the airport disability glare case study. I am also grateful to Tarek Rakha for his time in traveling to the airport with me as well as originally connecting me with the team from the Volpe Center.

Friends, colleagues, professors and supporters during my time at Harvard and MIT have made the efforts towards my degree infinitely more pleasant. The instruction and early advice received from Prof. Leon Glicksman was fantastic. I would like to thank some former and current members of the Harvard G(SD)<sup>2</sup> and MIT SDL research groups: Andrew, Azadeh, Carlos, Chris,

Cody, Diego, Eduardo, Elliot, Holly, Jeff, Jon, Karthik, Kera, Nathaniel, Rashida, Seth, Tarek and Timur. Kathleen Ross, Alexandra Golledge and Renée Caso kept the administrative wheels moving with minimal friction. I also thank my close friends Max Doelling for many productive discussions about the work and Erin Christian for her invaluable moral support and input on the finer points of the English language.

Prof. Franca Trubiano and Prof. Ruchi Choudhary believed in me with no clear reason to do so, consequently sparking my interest in building performance for which I will always be thankful. They have continued to offer their support and friendship. I am thankful to Prof. Yun Kyu Yi for introducing me to building simulation and offering me a first chance to perform research and teach.

I am indebted to my family for their lifelong support; Mom, Dad and Tess, thank you.

I am of the good fortune to have been financially supported by the National Science Foundation's Department of Emerging Frontiers in Research and Innovation (award number EFRI-1038264), the US Department of Transportation (contract number RVT-42) and a Martin Family Fellowship for Sustainability.

I am thankful for the contributions of my wife, Felicia. Her careful proofreading and feedback was always illuminating. Most of all her love, even while pursuing her own career, was always a beacon leading me through the night.





To Oskar.





# Table of Contents

<b>1 Introduction</b> .....	19
1.1 Research Goals.....	20
1.1.1. Plausibility of Predicting Visual Discomfort.....	20
1.1.2 Behavioral Reactions to Visual Discomfort.....	21
1.1.3 Frameworks and Communication.....	21
1.2 Dissertation Overview.....	21
<b>2 Literature Review</b> .....	25
2.1 Luminance and Illuminance.....	26
2.2 Discomfort Glare.....	27
2.2.1 Daylight Glare Index (DGI or Cornell Equation).....	28
2.2.2 New Daylight Glare Index (DGI <sub>N</sub> ).....	29
2.2.3 CIE Glare Index (CGI).....	29
2.2.4 Visual Comfort Probability (VCP).....	30
2.2.6 Daylight Glare Probability (DGP).....	31
2.3 Computer Monitor Contrast Ratio.....	31
2.4 Direct Sunlight.....	32
2.4.1 On Horizontal Surfaces.....	32
2.4.1 Direct Solar Visibility.....	32
2.5 Disability Glare.....	32

2.6 Research Context .....	33
2.6.1 Validity and Usefulness of Discomfort Glare Metrics.....	34
2.6.2 Design of Daylit Spaces .....	34
2.6.3 Window Shade Control .....	37
2.6.4 Luminance Ratios.....	38
2.7 Simulation Programs and Tools Employed .....	39
2.7.1 Simulation Tools .....	39
2.7.2 Evaluation Tools .....	39
2.7.3 Measurement Tools .....	39
2.7.4 User Surveys .....	39
<b>3 Examination of Discomfort Glare Metrics .....</b>	<b>41</b>
3.1 Chosen Glare Metrics .....	42
3.2 Methodology .....	42
3.3 Results.....	46
3.4 Discussion .....	51
3.4.1 Appropriate Use of Metrics.....	51
3.4.2 Interpreting Glare Predictions .....	51
3.5 Conclusion .....	51
<b>4 An Adaptive Visual Comfort Model – The ‘Adaptive Zone’ .....</b>	<b>55</b>
4.1 Yearly Hour-by-hour Discomfort Glare Simulation with Daysim and Enhanced Simplified DGP.....	58
4.2 Considering User Blind Behavior .....	60
4.3 Required Simulation Effort.....	61
4.4 Conclusion .....	62
<b>5 Predicting Long-term Visual Satisfaction .....</b>	<b>65</b>
5.1 Discomfort Metrics .....	66
5.2 Methodology .....	66
5.2.1 Survey on Visual Comfort.....	66
5.2.2 Visual Comfort Simulations.....	67

5.3 Results.....	70
5.3.1 Survey Results.....	70
5.3.2 Predicting Long-Term Occupant Evaluations.....	71
5.3.3 Spatial Display of Results.....	71
5.3.4 Ability to Predict Occupant Visual Satisfaction.....	72
5.4 Discussion.....	76
5.4.1 Using Multiple Visual Comfort Criterion.....	76
5.4.2 Occupant Variability.....	78
5.4.3 Adaptation.....	78
5.4.4 Survey Bias.....	79
5.4.5 Limitations of Study.....	81
5.5 Conclusion.....	81
<b>6 Integrated Luminance-based Analysis for the Prediction of Visual Discomfort.....</b>	<b>83</b>
6.1 Methodology.....	84
6.1.1 Data Source and Subject Evaluations.....	84
6.1.2. Luminous Overflow and Correction.....	84
6.2 Calculation of Image-based Analysis Metrics.....	86
6.1.1 Vertical Eye Illuminance.....	87
6.1.2 Discomfort Glare.....	87
6.1.3 Direct Sunlight.....	87
6.1.4 Monitor Screen Visibility.....	88
6.3 Results.....	88
6.4 Discussion.....	91
6.4.1 Identifying Subjective Discomfort Thresholds.....	91
6.4.2 Application to Design.....	92
6.4.3 Research Limitations.....	92
6.4.4 Luminous Overflow Methodology.....	92
6.5 Conclusion.....	95
6.5.1 Future Outlook.....	96

<b>7 Disability Glare</b> .....	99
7.1 Qualifying Disability Glare due to Specular Reflections .....	100
7.1.1 Disability Glare at the Case-study Airport .....	100
7.1.2 Dynamic Range of Human Vision .....	103
7.1.3 Existing Disability Glare Metrics from Specular Reflections.....	104
7.2 Methodology .....	104
7.3 Results.....	107
7.4 Discussion .....	110
7.4.1 Option 1: A Less Reflective PV Panel .....	111
7.4.2 Option 2: Rotate the Panels 90-degrees to the East, Away from the ATCT.....	111
7.5 Conclusions.....	112
<b>8 Conclusions: A Framework for Design Analysis</b> .....	115
8.1 Implementation into Design Processes .....	115
8.1.1 Proposed Visual Comfort Metrics.....	115
8.1.2 Simulations, Process and Time .....	116
8.1.3 Visualization and Communication .....	118
8.2 Summary of Contributions.....	124
8.2.1. Plausibility of Predicting Visual Discomfort .....	124
8.2.2 Behavioral Reactions to Visual Discomfort.....	124
8.2.3 Frameworks and Communication .....	124
8.3 Future Work.....	125
8.3.1 Behavioral and Control System Models for Window Shades.....	125
8.3.2 View .....	125

<b>Appendices</b> .....	127
A Free Response Survey Answers.....	129
B Calculating Luminance-based Metrics from Radiance RGBE Format Images .....	133
B.1. Masking a HDR Image.....	133
B.2. Calculating Illuminance from a Masked Hemispherical Image .....	133
B.3. Finding the Maximum Pixel Luminance .....	134
B.4. Determining the Solid Angle of Pixels Greater Than a Luminance Threshold .....	134
B.5. Increasing Select Pixel Luminances to Achieve a New Illuminance Value.....	134
<b>References</b> .....	137



# Chapter 1

## Introduction

Humans perceive the world, visually at least, in terms of the distribution of brightness. Brightness is the physiological sensation created by our visual system in response to light projected through the lens of the eye onto the retina. When we feel that it is too bright or too dark, this is a sensation of brightness. The brightness sensation allows us to discriminate the contrast between adjacent objects, images on a page or words on a computer screen. Literally everything that is seen is through the brightness sensation, yet the metrics and measures utilized most often in the evaluation of architectural daylighting have little relationship to brightness. The research presented herein aims to advance the analysis of built and unbuilt spaces to more closely align with the way humans experience the physical world.

It is desirable to design buildings and spaces with daylit qualities: having a connection to the outside through view and natural lighting, minimizing electric lighting use and maintaining visual comfort. Daylight is generally thought to improve feelings of health, wellbeing and alertness; however, if visual discomfort occurs, these benefits are likely to be negated. Knowing the total quantity of light incident on a surface, illuminance, is useful for ensuring that there is enough light in a space to perform work or for navigation. When designing or analyzing daylit buildings, the vast majority of recommendations and standards account only for illuminance landing upon a horizontal surface (USGBC 2009; IESNA 2012) but have little to say about the perception or comfort of such spaces, recommending only to avoid direct sunlight.

Illuminance-based metrics have been extremely successful at predicting and resolving the amount of daylight available in a space, but at the same time it is important to consider that the presence of daylight is not always a positive one. In this context, there has been a research interest in predicting visual discomfort for nearly 90 years (Holladay 1926; Luckiesh 1927). This research uses measures of luminance, a physical measure used to describe the distribution of light which relates directly to our visual perception. Often, excessive luminances, strong contrast or intense reflections cause visual discomfort or disrupt the ability to perform tasks. In such cases simply knowing the total quantity of light incident upon the eye is rarely enough to resolve this

discomfort. As illuminance is equivalent to the mean luminance divided by  $\pi$ , it is incapable of resolving perception of high contrast, bright reflections and veiling luminances on monitor screens that can lead to visual discomfort. Instead it is important to know how light is perceived, through brightness perception rather than total illuminance. Unfortunately, the results of the 90 years of research have not been embraced by the community of daylight practitioners.

One is left to wonder why daylighting measures of visual comfort that account for actual perception have not been embraced more widely. There are several reasons for this. Until recently, available computational power and methods have not been adequate to efficiently implement such measures into a design process. Beyond that, there is still no clear consensus that such measures are capable of differentiating between visual discomfort and comfort as experienced by space occupants (Painter et al. 2009; Hirning et al. 2013; Van Den Wymelenberg & Inanici 2014). Finally, even if the available measures are taken at face value, the way in which a result which classifies visual discomfort as ‘disturbing’ or ‘intolerable’ at a specific point of time but ‘imperceptible’ at another should be interpreted is unclear. In other words, how much visual discomfort is too much?

These conditions however are primed for change. The widespread availability of high dynamic range photography, a method of capturing physically-precise luminance distributions with normal camera equipment, has made it possible to investigate the realities of human perception as never before. Now it is also possible to accurately generate predicted luminance distributions (Ward 1994; Wienold 2009; McNeil 2013) using computational building performance simulation. The speed and ease by which this can be achieved is much greater than in the past and will only improve with time as computers become faster and technologies mature. As buildings are being designed with greater percentages of glazing and more reflective surfaces such as glass and polished metal, there is a new and strong interest in avoiding visual discomfort. This new interest parallels the appearance of some telling examples of high-profile problems related to visual comfort in modern buildings reported in the media. For example, the Walt Disney Concert Hall’s polished steel cladding panels caused high levels of glare to occupants of neighboring condominiums (The Associated Press 2004), and the Museum Tower in Dallas reflects enough light to endanger artwork through the glass roof of the neighboring Nasher Sculpture Center (The Dallas Morning News 2013).

## 1.1 Research Goals

Overall this research intends to advance the understanding and usefulness of visual comfort prediction to the point that it can become commonly used in architectural design processes. The path to achieve this goal is broken down into three parts: to develop and test methods of predicting visual discomfort with regards to their plausibility, investigating behavioral reactions to visual discomfort, and developing analysis frameworks and communication methods.

### *1.1.1. Plausibility of Predicting Visual Discomfort*

Currently the notion of how applicable any given prediction of visual comfort is to actual perception is suspect, because detailed survey and measurement studies of discomfort glare metrics have not shown a strong correlation between perceived comfort and predicted comfort (Painter et al. 2009; Hirning et al. 2013; Van Den Wymelenberg & Inanici 2014). This is one of the major obstacles to meaningful comfort prediction that could be employed in a design process. Furthermore, most visual comfort assessments are calculated based on a fixed position and view



direction in a space. The meaning that a user looking in specific direction at a specific point in time is likely to experience discomfort is difficult to assess for design, and issues of spatial visual discomfort and changing view are not well understood. There is a need to evaluate visual comfort conditions throughout a space rather than in a fixed viewing direction. Finally, it is not understood how individuals assess spaces based on the frequency and intensity of visual discomfort over a long period of time. This is important in order to design satisfying spaces where occupants experience a sense of well-being.

The first research goal is therefore to establish which metrics yield results that are plausible in the sense that they match our expectation of how different spaces perform. The research herein also investigates the potential for new visual comfort metrics and thresholds using measured photometric data and survey responses. These results will be evaluated with differing views and positions in order to assess entire spaces in their potential for visual discomfort.

### *1.1.2 Behavioral Reactions to Visual Discomfort*

In order to predict the daylighting and energy-use performance of buildings, it is important to know when occupants are uncomfortable and how they react to visual discomfort. For example, it may be that users lower window shades<sup>1</sup>, improving visual comfort but reducing the availability of daylight and solar gains into the space. The second research goal is to establish comfort baselines (closely related to the goal in Section 1.1.1) and occupant behavioral models that relate to comfort perception for the operation of window shades.

### *1.1.3 Frameworks and Communication*

Finally, once plausible discomfort predictions and behavioral models are established, they need to be made useful in order to become applicable to design, real-world evaluations of daylit spaces and remediation of visual discomfort issues. The third research goal is to propose methods for integrating the findings of the goals in Sections 1.1.1 and 1.1.2 into comprehensive comfort predictions and visualization schemes, ready for use in simulation and design workflows.

## **1.2 Dissertation Overview**

Chapters 1 and 2 constitute an introduction to the research. Much of the work in this thesis has already been published or is currently in the process of being published (Jakubiec & Reinhart 2012; 2013; 2014; Jakubiec et al. 2014) and is presented as a series of five studies related to the research goals in Chapters 3 through 7. Finally, Chapter 8 aims to bring the work together and propose a framework for evaluating visual comfort in daylit spaces.

Chapters 1 and 2 contain a background of research and practice that informs the need for this work as well as the current state of the art in visual discomfort and daylighting analysis. Existing discomfort glare, task visibility and direct sunlight criteria for comfort are reviewed. A brief history of lighting metrics and window shade controls is authored to place the thesis research within the context of current daylighting research. Finally the lighting simulation tools, analysis tools, and luminous capture methods commonly employed in the research are described.

Chapter 3 begins by evaluating the plausibility of discomfort metrics through a study that evaluates the results of previously reported discomfort glare metrics for three different space types. The results are evaluated in order to understand how applicable these metrics are to

---

<sup>1</sup> See Section 2.6.3.

various spaces and daylight conditions. The daylight glare probability (DGP) metric is found to be the only metric that yields plausible results for all space types as it considers overall brightness and contrast.

Chapter 4 continues with the results from Chapter 3 by investigating in greater detail how the DGP metric could actually be applied in design. It addresses multiple positions and view directions simultaneously, allowing the evaluation of glaring conditions throughout a space rather than using a single, specific view. The concept of an ‘adaptive zone’ adaptive visual comfort model is introduced within which building occupants may freely adjust their position and view in order to minimize the effects of discomfort glare.

Chapters 5 and 6 use human subject research to validate the ideas presented in Chapters 3 and 4 as well as to investigate other means of analyzing visual comfort besides the notion of a single discomfort glare index. The study presented in Chapter 5 investigates long-term visual satisfaction in a complex daylight and electrically lit space. A series of calibrated semester-long visual comfort simulations are used to test the capability of comfort simulations to resolve reported subjective comfort from participants in many different lighting conditions throughout the space. Discomfort glare, monitor screen visibility, and the presence of direct sunlight were found to contribute to participants’ visual satisfaction. The ability for occupants to adapt to their spaces in order to avoid glare using the ‘adaptive zone’ concept is also explored. The measures identified in Chapter 5 are further tested with an independent laboratory-collected dataset in Chapter 6. Chapter 6 presents a dataset of luminance-calibrated high dynamic range photographs with associated subjective data evaluated against a set of plausible visual comfort metrics: vertical eye illuminance, direct sunlight on the workplane, direct vision of the sun, monitor contrast ratio, and discomfort glare. The results identify several thresholds that indicate discomfort in the participant study and confirm that a multiple-metric mode of analyzing visual discomfort is warranted.

Chapter 7 is concerned with the appearance of disability glare from exterior reflections, and constitutes a case study for how visual metrics can be used in a design process. It presents an analysis of a disability glare hazard at an airport created by the installation of a large array of photovoltaic panels between an air traffic control tower and the aircraft taxiway. The panels reflect blinding quantities of daylight into the control tower, produce temporary after images and dangerously obscure taxiing aircraft. New metrics and simulation methodologies are created to use in an analysis of remediation strategies.

Finally, Chapter 8 provides concluding insight into the studies of visual comfort presented here and makes proposals as for how the results of this research can be used in an architectural design and analysis framework.





## Chapter 2

### Literature Review

As noted in Chapter 1, daylight has been shown to improve health, awareness and feelings of well-being in spaces where it is present; however, simply maximizing daylight is potentially undesirable. The suitability of a space for inhabitation can be compromised if glare is experienced in its use. It is hence dependent on the lighting distribution seen by an observer which may correlate very poorly with work plane illuminance metrics such as the daylight factor or daylight autonomy, especially in toplit spaces (Reinhart et al. 2006). In this chapter, existing literature relevant to the thesis is chronicled.

In Section 2.1, primary lighting units are established. Glare is a measure of the physical discomfort of an occupant caused by excessive light or contrast in a field of view. Glare, a major cause of visual discomfort, is typically categorized as either discomfort glare, veiling glare or disability glare. Discomfort glare, is merely irritating, and its root cause is a bright, visible light source that creates uncomfortable levels of contrast or overall brightness. Discomfort glare metrics are discussed in Section 2.2. Section 2.3 discusses veiling glare, which is when a bright light source is reflected by a surface, for example when light falling on a monitor display screen obscures the transmitted image by lowering the perceived monitor contrast ratio. Section 2.4 discusses other potential causes of visual discomfort, such as the presence of direct sunlight. Section 2.5 discusses disability glare, which measurably impairs vision, reducing the contrast of the retinal image by the presence of a very bright light source in the field of view (Commission Internationale de l'Eclairage TC3-13 1995). As disability glare and discomfort glare have the same root causes – bright, visible light sources – as discomfort glare intensifies it will turn to disability glare. Finally, Section 2.6 describes daylight simulation tools and methodologies employed in the research.<sup>2</sup>

---

<sup>2</sup> Large portions of this chapter borrow from the paper, Jakubiec, J. & Reinhart, C., 2012. The “adaptive zone” - A concept for assessing discomfort glare throughout daylight spaces. *Lighting Research and Technology*, 44(2), pp.149–170.

## 2.1 Luminance and Illuminance

Luminance is the physical correlate to the sensation of brightness (Hopkinson & Collins 1970). Luminance is technically defined as the luminous intensity per unit area of light travelling in a specific direction; it indicates how much luminous power reaches an observer viewing the surface from a particular vantage point and in the context of this work is described in SI units of candela per square-meter,  $\text{cd}/\text{m}^2$ . Through processes of physical and psychological adaptation, the human visual system chooses how to perceive luminance. In bright outdoor conditions, the pupil constricts (physical adaptation), our retinas become less sensitive to luminance (psychological adaptation), and photoreceptor pigments break down in response to the lighting change (chemical adaptation) (Boyce 2003). These three complex processes are changes the visual system makes to respond to varying levels of luminance. The relationship between luminance and perceived brightness is known, illustrated in Figure 2.1. Depending on the adaptation luminance of the visual system, a specific luminance will be perceived differently. Adaptation luminance is the mean luminance of the objects of viewing interest that the visual system adapts to such that they can be easily seen. For example, one might perceive a small light emitting diode (LED) as exceptionally bright during a moonlit night but not notice it at all during a bright day. In both cases, it has the same luminance, but the perception of brightness varies.

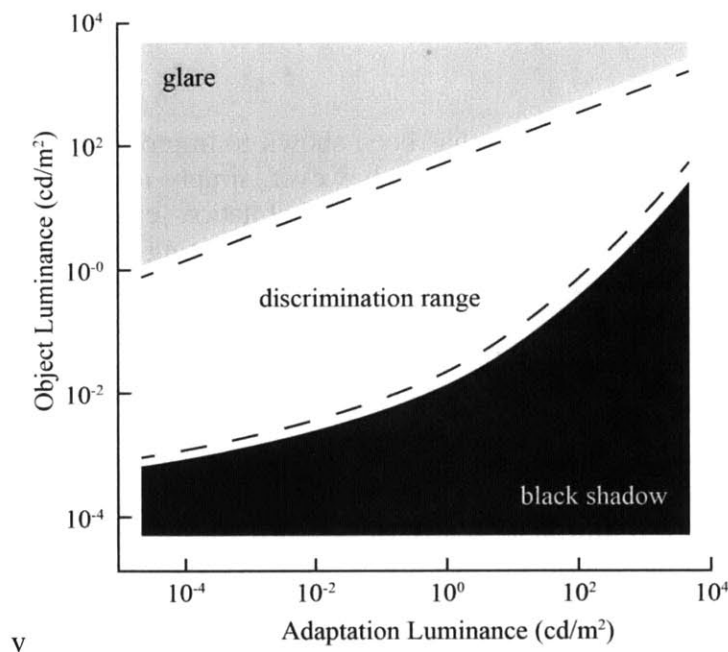


**Figure 2.1** The luminous range the visual system can distinguish depending on the adaptation luminance. On average, we can perceive between 2 and 3 log units of luminance simultaneously. After Hopkinson (1970).

Despite the somewhat complex relationship between measured luminance, the visual system and the perception of brightness, images calibrated to units of luminance are an excellent way to study human perception and visual comfort.

Illuminance, in contrast to luminance, is the sum luminous flux falling upon a surface per unit of area. It indicates how much light falls upon a surface, and in this research is referred to in the SI units of lux, lx (or  $\text{lm}/\text{m}^2$  or  $\text{cd}\cdot\text{sr}/\text{m}^2$ ). As mentioned in the introduction to this chapter, most architectural design decisions with regards to natural daylight and electric lighting are made

using measures of illuminance. Automated window shading and electric lighting systems are also commonly automated using measures of illuminance. By integrating across a hemispherical luminance distribution, illuminance can be derived; however, all of the spatial and contrast clues from a complete luminance distribution are not present in the single number which represents illuminance. Figure 2.2 compares the meaning of vertical luminance, a correlate to brightness perception of vision, to horizontal illuminance.

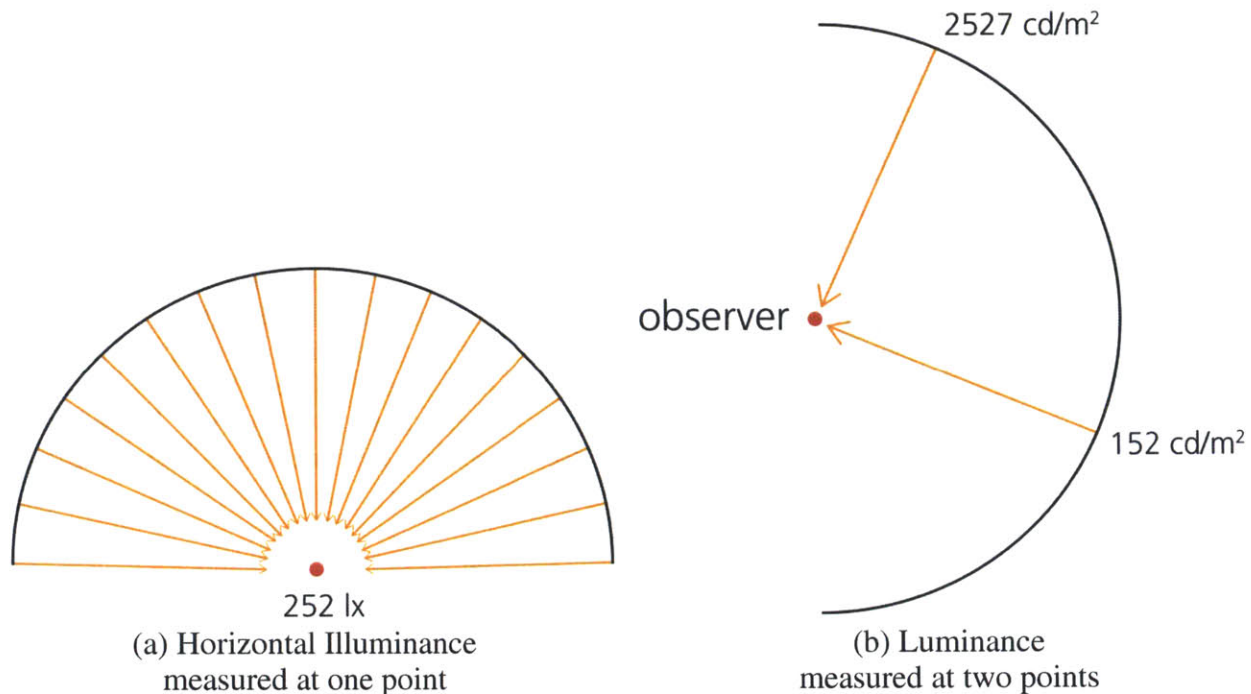


**Figure 2.2** A visual comparison of the meaning of illuminance and luminance measurements.

## 2.2 Discomfort Glare

While many architects have sensibilities for other subjective factors concerning the light within a space such as how ‘pleasing’ a space is or what a ‘good’ view is, they lack an intuition for what amount of glare is acceptable. Discomfort glare is even more difficult to discern than disability and veiling glare, as it does not initially produce observable effects such as the inability to perform a task (Hopkinson 1972). To further complicate matters, there is some evidence that suggests interesting views increase tolerance to glare (Tuaycharoen & Tregenza 2007). To improve our ability deal with glare, there has long been an interest in quantifying glare using the concept of a ‘glare index.’ A glare index is a numerical expression derived from the luminance distribution in the field of view of an observer. Within the context of a glare index, disability and discomfort glare are separated only by the brightness extremes of the glare sources, their sizes and their prominence in the field of view. An occupant will always feel discomfort when experiencing disability glare; therefore, preventing discomfort glare mostly precludes the possibility of experiencing disability glare. This is reflected in most glare metric calculations which predict the probability of experiencing visual discomfort, rather than visual disability, in a space.

Glare is typically expressed as the ratio of the size, location and luminance of glare sources in a field of vision when compared to the average luminance not inclusive of the glare source. This can be expressed as a simplified equation,

$$Glare = \sum_{i=1}^n \frac{L_{s,i}^{exp} \omega_{s,i}}{L_b^{exp} P_i^{exp}} \quad (2.1)$$

where exp is a weighting exponent applied to each variable. It can be observed that, in a generalized fashion, larger and brighter glare sources increase glare probability, where  $\omega$  is the solid angle size of a glare source, and  $L_s$  is its luminance. A brighter average or background luminance ( $L_b$ ) decreases the probability of glare, and the further away a glare source is from the center of the visual field, the less likely a viewer is to be disturbed by it. The value of  $P$ , the position index, grows larger as a glare source approaches the visual periphery with a value of one being perfectly centered in a field of view. The position index was originally developed by Guth, and it is a convenient way to weigh a glare source based on its location in a view (Figure 2.3) (Luckiesh & Guth 1949); however, it is not an easily understood factor without some background information, while the luminance and size of a glare source are much easier to understand conceptually. From this basic concept of glare, many different datasets developed through subjective polling of space occupants have led to different equation fits. Therefore, the conditions under which each metric gathered its user data are very important in evaluating its applicability to a given situation.

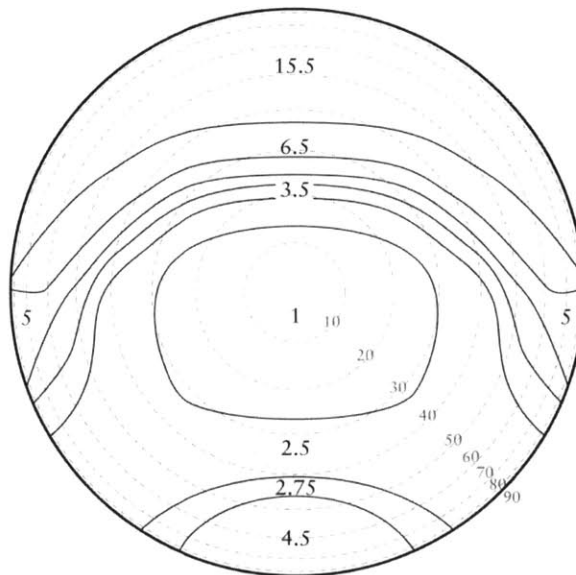


**Figure 2.3** Selected values of the Guth Position Index plotted on top of a 180 degree hemispheric view projection

### 2.2.1 Daylight Glare Index (DGI or Cornell Equation)

$$DGI = 10 \times \log_{10} 0.48 \sum_{i=1}^n \frac{L_{s,i}^{1.6} \omega_{pos s,i}^{0.8}}{L_b + (0.07 \omega_{s,i}^{0.5} L_{s,i})} \quad (2.2)$$

The Daylight Glare Index was originally formulated by Hopkinson in 1972 based upon earlier work he performed at the Building Research Station for small glare sources (Hopkinson



1972). DGI considers the possibility of large glare sources such as the sky visible through a window. Hopkinson's metric was derived from human subject studies in interiors with large diffusing screens backlit by fluorescent lights (Hopkinson 1971). In the study the glaring sources were subtended to various sizes and places at different locations in the field of view. This simulated sky brightness was measured and given a size and position index. DGI is not considered to be reliable when direct light or specular reflections are present in a field of view, because Hopkinson's experiment relied only upon a diffuse light source and not interior specular reflections or direct sources of light. The equation was later validated against daylighted interiors with acceptable results (Hopkinson 1972). DGI correlates the source luminance, size and its position in the field of view against the background luminance and a small percentage of the source luminance which compensates for additional eye adjustment to the visible luminance, resulting in a value where any number >31 corresponds to intolerable glare and <18 suggests that glare is 'barely perceptible'. Hopkinson also recognized the importance of adding new considerations to his metric by surveying those he asked to make subjective observations of spaces. He listed an evaluation of view and the consideration of interior specular reflections as the two most likely important missing factors in his formula.

### 2.2.2 New Daylight Glare Index ( $DGI_N$ )

$$DGI_N = 8 \times \log_{10} 0.25 \sum_{i=1}^n \frac{L_{exterior,i}^2 \Omega_{s,i}}{L_{adapt} + 0.07(\sum_{i=1}^n \omega_{s,i} L_{window,i}^2)^{0.5}} \quad (2.3)$$

The New Daylight Glare Index, developed by Nazzal in 2001 (Nazzal 2001), is a modification of Hopkinson's original equation which introduces several new variables into the metric:  $L_{adapt}$ , adaptation luminance, the average luminance of the surroundings;  $L_{exterior}$ , the average exterior luminance; and  $L_{window}$ , the average window luminance, treating the window as a uniform glare source. Exacting geometric information on the dimensions of the window and its distance from the viewing location are necessary for calculation.  $DGI_N$ 's results are correlated and validated only against those of the original DGI method; no significant human validation studies have been performed at this time, so  $DGI_N$  may contain substantial errors in correlation to discomfort that are unknown (Nazzal et al. 2005).  $DGI_N$  specifies exacting measuring techniques utilizing three sensors which measure the shielded window illuminance, total vertical illuminance and the total exterior vertical illuminance which is a great clarifying measure that somewhat allows the consideration of direct sunlight in the scene; however, it is still subject to the same weaknesses as the original DGI, that specular reflections and direct luminance sources are not adequately considered.

### 2.2.3 CIE Glare Index (CGI)

$$CGI = C_1 \times \log_{10} C_2 \frac{\left(1 + \frac{E_d}{500}\right)}{E_d + E_i} \sum_{i=1}^n \frac{L_{s,i}^2 \omega_{s,i}}{P^2} \quad (2.4)$$

Published in 1979, the CIE Glare Index was an attempt by Einhorn to develop a formula that took into account all peer-reviewed glare research in order to be used as a standard glare index adopted by the Commission Internationale de l'Eclairage (CIE) (Einhorn 1979). Care was taken that the summation of solid angles of luminance sources ( $\omega$ ) were to an exponent of one for mathematical clarity. Adaptation to glaring sources is weighted by the ratios of vertical eye

illuminance which are multiplied by the summation in the equation. For C1 of 8 and C2 as 2, which are optional scaling factors defined by Einhorn, values >28 are intolerable while those <13 are imperceptible. These values correlate with the later-discussed UGR metric, also adopted by the CIE. There were no user perception studies conducted during the development of the CGI metric; however, correlation studies were performed with other contemporary glare metrics.

#### 2.2.4 Visual Comfort Probability (VCP)

$$VCP = 279 - 110 \left[ \log_{10} \sum_{i=1}^n \left[ \frac{0.5L_{s,i}(20.4\omega_{s,i} + 1.52\omega_{s,i}^{0.2} - 0.075)}{P \times E_{avg}^{0.44}} \right] \right]^{n^{-0.0914}} \quad (2.5)$$

Visual Comfort Probability expresses “the probability that a normal observer does not experience discomfort when viewing a lighting system under defined conditions” (Harrold 2003). While a rather complex assemblage of factors, VCP essentially weighs the glare source luminance and size against its position in the scene and the average illuminance for a viewing solid angle of 5 steradian. It is only valid for typically-sized, ceiling-mounted, artificial lighting installations with uniform luminances, as it was derived under these conditions. It is not valid for very small or very large glare sources, and therefore should not be used to evaluate glare from daylight sources nor compact types of luminaires such as halogens. VCP evaluates in a numerical range from 0 to 100, specifying a percentage of people who would feel comfortable under similar lighting circumstances.

#### 2.2.5 CIE Unified Glare Rating System (UGR)

$$UGR = 8 \times \log_{10} \frac{0.25}{L_b} \sum_{i=1}^n \frac{L_{s,i}^2 \omega_{s,i}}{P^2} \quad (2.6)$$

The Unified Glare Rating (Commission Internationale de l’Eclairage TC3-13 1995) was developed in response to difficulties in calculating direct illuminance required under the CGI metric. Thusly, visual adaptation to direct sources of light in the scene is not considered in this metric; however, the CIE technical committee 3-13 created the UGR formula so that its abstraction has “little effect when [...] applied to rooms having illuminances within the usual range recommended for working interiors.” For this reason, UGR typically predicts less probability of discomfort glare than does CGI. In essence, UGR is a simplification of CGI for computational ease; however, with current technologies it is now easy to separate direct and diffuse illuminances so that this simplification is no longer required. UGR uses a similar numerical scale as DGI; however, UGR predicts intolerable discomfort at a lower threshold. Any value >28 is intolerable while values <13 are considered imperceptible. The exact testing and user polling conditions that lead to UGR’s derivation are not clearly discussed in the technical report released by the CIE.

### 2.2.6 Daylight Glare Probability (DGP)

$$DGP = 5.87 \times 10^{-5} E_v + 0.0918 \times \log_{10} \left( 1 + \sum_{i=1}^n \frac{L_{s,i}^2 \omega_{s,i}}{E_v^{1.87} P_i^2} \right) + 0.16 \quad (2.7)$$

Daylight Glare Probability is a metric derived from subjective user evaluations in sidelit office spaces (Wienold & Christoffersen 2006). One major departure of DGP relative to other metrics summarized in this section is that glare sources are determined by comparing areas of bright luminance against the total vertical eye illuminance for a viewing hemisphere of  $2\pi$  sr. Therefore, DGI can evaluate direct sunlight falling on a workplane as a glare source while at the same time a dim visible sky might not be perceived as such. Specular reflections can also be seen as glare sources. A second major change present in DGP is the addition of a novel first-half of the equation, utilizing vertical eye illuminance,  $E_v$ , as its sole input. This means that in exceedingly bright scenes, discomfort can be predicted even without significant visual contrast. The latter-half of the equation uses the familiar comparison of the source luminance and size against the scene luminance and the position index of the glare source, an evaluation of visual contrast. In this sense, DGP is the evaluation of glare which considers the most factors that contribute to discomfort. It also resolves some of Hopkinson's original concerns about the DGI metrics' validity by allowing for direct glare sources other than the sky, something which no other subsequent metric has done. Similar to VCP, DGP's value scale is more intuitive, representing a percentage of people who would feel uncomfortable under specific lighting conditions. Unintuitively, a glare probability of 0.45 corresponds to intolerable glare – an estimated 45 percent of people would feel discomfort in such a lighting situation, while a value of 0.35 is considered imperceptible. DGP's equation is fit to substantial subjective user sampling in both Denmark and Germany under careful testing conditions in real daylit spaces.

### 2.3 Computer Monitor Contrast Ratio

When light reflects from a monitor screen, the observable contrast between pixels is lowered. For specular (shiny) LCD screens, this problem is exasperated by veiling glare, when bright light sources manifest as visible reflections in the monitor. The observable contrast ratio between bright (high state) and dark (low state) pixels can be calculated based on the amount of light reflected from a monitor as shown below,

$$CR = \frac{L_H + L_r}{L_L + L_r} \quad (2.8)$$

where  $L_H$  is the high state luminance,  $L_L$  is the low state luminance and  $L_r$  is the amount of reflected light. According to ISO standard 9241-3:1992, contrast ratios above three are necessary to preserve readability (International Standards Organization 1992). Later standards suggest contrast ratios as high as four are necessary (International Standards Organization 2008).

## 2.4 Direct Sunlight

### 2.4.1 On Horizontal Surfaces

Direct sunlight falling on the workplane or the eye directly is likely to cause discomfort. IES standard LM-83-12 states that horizontal illuminance from direct solar exposure over 1000 lx, as derived by running a simulation accounting for the direct solar beam alone, is a good indicator for visual discomfort (IESNA 2012). When greater than 2% of a daylight space is illuminated by 1000 lx of direct solar insolation calculated in this way, IES recommends that blinds be closed. The Lightswitch algorithm (Reinhart 2004) employed in Daysim (Reinhart 2010) suggests window shades be closed when greater than 50 W/m<sup>2</sup> direct normal irradiation falls on the workplane. Lightswitch also considers only the direct solar beam; however, it has provisions to allow the setting of measurement points to be located where occupants are actually seated.

### 2.4.1 Direct Solar Visibility

Experience shows that viewing the sun directly is uncomfortable; however it is also likely to affect the ability to see other objects in the scene. Therefore, direct visibility of the sun might be quantifiable as disability glare under certain conditions. This is described in the following section.

## 2.5 Disability Glare

Disability glare impairs vision in measurable ways, as opposed to discomfort glare which is merely uncomfortable. Typically it is caused by the scattering of light in the eye which obscures the source image by reducing its contrast (Commission Internationale de l'Eclairage 2002) or by very bright sources which might cause temporary after images or permanent retinal damage.

Ho and colleagues (2011) have created a metric to quantify glare and glint hazards as might be experienced from bright sources such as the sun. Their metric is evaluated using irradiance at the retina and the size of the glaring source and is based on previous research on the physiology of the human eye to experience after images and retinal burning. In order to calculate irradiance at the retina, the below series of three equations are useful,

$$d_r = f\omega \quad (2.8)$$

$$\omega = d_s / r \quad (2.9)$$

$$E_r = E_c \left( \frac{d_p^2}{d_r^2} \right) \tau \quad (2.10)$$

Where  $d_r$  is the diameter of the image projected on the retina,  $f$  is the focal length of the eye ( $f \cong 0.017m$ ),  $\omega$  is the subtended source angle in radians,  $d_s$  is the source size,  $r$  is the radial distance between the eye and the source,  $E_r$  is the retinal irradiance,  $E_c$  is the irradiance at a plane in front of the cornea in W/cm<sup>2</sup>,  $d_p$  is the daylight adjusted pupil diameter ( $d_p \cong 2mm$ ), and  $\tau$  is a transmission coefficient ( $\tau \cong 0.5$ ). The relationship of retinal irradiance and the source size to the potential for after image and eye damage is shown in Figure 2.4.

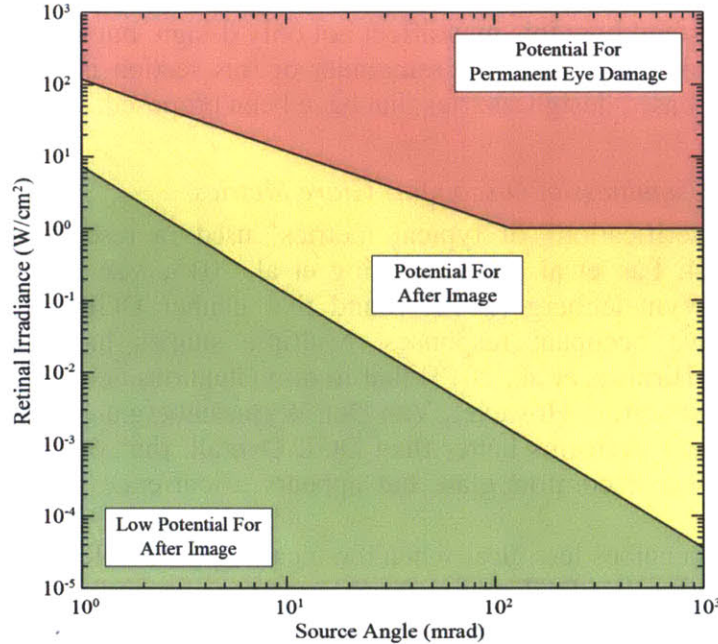


**Figure 2.4** Ho and colleagues’ metric for experiencing after images and eye damage from bright sources.

The CIE has also produced a general equation to represent disability glare, shown in Equation 2.11. The equation asserts the amount of light scattered in the eye relative to the glaring source, and is only valid for light sources between 0.1 and 30 degrees from the center of vision (Commission Internationale de l’Eclairage 2002).

$$\left[ \frac{L_{veil}}{E_{glare}} \right] = \frac{10}{\theta^3} + \left[ \frac{5}{\theta^2} + \frac{0.1p}{\theta} \right] \times \left[ 1 + \left( \frac{A}{62.5} \right)^4 \right] + 0.0025p \quad (2.11)$$

where  $L_{veil}$  is the veiling luminance,  $E_{glare}$  is the illuminance on the eye from a glaring source,  $\theta$  is the angle between the direction of the glare source and the viewing direction,  $A$  is the age of the person experiencing glare, and  $p$  is a value associated with eye pigmentation (0 for black eyes, 0.5 for brown eyes, 1.0 for light eyes, and 1.2 for very light-blue eyes). However, there is no guidance for how to evaluate these results.

## 2.6 Research Context

Beyond establishing key measures (Sections 2.1 through 2.5) of visual discomfort, it is important to set the stage for the context of the thesis research. As alluded to in the introduction, researchers have been studying the effects of glare since the 1920s (Holladay 1926), and specifically visual discomfort has been studied since the 1940s (Hopkinson 1940; Luckiesh & Guth 1949). Then one must ask, why has this area of study not produced any impact on the design of architecture as arguably other methods of building performance analysis such as thermal modeling, computational fluid dynamics, and daylighting have? Secondly, as the goal of this thesis is to establish a means for visual comfort analysis to be used in the design process,

it is useful to understand how this may affect not only design, but other important measures such as window shade control. Finally the remainder of this section is dedicated to exploring other types of luminance-based design metrics that have been proposed, such as luminance ratios.

### 2.6.1 Validity and Usefulness of Discomfort Glare Metrics

Independent verifications of typical metrics<sup>3</sup> used in research and practice are sparse (Rubiño et al. 1994; Fan et al. 2009; Hirning et al. 2013; Van Den Wymelenberg & Inanici 2014). Van Den Wymelenberg (2012) found that neither DGP nor DGI was successful at predicting subjective occupant responses. Multiple studies have found (Painter, Fan and Mardaljevic, 2009; Hirning, et al., 2013) that in dim situations neither DGP nor DGI can resolve subjective visual discomfort. However, Van Den Wymelenberg and colleagues (2010, 2014) note that DGP consistently performs better than DGI. Overall, the consensus is that DGP responds less to contrast-based discomfort glare but appears to correlate most strongly with subjective ratings.

The situation becomes less clear when the meaning and implementation of glare predictions are considered. Taking the DGI metric as an example, discomfort predictions greater than 31 indicate intolerable glare, but this value has no relationship with reality. DGI is implemented in EnergyPlus (EnergyPlus Development Team 2012); however, it is well known that the Split Flux lighting calculation method (Hopkinson et al. 1954; Lynes 1968) used in EnergyPlus is not very accurate. In a mostly unrelated study by the author, DGI predictions in EnergyPlus were highest during the Summer season when far less sunlight enters the space due to the higher solar elevation (Jakubiec & Reinhart 2011). By using such a highly simplified model, it is difficult to inspire confidence in metrics such as DGI. DGP evaluates between 0.16 and 1, suggesting a percentage of people who are uncomfortable; however, its real range of meaning is much more narrow: values less than 0.35 are typically imperceptible and values greater than 0.45 are typically intolerable (Wienold 2009). This suggests that further study into how DGP glare predictions are evaluated is necessary.

### 2.6.2 Design of Daylit Spaces

Although building occupants experience spaces visually, most daylighting goals strictly deal with the total amount of luminous flux normalized per area, illuminance, present on a horizontal working surface. For example, the IESNA recommends certain illuminance minimums for various tasks (Harrold 2003), shown in Table 2.1. Providing 500 lx on the workplane is a typical goal in the design of new office spaces.

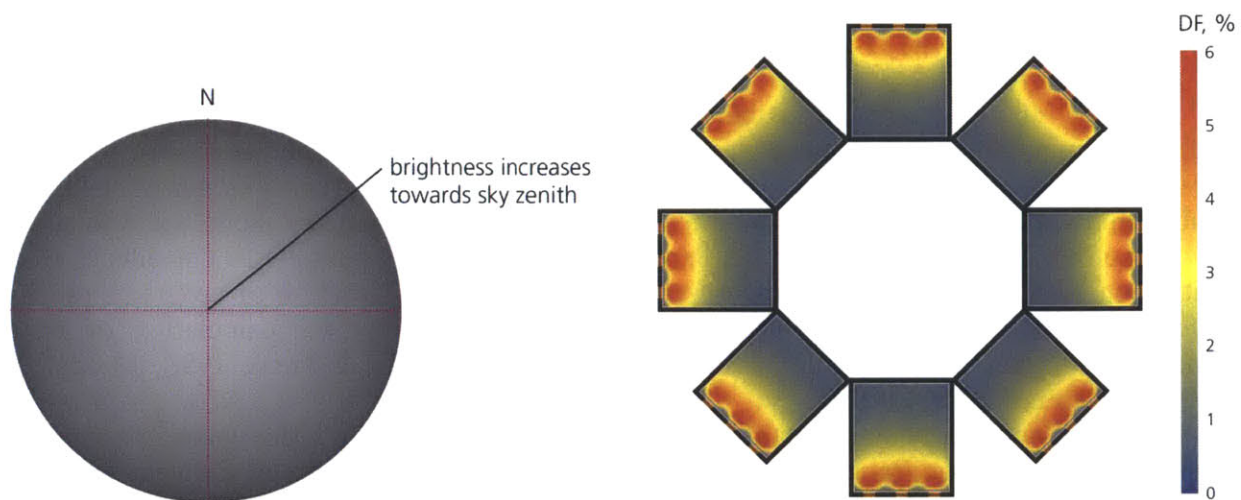
**Table 2.1** IESNA recommended illuminance guidelines.

<b>Task</b>	<b>Illuminance Recommendation</b>
Reading (Computer Screens)	30 lx
Meeting Rooms	300 lx
General Classrooms	300 lx
Office Spaces (intensive computer tasks)	300 lx
Office Spaces (variety of tasks)	500 lx
Fine Machine Work	3,000 – 10,000 lx

<sup>3</sup> See Section 2.2.



At the advent of daylighting simulation, a metric known as the daylight factor (DF) was used to quantify the amount of a space that is daylit. DF is simply defined as the ratio of indoor illuminance to the ratio of outdoor illuminance expressed as a percent; however, in practice the method is calculated using the CIE overcast sky (Commission Internationale de l’Eclairage 1996) shown in Figure 2.5a, which is a rotationally invariant sky that has no direct solar component. What this in essence means is that buildings designed using DF as the primary daylighting metric do not account for climate. Neither the climate-specific solar position nor specific climate data is included. Identical buildings located in Alaska and Singapore will have the same DF results; however, the actual daylighting would be very different. The relationship of calculated daylight factor to the orientation of several spaces is displayed in Figure 2.5b. Typically a DF of between 2 and 6 percent is a design goal (USGBC 2001; USGBC 2003), and values of greater than 6% are thought to correlate with overlighting.



(a) Visualization of the CIE Overcast Sky      (b) DF results visualized for many orientations.  
**Figure 2.5** Sky and results visualizations for typical DF calculations.

Later it became commonplace to calculate illuminances in practice, with the goal of achieving the IESNA targets described in Table 2.1 without obtaining results that would be so bright as to be uncomfortable. The definition of uncomfortable daylighting ranged between 2000 lx (Nabil & Mardaljevic 2006) and 5382 lx (USGBC 2009). Practically, illuminance is calculated using the CIE clear sky, which accounts for the geographic location by accurately positioning the sun, but still not accounting for any climatological data. An illustration of the CIE clear sky and a typical illuminance calculation is shown in Figure 2.6.

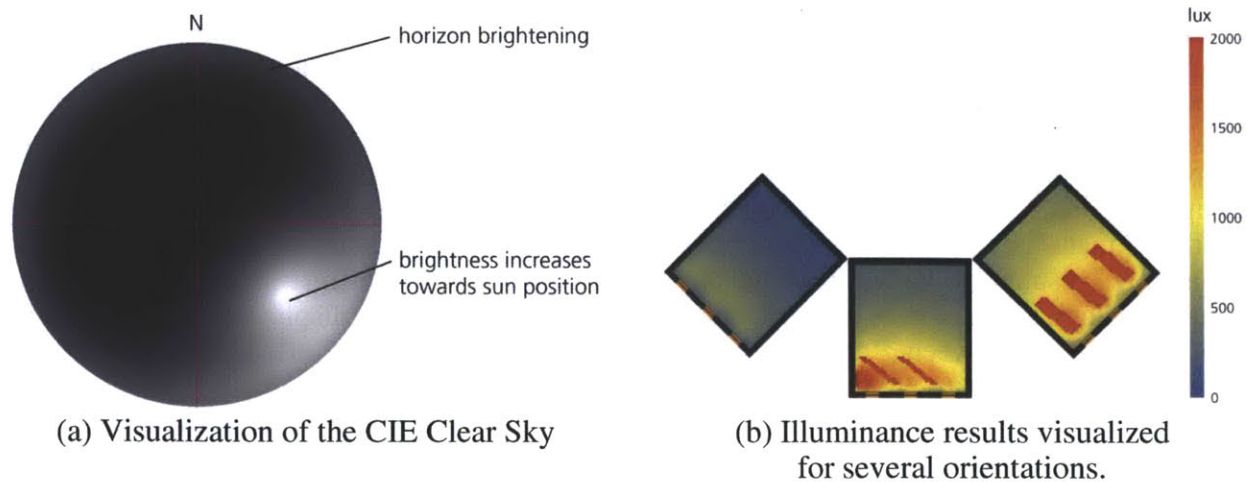


**Figure 2.6** Sky and results visualizations for typical illuminance calculations.

Bringing this brief history to the present, the conceptualization of daylight coefficients (DC), mathematical relationships between the sky outside and illuminance at a point in a room, allowed the simulation of illuminance for every hour in the year (Tregenza 1983). In combination with measured median weather data (USDOE 2014) and sky models that relate that data to more realistic sky distributions (Perez et al. 1993), it was possible to consider not only position on the earth but typical climatological factors as well. A wealth of programs (such as ADELINe, ESP-r and Daysim) and methodologies emerged for the calculation of annual illuminance distributions using DCs (Erhorn et al. 1997; Clarke & Janak 1998; Mardaljevic 2000; Reinhart & Herkel 2000).

Suddenly new methods of qualifying the daylight qualities of a space were imagined that considered lighting conditions in terms of percentages of occupied hours in the year when they occur. For example, Daylight Autonomy (DA) is defined simply as the percentage of occupied hours in a year where lighting is above a certain threshold. If a space is being designed to achieve 500 lx, a DA value of 50% means that half of the time there will be enough light through daylight alone. More useful metrics separate lighting into several bins. Useful Daylight Illuminance (UDI) has four lighting criterion (Nabil & Mardaljevic 2006; Mardaljevic et al. 2012),

- fell short  $E < 100 \text{ lx}$
- supplemental  $100 \text{ lx} < E < 300 \text{ lx}$
- autonomous  $300 \text{ lx} < E < 3000 \text{ lx}$
- exceeded  $3000 \text{ lx} < E$

which suggests that horizontal illuminances greater than 3000 lx ( $UDI_{\text{exceeded}}$ ) may cause some sort of visual discomfort. Daylight Availability ( $DA_{\text{avail}}$ ) is defined in two steps. It considers overlit areas, those which achieve an illuminance 10 times the lighting threshold for more than 5% of the occupied hours in the year. Areas which are not overlit are defined in the same way as DA, the percentage of occupied hours in a year where lighting is above a certain threshold. Figure 2.7 compares these types of ‘climate-based’ annual metrics.



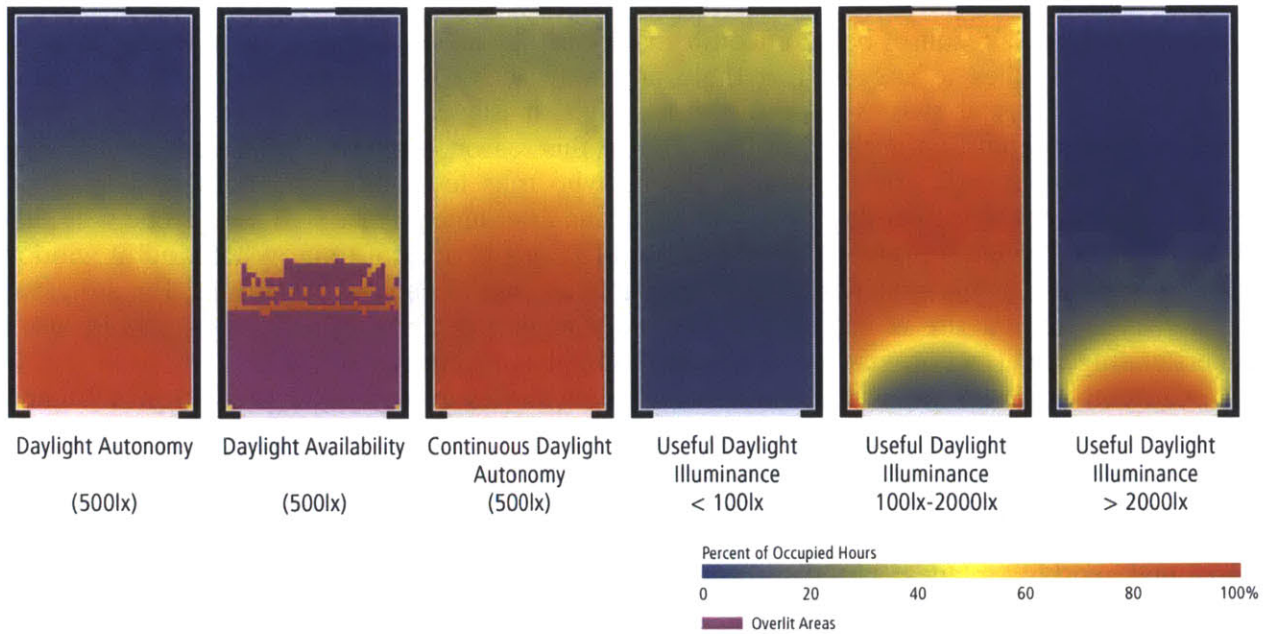


**Figure 2.7** Comparison of several types of climate-based daylighting metrics generated using measured climate data and daylight coefficients.

Throughout this explanation, it should become obvious that the actual perception of light in a space was never a major concern in terms of daylighting metrics. There has long been an emphasis on quantifying the daylight availability in spaces. This interest triggered the introduction of climate based daylight availability metrics, such as those shown in Figure 2.7, into standards. At this point daylighting research is turning towards more complicated, data rich luminance-based metrics. This thesis contributes to these efforts. Regardless, there is no denying that as a method for predicting comfort and successful daylighting in spaces, illuminance-based metrics are currently dominant. Visual comfort analysis in daylit spaces is, more often than not, taken care of with an overlighting provision expressed as a maximum illuminance value. Looking towards the future, there are exciting new technologies that allow the simulation of annual luminance visualizations (McNeil 2013). With appropriate measures, such imagery could be utilized to not only predict visual comfort, but to predict well-daylit qualities of a space. Furthermore, they could be used to visualize annual aesthetic and comfort-relevant luminance information (Rockcastle & Andersen 2012).

### 2.6.3 Window Shade Control

Another area where predicting visual discomfort or comfort is important is in the control of window shades. It seems plausible that occupants may adjust the blinds for several reasons: maintaining comfort, privacy, or view. While there are some studies that suggest interesting views have a limiting effect on discomfort glare (Tuaycharoen & Tregenza 2005), this section is primarily concerned with predicting when an occupant will desire to close a window shading system. This has implications for both the design of shading systems and for programming automated shading control algorithms.

Research on manually controlled blind systems has shown that users are often not eager to change their shading systems. For example, some studies find that 35 percent of users go for four months without adjusting their window shades (Pigg et al. 1995). Such users may lower their

window shades as a result of being uncomfortable one day and never raise them again. However there are also studies to suggest that there are more active shade operators who adjust their shades as frequently as two or more times per day (Lindsay & Littlefair 1992; Reinhart 2004). The Lightswitch control algorithm in Daysim, for this reason, allows the modeling of an active user and a passive user. An active user is one who tries to maintain daylight in a space by opening the shades twice per day: in the morning and after lunch. A passive user is one who, like in the study of Pigg et al., keeps the blinds closed for long periods of time. What kind of window shade users exists in any given building is probably a result of cultural conditions. Regardless of the user type and culture of the space, accurately predicting comfort conditions should aid in understanding the effect of window shades on daylight availability in a space.

Currently Daysim allows the control of window shades through DGP predictions (Wienold 2007; Reinhart 2010); however, it has already been noted that DGP alone does not fully predict discomfort compared to subject studies.<sup>4</sup> The most common shading control systems by far are, again, illuminance or irradiance-based. A description of two such control algorithms is located in Section 2.4.1. Essentially, users deploy window shades in the presence of direct sunlight on horizontal working planes, but there are also more causes of visual discomfort than direct sunlight alone. Studies have found that exterior vertical illuminances between 40,000 and 50,000 lx typically lead to shade closure (Reinhart & Voss 2003; Sutter et al. 2006). Other studies have found that no more than 10% of the view should exceed 2000 cd/m<sup>2</sup> (Van Den Wymelenberg et al. 2010) or that mean window luminance values should not exceed 3200 cd/m<sup>2</sup> (Sutter et al. 2006).

#### 2.6.4 Luminance Ratios

One commonly used luminance-based design metric is that of maximum luminous ratios, which was not discussed previously because of its lack of any human or perception-based rationale. Current recommendations from the IESNA (DiLaura et al. 2011) suggest that luminance ratios should not exceed the below list,

- 1:3      Between task and adjacent light-colored surroundings
- 3:1      Between task and adjacent dark-colored surroundings
- 1:10     Between task and distant light-colored surfaces
- 10:1     Between task and distant dark-colored surfaces
- 20:1     Between daylight admitting surfaces and adjacent surfaces

These are obviously established with the noble goal of preventing contrast-based glare.<sup>5</sup> However, Van Den Wymelenberg and Inanici (2014) recently published a thorough analysis of luminance ratios and concluded that currently such ratios are not able to identify subjective reported discomfort. They also note, however, that further research may be helpful in improving these results.

---

<sup>4</sup> See Section 2.6.1.

<sup>5</sup> See Section 2.2.

## 2.7 Simulation Programs and Tools Employed

### 2.7.1 Simulation Tools

This thesis employs two primary simulation tools: Radiance and Daysim. Radiance is a physically-based backward raytracer, developed at Lawrence Berkeley National Laboratory (Ward 1994). Radiance is a reasonable choice for representing the visual, luminous environment as it includes a series of material modifiers that allow users to set up custom materials based on optical measurements and has been validated by numerous studies (Ochoa & Capeluto 2006; Reinhart & Walkenhorst 2001; Mardaljevic 1995). Daysim is a validated daylighting analysis software which predicts yearly illuminance levels by performing two raytracing operations to a sky dome consisting of 145 sky segments and 3 ground segments and another of around 65 direct solar positions (Reinhart & Walkenhorst 2001). Each sky segment is weighted relative to its illuminance contributions in the scene. In this way, illuminance can be predicted across an entire year in any incremental time step without running thousands of separate raytrace simulations directly in Radiance.

### 2.7.2 Evaluation Tools

Gen\_dgp\_profile is a program that combines fast Radiance simulations calculating direct sunlight only by using zero ambient bounces (ab) for each hour of the year with the results of a yearly Daysim illuminance simulation. This yields a simplified prediction of DGP, enhanced simplified DGP (eDGPs). Developed by Jan Wienold, eDGPs is a validated method of predicting discomfort glare across an entire year using minimal computational resources (Wienold 2009).

Evalglare is a program developed at the Fraunhofer-Institut für Solare Energiesysteme in Freiburg for the evaluation of DGP and other glare metrics from the Radiance RGBE image format and also allows the visualization of contrast-based sources of glare (Wienold 2010).

### 2.7.3 Measurement Tools

Another important tool used in this thesis is high dynamic range (HDR) photography. HDR photography records the brightness indicated in units of luminance (candela per square meter,  $\text{cd}/\text{m}^2$ ) of each pixel in a photograph and can be used to calculate discomfort glare, glare and glint hazards, and other luminance-based metrics. The method used to create such images relies upon capturing several exposures at known shutter speeds, lens apertures and exposure times. Afterwards the photos are composited and calibrated to physical values using a camera-specific calibration function based on measured luminance data with calibrated instruments. Inanici found this method to have an average error of 5.8% for outdoor scenes and 10.1% for daylight interior scenes (Inanici 2006). The resulting HDR photograph is stored in the Radiance RGBE image format, a lossless format where each pixel corresponds to a physical value (Ward 1994).

### 2.7.4 User Surveys

Besides simulating, measuring and evaluating luminance distributions, it is important to know how occupants feel about such views. To achieve this, computer-based surveys are employed asking users to describe their visual comfort and the causes of discomfort described in chapters 5 and 6 of this thesis.



## Chapter 3

# Examination of Discomfort Glare Metrics

With modern buildings' increased use of glazing, the interest in and need to quantify and avoid discomfort glare have increased in tandem. Historically, there have been more than half a dozen separate attempts to quantitatively predict glare, each developed under varying experimental circumstances and for different purposes. Thus far, there have been only very limited attempts to directly compare predictions from these metrics and to define their ranges of applicability. As a result, it is currently difficult for a designer to decide which glare metric to use, if any. For example, green building rating systems, such as the US Green Building Council's LEED system, avoid the application of glare indices altogether (USGBC 2009). The only widely implemented glare prevention strategy is to generally keep direct sunlight away from vertical task planes such as computer monitors and horizontal task planes such as desks. This recommendation mainly addresses disability and veiling glare. In order to avoid discomfort within the field of view, a frequently quoted rule is to avoid luminance ratios larger than 1:3 and 3:1 between the work surface and the near visual field and 1:10 and 10:1 in the far visual field.<sup>5</sup> These recommendations are not based on any human subject studies, and there is a general attitude within the design community that they are too stringent for daylight spaces, and thus are applicable only for electrically lit environments.<sup>6</sup> Thereby one is left wondering whether the design community should begin adopting more sophisticated glare analysis methods.<sup>7</sup>

The increased use of three-dimensional digital models during building design combined with enhanced availability and usability of validated, physically-based daylight simulation engines (Reinhart & Breton 2009) means many architectural design teams now have access to

---

<sup>6</sup> See Chapter 2 for a more complete description of the subjects in this paragraph.

<sup>7</sup> The work presented in this chapter was originally published as,

Jakubiec, J. & Reinhart, C., 2012. The "adaptive zone" - A concept for assessing discomfort glare throughout daylight spaces. *Lighting Research and Technology*, 44(2), pp.149-170.

high dynamic range visualizations of existing and unbuilt spaces. One of the uses of these visualizations is to assess the likelihood of glare in spaces using the glare indices detailed in Section 2.2. In fact, the Radiance backward raytracer has supported this functionality since 1993 using the ‘findglare’ program (Larson & Shakespeare 1998). Varied discomfort glare metrics have been integrated into other simulation tools as well such as EnergyPlus (EnergyPlus Development Team 2012), Daysim (Reinhart 2010), and AGi32 (Lighting Analysts, Inc. 2014). However, as noted in Chapter 2, this functionality is rarely used by practitioners, likely due to a confusing number of competing metrics and little advice as to how and for what types of spaces these metrics should be investigated. Therefore it is worthwhile to understand the meaning and reliability of discomfort glare analyses in order to confidently apply the results to design projects.

On a practical level, a second barrier towards the use of glare metrics in building design is that glare depends not only on the current sky condition but also on the position and view direction of an observer in a space, i.e. on a sunny day one might experience severe glare facing a window but be perfectly comfortable facing towards the interior. A second example is that changing a seating position might obscure a luminance source, which would otherwise cause glare. In order to introduce glare into rating systems, it is hence desirable to summarize the overall glare sensation spatially and over the course of a year.

This chapter is therefore an attempt to make recommendations for determining the probability of discomfort glare in daylit spaces based upon simulations or real-world interior scenes. In examining the current state of various glare simulation processes and metrics predictions from five glare indices<sup>8</sup> are compared: Daylight Glare Index (DGI), CIE Glare Index (CGI), Visual Comfort Probability (VCP), Unified Glare Rating (UGR), and Daylight Glare Probability (DGP). The methodology section describes a large parametric simulation effort to evaluate predictions of these glare metrics in three daylit scenes. By analyzing glare for multiple view-directions and locations, a visualization of spatial comfort analysis which has the capacity to support design decisions is created. The discussion makes specific recommendations of which metrics are useful under varying daylit and spatial circumstances.

### 3.1 Chosen Glare Metrics

In Section 2.2, six discomfort glare metrics are described. Five of these six are compared in this chapter.  $DGI_N$  was not considered due to the geometric complexity involved in its calculation and its lack of significant validation studies (Nazzal 2001; Nazzal et al. 2005).

### 3.2 Methodology

Two differing spaces were analyzed for discomfort glare probability: a sidelit office with an exposed South-facing window and a large, open plan space lit primarily by East-facing clerestory windows. The open plan space is based on Gund Hall, the home building of the Harvard Graduate School of Design. The two spaces were chosen with the intent of observing the applicability of glare metrics in differing spatial conditions; however, it is worth stating that no glare metric has been developed under open plan spaces nor clerestory window lighting. The exact dimensions and locations of view in the two spaces can be seen in Figures 3.1 and 3.2. An

---

<sup>8</sup> See Section 2.2.

additional set of calculations were run of the sidelit office space with typical venetian blinds, the geometric properties of which are summarized in Figure 3.3. Both spaces are located in Boston, Massachusetts (42.37°N, 71.02° W).

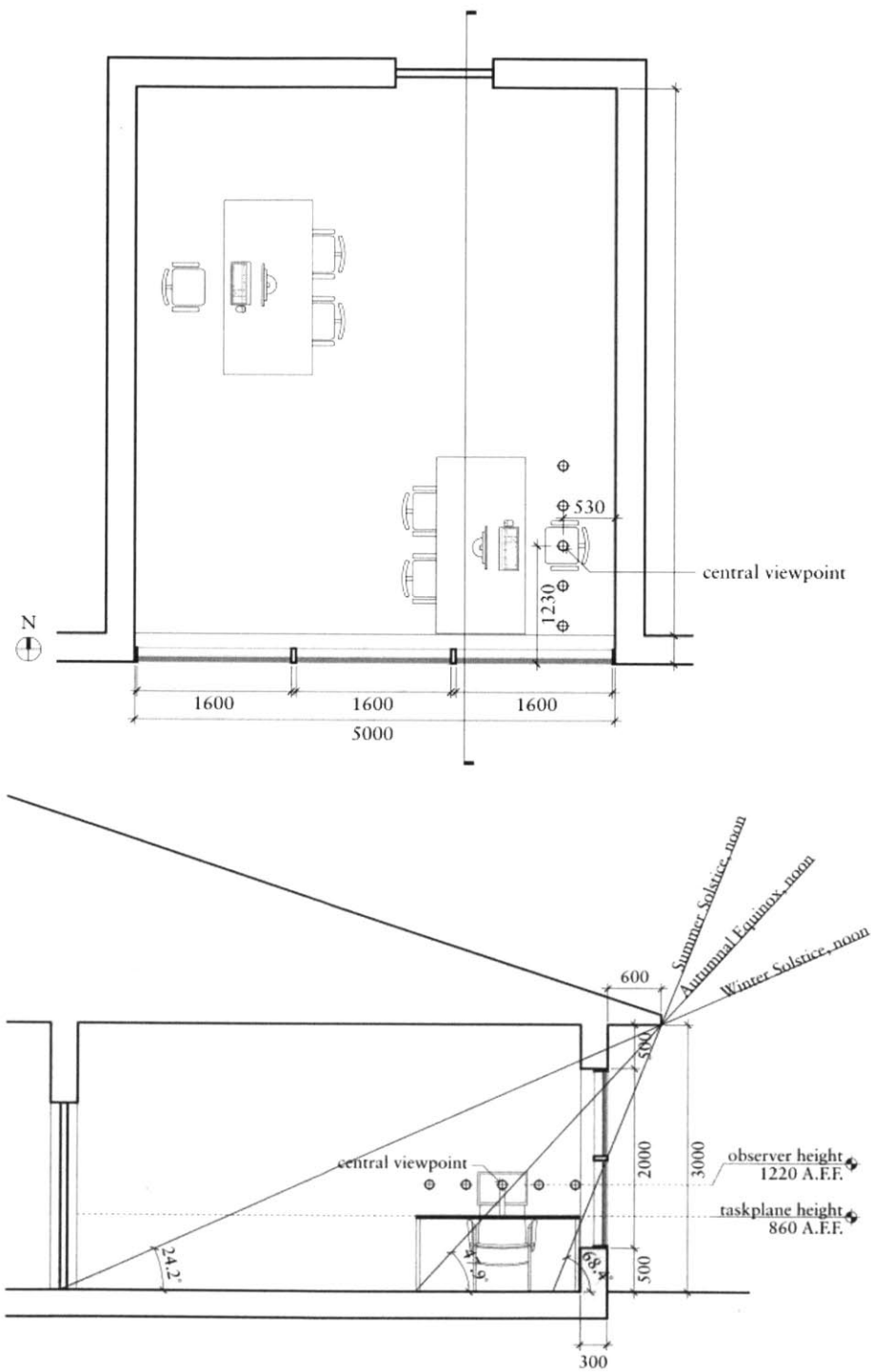


**Figure 3.1** Sidelit space geometric properties in plan and section. The sidelit space has one window on the South side, while the occupant faces west.



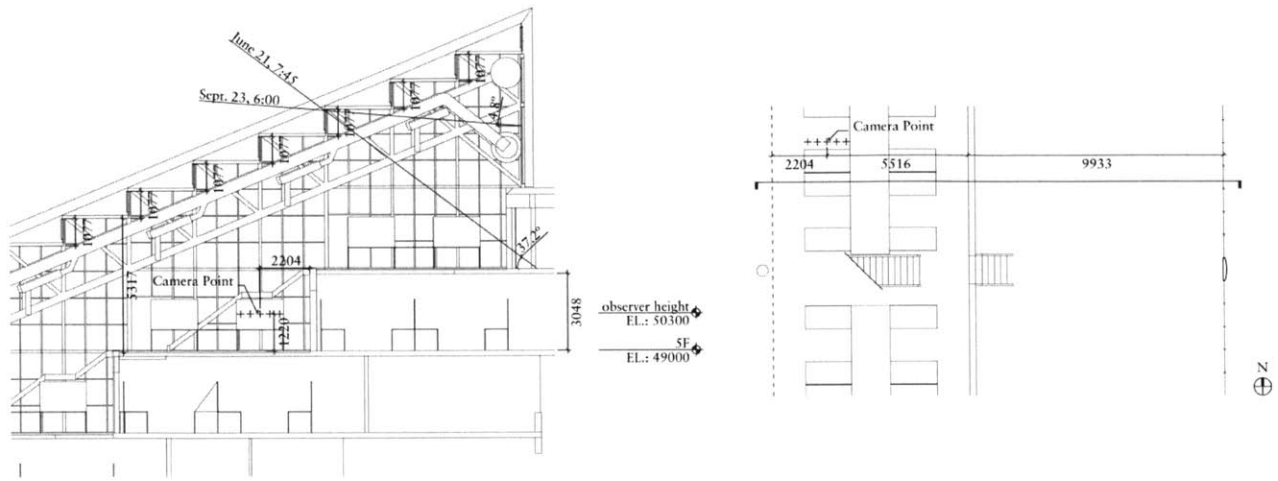


**Figure 3.2** Gund Hall geometric properties in plan and section. The desk faces south.

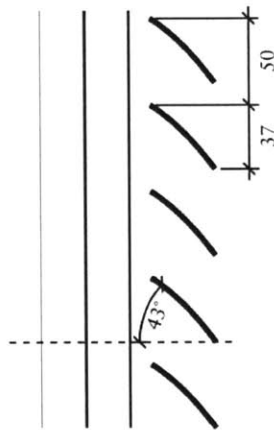


**Figure 3.3** Venetian blind geometric properties in section.

High dynamic range luminance images were generated using the validated Radiance backward raytracer in 15 minute time intervals for three discrete days during the year: the Winter and Summer solstices occurring on December 21 and June 21 respectively and the Autumnal equinox occurring on September 23. For all three days, simulations were run between the hours of 9am and 9pm local time. Each of the 48 resulting sky conditions was generated by the gensky Radiance program utilizing the CIE clear sky model with sun ('+s' option in gensky) (Commission Internationale de l'Eclairage 1996). The CIE clear sky was chosen because building occupants are likely to experience discomfort from direct sunlight in modern spaces with large window-to-wall ratios. In order to consider spatial discomfort, for each sky condition and space, 360 degrees of rotational views were simulated in three degree rotational increments centered about five separate viewpoints, giving the user a degree of rotational and positional freedom. The locations of these viewpoints are illustrated by points in Figures 3.1 and 3.2 above for each space. Each luminance image was then used in the calculation of five discomfort glare metrics: DGI, CGI, UGR, VCP and DGP. Glare analysis of the resultant images was performed



using the Evalglare program (Wienold 2010). Glare sources,  $L_s$  in Equations 2.1-2.7, were identified as any pixel which exceeds five times the mean image luminance. It should be noted that the evaluation of DGP by the Evalglare program was only valid for vertical eye illuminances greater than or equal to 380 lx at the time of this study; however, its functionality in low-light conditions has since been enhanced (Wienold 2012). The material properties and Radiance parameters used in the simulations are detailed in Table 3.1 below.

**Table 3.1** Radiance simulation parameters and material properties utilized in simulations.

Radiance Simulation Parameters		Material Properties	
Ambient bounces (ab)	6	Floors	20% Diffuse Reflectance
Ambient accuracy (aa)	0.15	Walls	50% Diffuse Reflectance
Ambient divisions (ad)	3000	Ceilings	80% Diffuse Reflectance
Ambient super-samples (as)	16	Desk Surfaces	50% Diffuse Reflectance
Ambient resolution (ar)	93	Outside Ground	20% Diffuse Reflectance
		Glazing	72% Transmittance

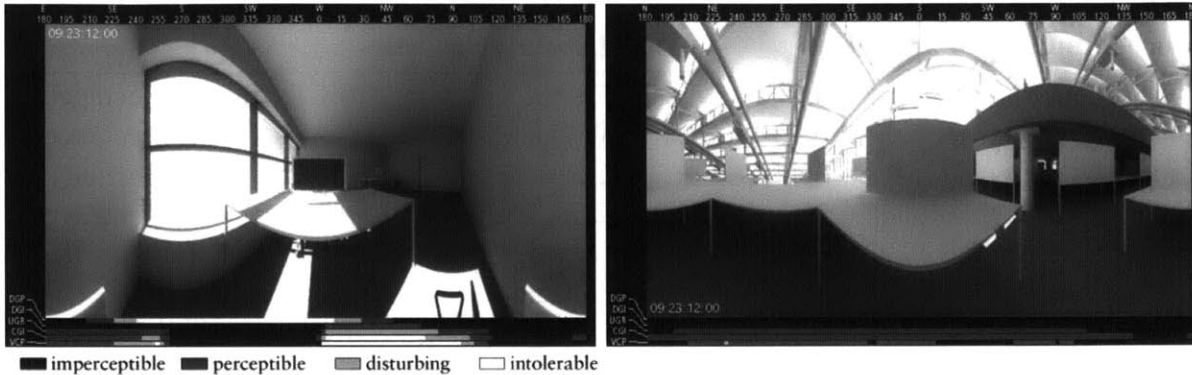
In order to directly visually compare the results from the various glare metrics, DGI, UGR, VCP and CGI results were normalized to a range between 0 and 1 where 0 corresponds to no likelihood of discomfort and 1 corresponds to 100 percent probability. DGP already evaluates in a range between 0.16 and 1, so no normalization was necessary in that case. DGI was multiplied by a factor of 0.01452, UGR and CGI were multiplied by 0.01607, and VCP was normalized by subtracting its value divided by 100 from 1. The multipliers used in normalization for CGI, UGR and DGI were chosen to correlate the intolerable value ranges with those defined by the DGP metric. Table 3.2 shows the value ranges in which glare is considered to be ‘imperceptible,’ ‘perceptible,’ ‘disturbing’ and ‘intolerable’ for the different metrics.

**Table 3.2** Glare prediction value–color assignments used in all visualizations.

Discomfort classification	Glare value ranges				
	DGP	DGI	UGR	CGI	VCP
Imperceptible (black)	< 0.35	< 18	< 13	< 13	80 – 100
Perceptible (dark grey)	0.35 – 0.4	18 – 24	13 – 22	13 – 22	60 – 80
Disturbing (light grey)	0.40 – 0.45	24 – 31	22 – 28	22 – 28	40 – 60
Intolerable (white)	> 0.45	> 31	> 28	> 28	< 40

A series of time lapse animations was produced from this dataset in 15 minute intervals, mapping the probability of experiencing glare as defined by each metric in relationship to a 360 degree cylindrical projection from the middle viewpoint of the five view positions. In this way, lighting conditions can be visually correlated to the probability of experiencing discomfort glare in many directions of view in an easily understandable format. Figure 3.4 shows two typical frames from the output. Falsecolor evaluations of glare metrics are displayed across the bottom of each image with degrees rotation from the center of the view and the corresponding cardinal directions shown at the top. Each frame has a time stamp applied in the format of month : day : hour : minute. For example, in Figure 3.4 both scenes were rendered on September 23<sup>rd</sup> at noon

under CIE clear sky conditions. The DGP color-coding for the sidelit office space (3.4a) is white, intolerable, for a user facing either straight west (towards the center of the visualization) or towards the window (south to southwest 240 to 330 degrees). DGI does not predict significant glare for any orientation whereas the other metrics also predict glare for the occupant facing west to northwest. There is no ‘disturbing’ or ‘intolerable’ glare predicted by any metric for Gund Hall at that selected timestep (3.4b).



(a) sidelit office space, facing West (b) Gund Hall, fifth floor, facing South

**Figure 3.4** View-direction dependent glare evaluations on September 23 at noon. The greyscale bars across the bottom of each image illustrate predicted levels of discomfort glare in the indicated orientation for each analyzed metric.

While it is not possible to publish the full animation results in this format, they are available in color online from the following URL,  
<http://www.gsd.harvard.edu/research/gdsquare/GlareRecommendationsForPractice.html>

### 3.3 Results

Figure 3.6 illustrates results normalized to a range between zero and one as previously explained for the primary viewing angle (center of the visualization) and occupant position for each sky condition simulated. Simulation results from September 23 were chosen for further analysis, because a variety of lighting conditions in the three model spaces were observed as detailed in Table 3. Areas of interest on September 23rd are marked with vertical dashed lines which will be analyzed in further detail with regards to view rotation and predicted glare reduction. Figure 3.5 shows typical hemispheric images of the type used in glare evaluation for the three scenes at noon on September 23rd.

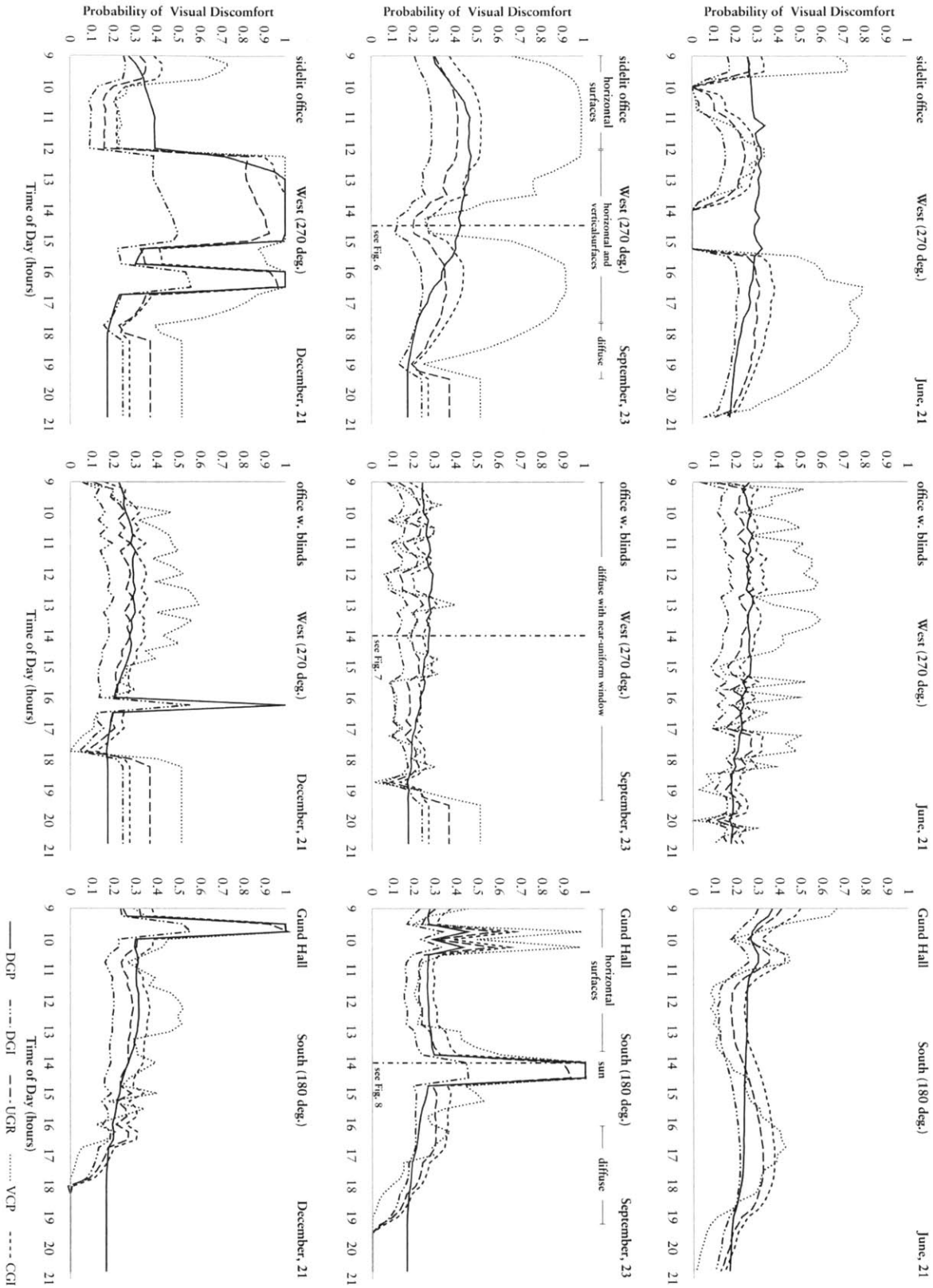


**Figure 3.6** Discomfort glare probabilities for three spatial conditions on July 21, September 23 and December 21.

**Table 3.3** Lighting conditions observed in simulation models on September 23.

Simulation model	Lighting conditions and time ranges observed		
sidelit office space	light falling on horizontal surfaces	light falling on horizontal and vertical surfaces	diffuse light from windows with visible sky
	9:00 - 12:00 local time	12:15 - 17:30 local time	17:45 - 19:15 local time
sidelit office space w. blinds	window as near-uniform diffuse light source		
		9:00 - 19:15 local time	
Gund Hall	light falling on horizontal surfaces	sun directly visible	diffuse light from clerestory and south windows
	9:00 - 13:45 local time	14:00 - 14:30 local time	16:00 - 19:15 local time

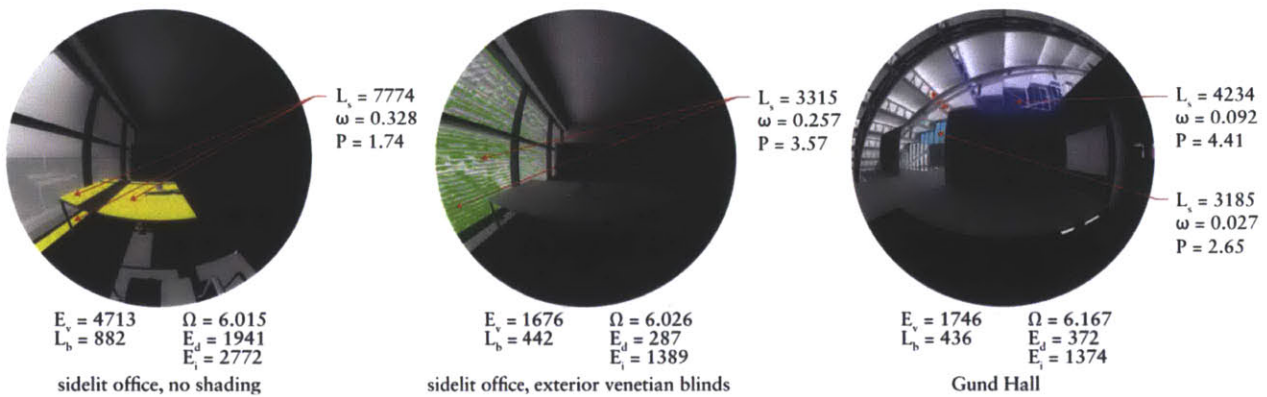


**Figure 3.5** Sample hemispheric views used in glare metric calculations at noon on September 23 with glare sources and associated values identified by Evalglare.

The direct comparison of the different glare indices over the course of a day in Figure 3.6 shows that VCP, which is derived for glare originating from electric, typically-sized, ceiling-mounted light sources, often predicts discomfort probabilities much higher than that of the other metrics regardless of whether they were developed for use under electrically lit or daylight conditions. DGI, UGR and CGI correlate strongly, differing most often in their relative intensities. In general it was found in nearly all test cases, during times when the space is daylight, that CGI predicts the highest likelihood of discomfort between the three similarly defined metrics. DGI predicts the lowest values of the three metrics due to its use of a percentage of the source luminance in its denominator. DGP typically evaluates within the upper and lower bounds that DGI, UGR and CGI establish for most lighting conditions for the three simulated days. DGP in general is less sensitive to changes in contrast; this makes sense as its formula is based on two parts which evaluate contrast and total vertical eye illuminance.<sup>9</sup> However, an analysis of these results spatially using many view directions is warranted for further study as the evaluation discomfort glare is affected strongly by view within a space.

When direct sunlight is present in the scene and the visible sky from the window is very bright, DGP performs better than other existing metrics, predicting a much higher likelihood of discomfort glare. This is the case between 13:15 and 15:15 local time in the sidelit office model with no exterior shading on September and June 21. Under this condition, DGI, UGR, VCP and CGI all predict no likelihood of glare for most view directions when large solid angle luminance

<sup>9</sup> See Section 2.2.6.

sources are in the field of view. Due to DGP's consideration of total vertical eye illuminance as one factor in determining glare, it predicts discomfort when significant contrast does not exist, but excessive luminance is present in the field of view which peaks at around 12000 cd/m<sup>2</sup>. For the central field of view at 0 degrees rotation, 4515 lx falls upon the eye. In this case, DGP's prediction is likely reliable as bright, direct sunlight is generally associated with glare. The discrepancy in prediction with other metrics probably occurs due their purely contrast-based nature. The combined brightness of the window and direct sunlight saturate large portions of the scene except when facing between 30–150 degrees; therefore, significant contrast only exists peripherally in the least-bright directions. This phenomenon is illustrated in Figure 3.7.

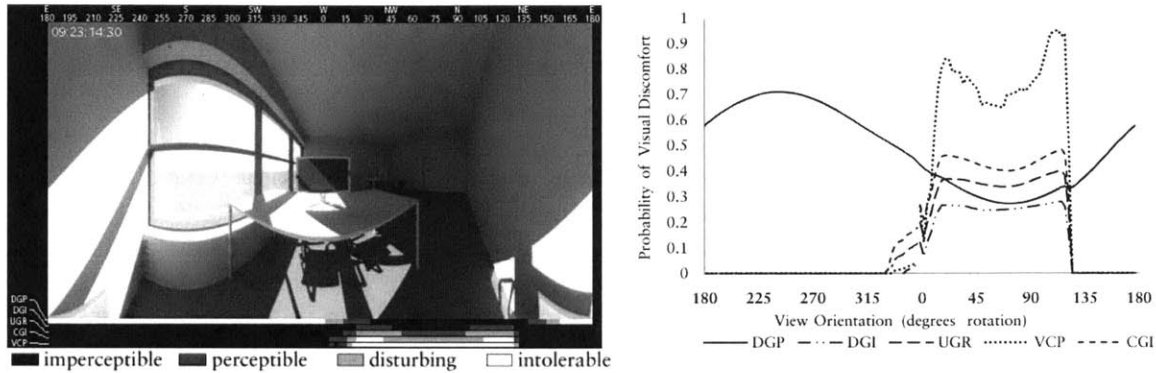


**Figure 3.7** Discomfort glare predictions on September 23rd, 14:30 local time in the sidelit office space.

All metrics appear to make reasonable predictions for the sidelit office space with exterior venetian blinds as long as direct sunlight is prevented from entering the space as is the case in Figure 3.8. This is expected as DGI, UGR and CGI were developed under presumed conditions of uniformly diffuse windows, although VCP also performs similarly in this lighting scenario. One concern is that the results for venetian blinds experience some seemingly random turbulence. This is most likely due to the ambient accuracy (aa) Radiance simulation parameter used being slightly too high for the complex geometry of the blinds and the ambient divisions (ad) being slightly too low; however, the results should still be reasonably valid as the blinds have no specular material component. In this case, DGP predicts perceptible to disturbing levels of discomfort glare (~0.35 – 0.40) when facing the area of bright luminance where the venetian blinds are present due to its evaluation of vertical eye illuminance; however, only VCP predicts significant glare under such lighting conditions.



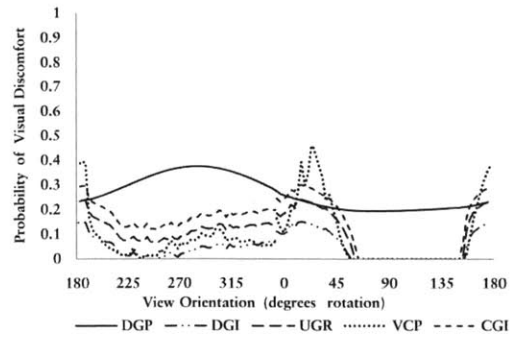
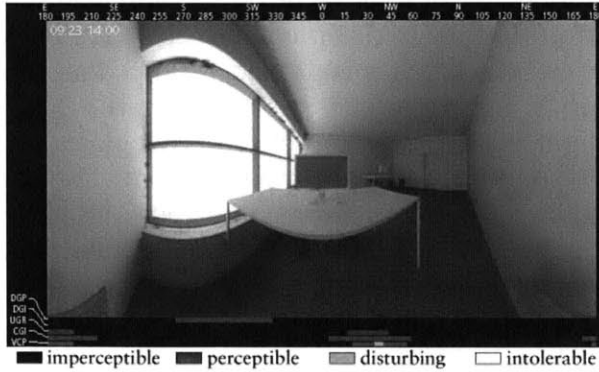


**Figure 3.8** Discomfort glare predictions on September 23rd, 14:00 local time in the sidelit office space with venetian blinds.

The chosen desk location in Gund Hall, with the large partition blocking the Southern view, does not typically experience much direct sunlight on the desk surface. VCP presents results that appear reasonable under these circumstances, though predicted discomfort increases rapidly when the sky behind the large, South-facing window is particularly bright or a glare source (the sun) is located proximate to the center of view (a low Guth position index<sup>10</sup> value) as seen in Figure 3.9. DGI reports comparably low glare probabilities even when the sun is directly visible, a serious weakness for a metric meant for daylight but not unexpected as it was developed under diffuse sky conditions and has a percentage of the source luminance in its denominator. When the sun is not directly visible, DGP, DGI, UGR and CGI correlate strongly, differing primarily in magnitude.

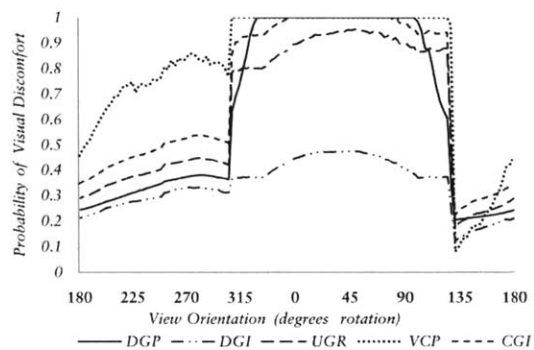
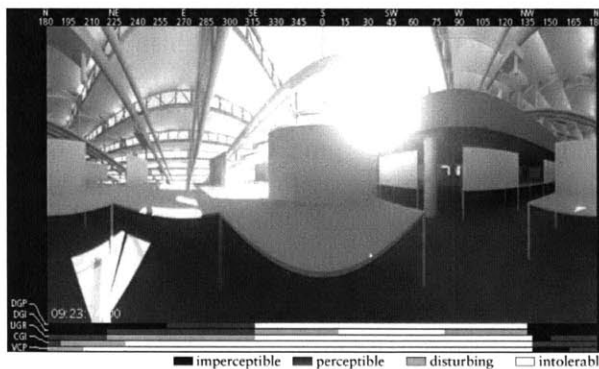


**Figure 3.9** Discomfort glare predictions on September 23rd, 14:00 local time in Gund Hall. The sun is in the direct line of sight of the observer

<sup>10</sup> See Section 2.1.

## 3.4 Discussion

### 3.4.1 *Appropriate Use of Metrics*

Based on the results from the previous section, the following use of the glare metrics investigated is recommended. As noted, computational evaluation produces very similar data for the Daylight Glare Index (DGI), CIE Glare Index (CGI) and Unified Glare Rating (UGR). These are useful and valid only under conditions where direct sunlight will not enter the space and where the window can be considered as a medium-sized source of contrast-based glare; however, CGI is the most robust of the three metrics as it consistently predicts a higher likelihood of discomfort, thereby representing a worst-case comfort scenario. As  $DGI_N$  requires geometrically complex information and has had no conclusive user validation studies performed, its use, at this time, is not recommended; an ideal design analysis workflow is to calculate glare probability from a high definition luminance image without associated geometric and outside sensor data.<sup>11</sup> Under daylight conditions, VCP produces values least in line with other metrics. As VCP was developed only for very specific, artificially-lit circumstances, its use is not recommended for daylight scenes. While the five studied discomfort glare metrics may be useful under some lighting conditions, the results have shown that they are not applicable under every lighting circumstance that occurred in the simulations (Table 3.3). In this regard, DGP was found to be the most robust glare metric. DGP responds predictably to most simulated daylight scenes including those with many or large solid angle direct or specular luminance sources. For this reason, the running of iterative time-step simulations with direct solar ray casting can be achieved and compared with less chance of unreliable or questionable results when using DGP.

### 3.4.2 *Interpreting Glare Predictions*

The simulation results have shown that cylindrical image projections overlaid with a view direction dependent glare evaluation are an effective way to visually represent the directionality and spatiality of discomfort glare in a single image. These new type of images probably constitute a useful diagram for use in design as they show the perception of discomfort glare under daylight conditions throughout a space in relation to occupant orientation. When compiled as an animation that loops over one or several days of the year, this information helps designers to quickly understand the glare situation within a space over time and in varied directions at least under clear sky conditions.

A limitation of this approach is that it does not take actual climate data into account as, for example in the Boston climate, clear sky conditions in December might be rare. Another limitation is the difficulty in correlating visual comfort data to the illuminance availability in a space as the former is perceptual and view dependent while the latter is a measured minimum distribution of light in a space (Ochoa & Capeluto 2006).

## 3.5 Conclusion

This comprehensive study of popular discomfort glare metrics clarifies which are meaningful for architectural design and under what conditions they remain reasonable predictors of comfort. Such information should clear the air of ambiguities surrounding glare metrics and allow them to be used as a design parameter for buildings. Experimental results in three spaces utilizing individual Radiance simulations for many sky conditions in each space showed that

---

<sup>11</sup> See Section 2.2.2.

DGP, daylight glare probability, is the most robust of the five tested metrics and least prone to produce misleading or inaccurate glare predictions under a wide variety of analyzed daylight conditions. It seems sensible at this time to recommend the use of DGP to quantitatively predict discomfort glare in daylight scenes during design and afterwards using HDR photography (Inanici 2006). The newly created cylindrical images with glare prediction data overlaid are an effective tool for design and presentation, illustrating lighting quality, spatial distribution, and comfort in one image. As rendering is already a key element in the architectural design process, generating a set of these images lends additional value beyond environmental simulation such as for daylight animations and client presentations.

Several questions are also raised by these new cylindrical image types. For example, how do space occupants react when there is glare in one viewing direction but not in another? Chapter 4 continues this line of thought brought on by spatializing visual comfort predictions through investigating what it means for design and behavior in daylight spaces.







## Chapter 4

# An Adaptive Visual Comfort Model – The ‘Adaptive Zone’

Chapter 4 continues analysis of the dataset generated in the previous chapter. One aspect that required further inquiry is how a designer should actually interpret the result that an occupant might experience glare at a certain point in time when facing in one direction but not if facing in another, i.e. is the glare at a particular location in a building acceptable if an occupant is likely to experience severe glare looking in one direction and less or no glare facing another direction? The answer depends on the space type, furniture layout and culture of a space. A typical response to visual discomfort from the students in Gund Hall is to change their viewing position as to obscure the glare source or move it further from the center of view. The design students who inhabit the space also often construct their own makeshift shading devices which further serve to illustrate how important user interaction and behavior can be in determining visual comfort.

The new concept of an ‘adaptive zone’ is proposed within which an occupant can change position and view direction in order to adapt to the visual environment for a particular workplace and minimize the occurrence of glare.<sup>12</sup> In the sidelit space from Figure 3.7 with a simple rectangular desk, the range of such an ‘adaptive zone’ would be from about 315 to 45 degrees, a +/-45 degree rotational freedom while also allowing an occupant to move his or her chair about 0.75m to the left or right. This concept is shown in Figure 4.1. Assuming that an occupant is going to select the least visually disruptive position within the adaptive zone, the designer may pick for each time step the lowest glare prediction in either of these directions (or positions if applicable). The key advantage of this interpretation is that glare relative to occupant orientation

---

<sup>12</sup> The work presented in this chapter was originally published as, Jakubiec, J. & Reinhart, C., 2012. The “adaptive zone” - A concept for assessing discomfort glare throughout daylight spaces. *Lighting Research and Technology*, 44(2), pp.149–170.

and position can be considered by a single number for each moment in time. The resulting reduced daily glare profile,  $DGP_{\text{adaptive}}$ , is shown in Figure 4.2 on September 23rd plotted against the original fixed view glare results (DGP). In the case of the sidelit office, the fixed-view DGP profile results mostly in intolerable discomfort glare for the occupant; however, adapting allows the occupant to avoid any significant discomfort. The same results can be seen in Gund Hall where the occupant is successfully able to avoid a direct view of the sun within the adaptive zone between 13:45 and 14:45.

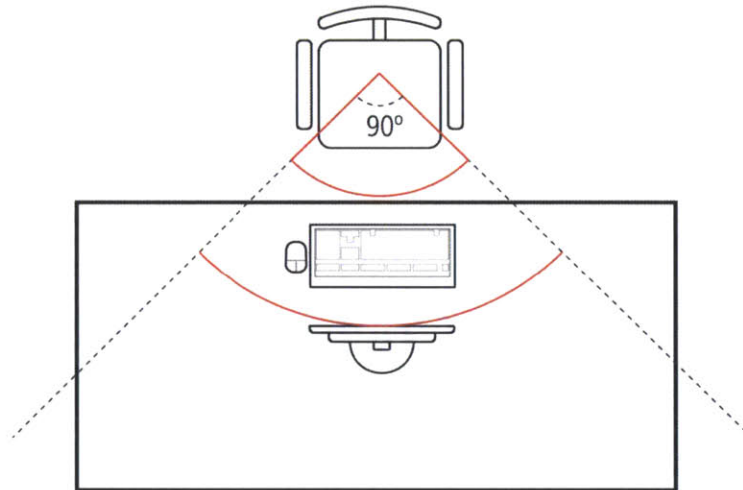


**Figure 4.1** Illustration of the adaptive zone concept where a user can change their view orientation by +/- 45 degrees.

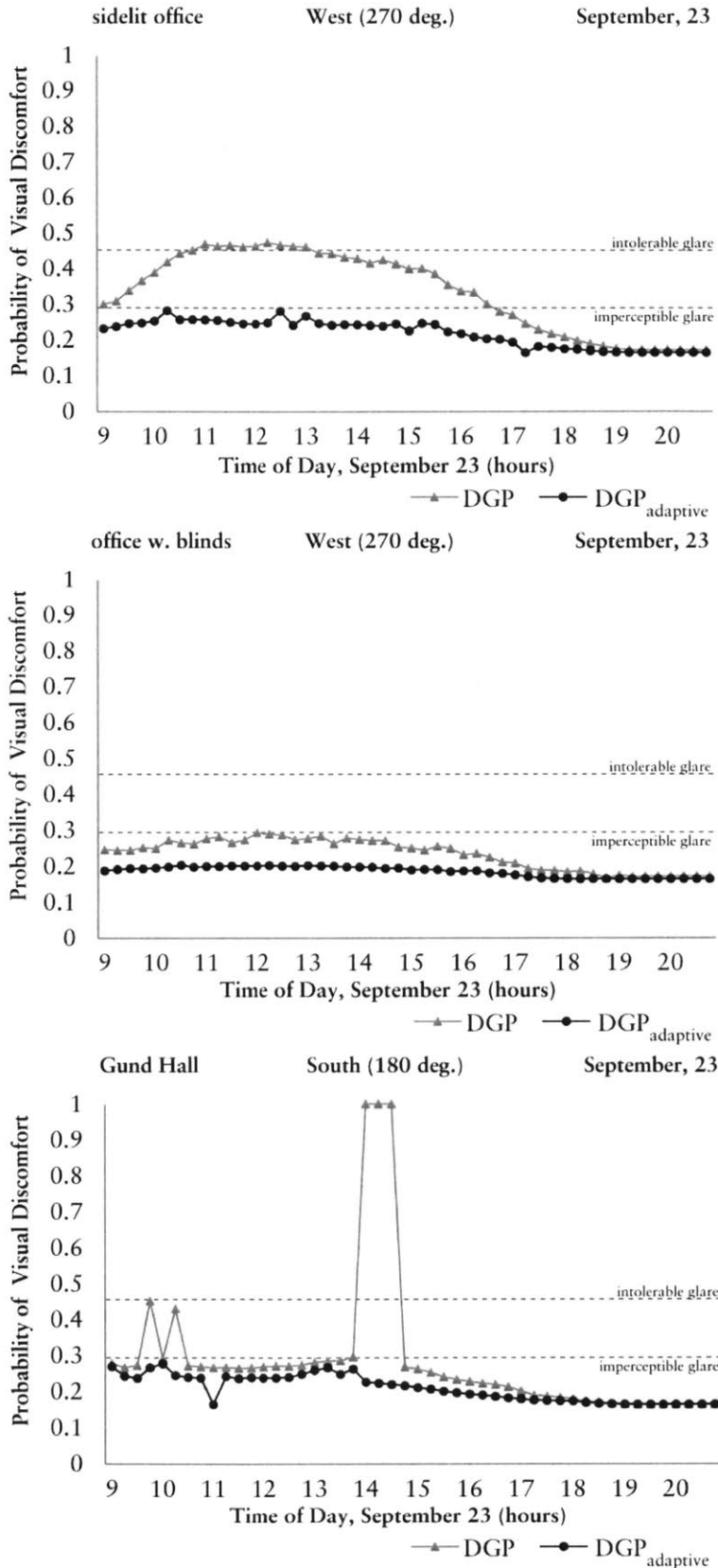


**Figure 4.2** DGP and DGP<sub>adaptive</sub> timelapse plots for three simulated spaces on September 23rd.

What is the effect of allowing occupants to adjust their orientation within a certain range? Allowing occupants to avoid glare obviously reduces the predicted glare. The larger the adaptive zone, the greater on average will be this reduction. Table 4.1 shows the mean and maximum reduction of predicted glare for all 144 simulated sky conditions across the three simulated days in all seating positions and for various degrees of rotational freedom with respect to an occupant that is only allowed to face forward from a central, fixed position as the reference value.

The mean and maximum values were taken from the rotational ranges of +/- 15, +/- 30, +/- 45, +/- 90, and +/- 180 degrees across the five seating positions. For the typical, sidelit space it becomes apparent that giving occupants, via furniture layout, the ability to adjust themselves substantially reduces predicted glare within a space. For DGP this amounts to a mean reduction of 14% in the case of a workplace which allows the rotation from -45 to +45 degrees from the center. As the difference between the tolerance for 'perceptible' and 'intolerable' glare in the DGP metric is only 10%, a 14% reduction in predicted discomfort glare is significant. Maximum glare reduction probabilities show that simple changes in view position and orientation can have even larger user comfort effects. The reductions for the sidelit space with blinds and the Gund Hall workspace are smaller, because the glare indices are lower in these situations than for the sidelit office without blinds. Table 4.1 is therefore an effective argument to providing occupants with flexible workspace options. A caveat within this analysis is that computer monitors tend to be fixed in most workspaces. Unless the occupants work on laptops, it is necessary that they are able to move their chairs or monitors in order to adjust their view.

**Table 4.1** Yearly mean and maximum discomfort glare reduction probability with user freedom of adaptation. Simulated users were allowed to move their chairs in front of desks and given degrees of rotational freedom from 15 to 180 degrees in order to reduce discomfort.

Simulated Space Result		User Rotational Freedom				
		+/- 15	+/- 30	+/- 45	+/- 90	+/- 180
sidelit office	mean reduction	0.11	0.13	0.14	0.16	0.16
	maximum reduction	0.77	0.78	0.79	0.79	0.79
sidelit office w. venetian blinds	mean reduction	0.04	0.05	0.05	0.06	0.06
	maximum reduction	0.82	0.82	0.82	0.82	0.82
Gund Hall	mean reduction	0.04	0.05	0.05	0.06	0.07
	maximum reduction	0.76	0.77	0.78	0.80	0.81

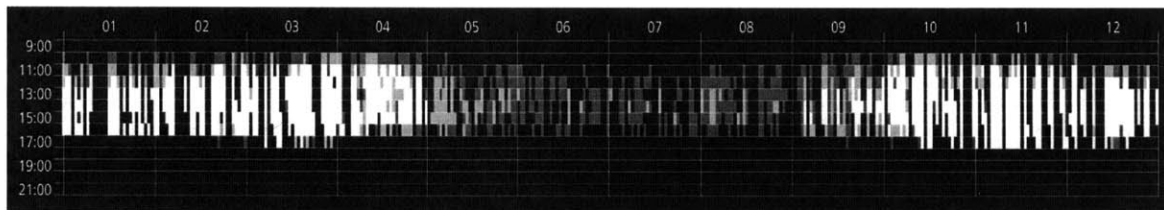
#### 4.1 Yearly Hour-by-hour Discomfort Glare Simulation with Daysim and Enhanced Simplified DGP

As mentioned above, the forgoing glare analysis did not take actual climate data into account but assumed clear sky conditions throughout the year. Advances in daylight simulations have allowed hour-by-hour illuminance predictions across an entire year based on typical meteorological year weather data. One program that enables such predictions is Daysim.<sup>13</sup> Daysim can calculate vertical eye illuminance across an entire year in any incremental time step without running thousands of separate raytrace simulations directly in Radiance (Walkenhorst et

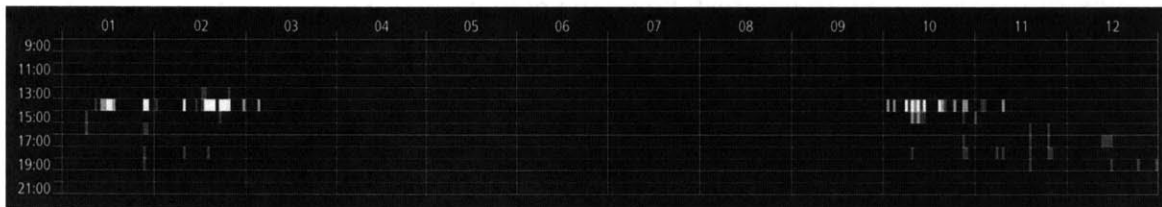
<sup>13</sup> See Section 2.7.1 for greater details on the capabilities and validity of Daysim.

al. 2002). Because DGP is defined by a two-part formula of total vertical eye illuminance and contrast, one-half of the formula can be satisfied by data generated from Daysim alone. By combining fast Radiance simulations showing direct sunlight only by using zero ambient bounces (ab) for each hour of the year with the results of a yearly Daysim illuminance simulation, enhanced simplified DGP (eDGPs) is a validated method of predicting glare across an entire year using minimal computational resources (Wienold 2009).

The enhanced simplified DGP method was used to predict discomfort glare in the sidelit office space from Chapter 3, and the results were visualized using a falsecolor temporal map between the hours of 9:00 to 21:00 for each day of the year. On the temporal map, the vertical axis describes the time of day, whereas the horizontal axis corresponds to the day of the year. The color scale corresponds to the same values as defined in Table 3.2. eDGPs simulations (155 total) were run in three degree rotational increments for each of five seating positions to cover a visual range of plus or minus 45 degrees rotation as in earlier non-dynamic simulation methods. Visually comparing the results of a simulation without (4.3a) and with adaptation (4.3b) dramatically underscores the potential importance of office furniture, flexibility and user behavior in the use of a daylit spaces as seen in Figure 4.3. For the adaptive DGP predictions, glare basically ceases to be a problem in the sidelit space from March to September. Table 4.2 contains the percentage of annual occupied hours when discomfort is predicted using DGP<sub>adaptive</sub> versus DGP.



(a) Annual DGP distribution, fixed view facing forward only



(b) Annual adaptive DGP distribution (+/- 45 degrees rotational freedom)

■ imperceptible ■ perceptible ■ disturbing □ intolerable

**Figure 4.3** Falsecolor visualizations of yearly glare predictions for the sidelit office space. The horizontal axis indicates the day with the numbers across the top representing the twelve months. The vertical axis illustrates the time of day each prediction was experienced.

**Table 4.2** Yearly percentage of predicted discomfort glare during occupied hours for the sidelit office space.

Metric	Percent of Occupied Hours			
	Imperceptible	Perceptible	Disturbing	Intolerable
DGP	70.1 %	9.3%	5.2%	15.4%
DGP <sub>adaptive</sub>	98.4%	0.9%	0.3%	0.4%

## 4.2 Considering User Blind Behavior

Glare predictions can be combined with an occupant behavior model in order to determine how a shading device is manually operated over the course of the year. Annual daylight glare probability predictions have already been used for this purpose as an extension to the Lightswitch behavioral model (Reinhart 2004). The Lightswitch model supports two types of users, an active user who opens the blinds in the morning and after a lunch break and closes them either when direct sunlight is incident on the workplace or the predicted DGP becomes intolerable (greater than 0.45) and a passive user who leaves blinds closed for days on end (Wienold 2007; Rubin et al. 1978; Lindsay & Littlefair 1992). The setting of the venetian blinds throughout the year has an obvious effect on both the glare experienced by the occupant, the amount of daylight available and electric lighting use within a space.

As freedom of rotation and seating position is introduced, the blinds are lowered less often as the occupant manages to avoid glare; however, this model operates under the assumption that the benefits of view are greater than the annoyance of changing position, and some users may opt to close blinds even in the presence of a flexible workspace. The effect of the behavioral model is shown in Figure 4.4 for the sidelit space with and without freedom of adaptation. Blinds are opened by a conscientious (active) user seated near the window each day in the morning and at a noon lunch break. If the same user experiences a DGP value of 0.45 or greater, the blinds are lowered until the end of the lunch break or until the next morning. The annual predicted illuminance resulting from this behavior model is used to determine the daylight autonomy (DA) distribution in the space at a minimum illuminance level of 500lx via Daysim simulations and the aforementioned behavior model. Daylight autonomy is the percentage of occupied hours in a year where lighting requirements can be met with daylight alone. Furthermore, the daylit areas of a space are defined as those which achieve half of the maximum DA value measured inside, indicated by the text in Figure 4.4. When blind behavior is controlled by a fixed-view DGP threshold (4.4a), the mean daylight autonomy in the space is 40.16% while the daylit area is 67.69% of the floor area. In contrast, when the prediction of  $DGP_{\text{adaptive}}$  controls blind behavior in the model (4.4b), the mean daylight autonomy is 72.01% and the daylit area 100% – a substantial difference. Notice that the daylit area using flexible workspaces and  $DGP_{\text{adaptive}}$  includes the entire room while a prediction using DGP alone leaves the rear portion of the room requiring electric lighting more often than not. The increase of the daylight autonomy and daylit area thus suggest a correlate decrease in predicted lighting energy use and internal heat gains from electric lighting (Bodart & De Herde 2002).



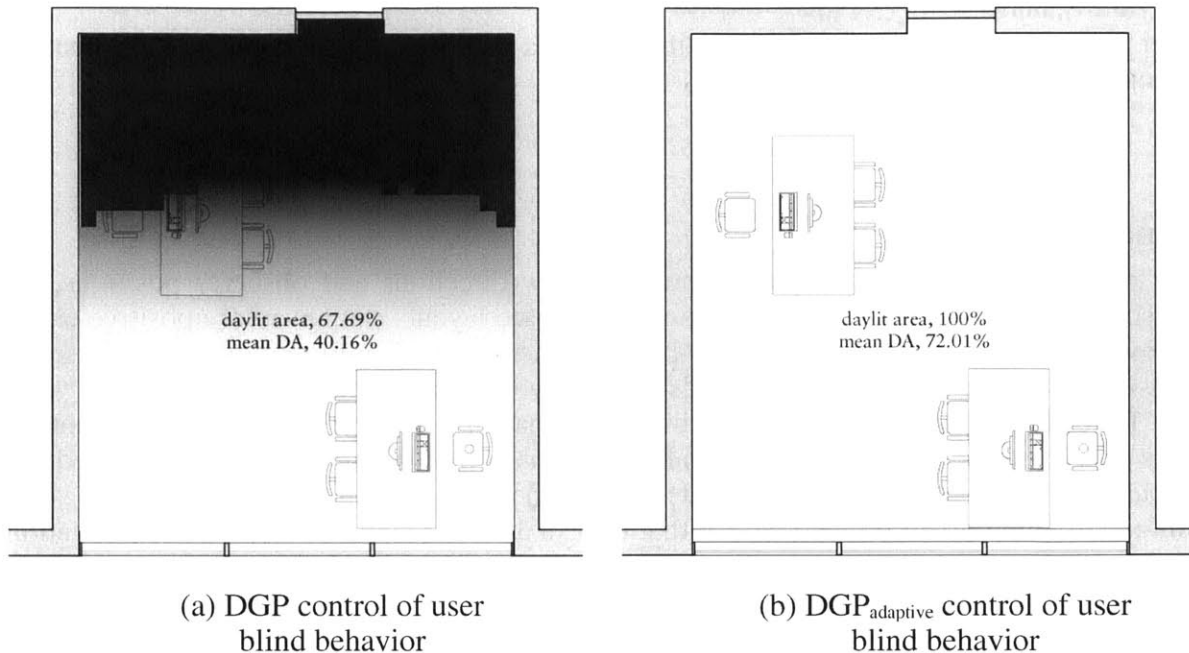


**Figure 4.4** Daylight autonomy distributions with occupant controlled blinds relative to predicted glare.

### 4.3 Required Simulation Effort

The method discussed above provides an effective way to visualize the likelihood of glare within a daylit space under selected days of the year as well as to take the effect of user adaptation into account. The latter extension of glare analysis can be directly integrated into holistic evaluations of daylight spaces concerning daylight availability, glare and energy use (Reinhart & Wienold 2011). One question that is likely on the reader’s mind now is, “how much effort is required for such an analysis?”

Increasing the simulation domain for variable user orientations versus a single orientation requires no additional simulation input from the user and minimal additional computational effort since global illumination information can be stored, maintaining associated luminance data for each lighting condition. Once an initial fisheye view had been calculated, each additional, rotational view took a fraction of the initial simulation time. The overall simulation time to generate a daily glare animation, as in Chapter 3, varies by model complexity, the number of time steps associated with that day and the number of occupant positions chosen; simulation times for one sky condition and position in each of the three spaces range from about 3.5 hours for the sidelit office space without blinds to 15.5 hours for the Gund Hall space on a standard laptop computer using a single-core of a 2.4 GHz processor and high-quality Radiance image parameters detailed in Table 3.1.

The annual enhanced simplified DGP simulations were performed using the `gen_dgp_profile` subprogram developed by Jan Wienold that has been implemented into Daysim version 3.1 (Reinhart 2010). The time involved in simulating a single yearly eDGPs profile using Daysim was comparable to the time required to generate one day’s worth of cylindrical projection glare overlay data using static Radiance simulations.

In summation, the analysis procedure presented here can be largely automated since additional simulation input required by the user is negligible. The required simulation time on

the other hand is substantial and requires the use of a dedicated calculation engine (ideally a simulation cluster) or overnight calculations.

#### 4.4 Conclusion

By expanding glare simulations to multiple view directions and observer positions, this chapter shows that designing flexibility into interior space layouts can have very positive effects on improving the comfort experienced in a space. Furthermore, this information can be presented in an easily communicable format that adds value beyond a single number representing visual comfort. Instead, the comfort probability is displayed spatially from the view of the occupant.

The adaptive zone discomfort glare analysis described in this chapter can be performed on a yearly basis using the enhanced simplified DGP method and then be combined with a set of medium-quality cylindrical projections. At that time, a designer could navigate glare predictions and their visual correlates for an entire year using a simple program interface, such as the conceptual one shown in Figure 4.5. The enhanced simplified DGP method allows a more comprehensive analysis of yearly comfort data for a specific space, requiring a much smaller computational effort than performing thousands of Radiance simulations for sky conditions across the entire year; however, to perform the simulation still takes a substantial amount of time and thus should only be attempted once basic performance and reasonableness have been established using luminance images from discrete time simulations. For example, it is prudent to check for glare and direct sunlight over several hours on the solstices and an equinox before investigating the annual presence of discomfort glare using climate-based daylight simulations.

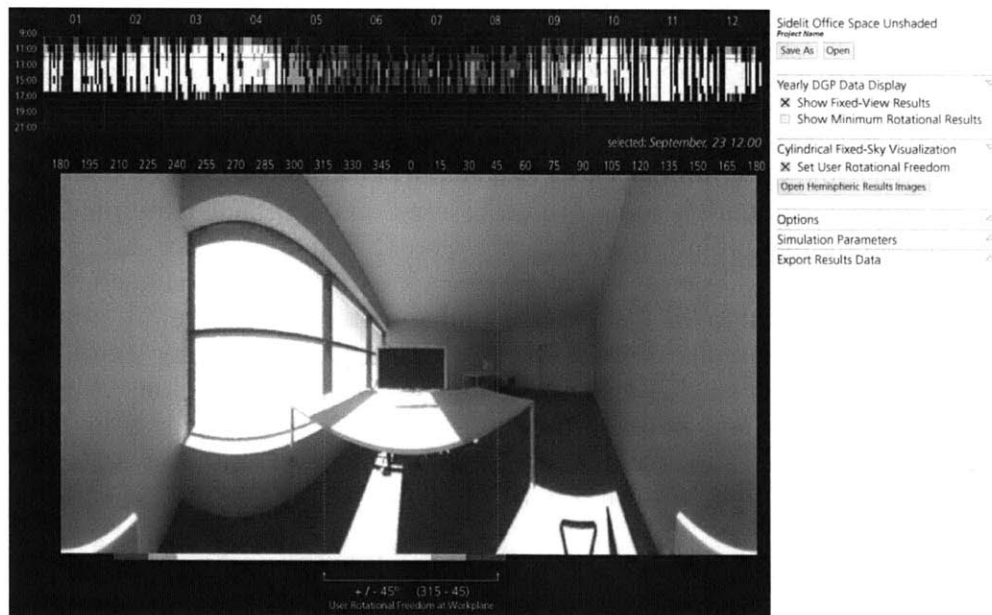


**Figure 4.5** Proposed computer program showing spatial, lighting and glare properties of a space.

This chapter deals with ways of applying discomfort glare analysis to daylit spaces in terms of visualizations, occupant behavior and shading effects; however, it still leaves several questions raised in the research goals section (1.1) unanswered. For example, how well does DGP resolve the actual sensation of visual comfort that occupants experience in daylit spaces? Furthermore, can DGP be used to predict an occupants' overall evaluation of a space based on the frequency and intensity of visual discomfort over a long period of time? Chapter 5 aims to investigate these questions.



## Chapter 5

# Predicting Long-term Visual Satisfaction

Chapter 3 focused primarily on the evaluation of metrics designed to analyze discomfort caused by contrast and overall brightness in the form of vertical eye illuminance ( $E = \bar{L} / \pi$ ). However, in Sections 2.2 through 2.4 several other means of evaluating visual discomfort are described, including monitor contrast and the presence of direct sunlight. Over prolonged analysis periods on the scale of annual building performance simulations, uncomfortable DGP results can occur separately from low monitor contrast ratios depending on whether glaring sources are located in front of or behind the occupant as the solar position changes. Chapter 4 introduced the idea that occupants may also adapt to uncomfortable daylit environments. Chapter 5 shows that discomfort probability simulations have the capacity to resolve subjective occupant discomfort in spaces over long periods of time.<sup>14</sup> This concept is termed visual satisfaction, to align with notions of long-term pleasure associated with a space, rather than visual discomfort, which is an instantaneous phenomenon.

No annual metric exists to assess the visual satisfaction of occupants in daylit spaces, and the application of visual comfort analysis to design problems is seriously limited. A number of comfort metrics have been proposed in the past that were created in the laboratory or via controlled studies; however, there have been few applications of these metrics to real, daylit interiors (Rubiño et al. 1994; Painter et al. 2009; Hirning et al. 2013). The results of those studies have not been positive thus far.<sup>15</sup> The research presented in this chapter shows that visual comfort analyses can be used to predict occupant visual dissatisfaction by applying them in the field.

---

<sup>14</sup> The work presented in this chapter was originally published as,

Jakubiec, J. & Reinhart, C., 2013. Predicting visual comfort conditions in a large daylit space based based on long-term occupant evaluations: a field study. In *13th International IBPSA Conference, Building Simulation*. pp. 3408–3415.

<sup>15</sup> See Section 2.6.1.

To this end, a comprehensive visual comfort analysis of the Harvard University Graduate School of Design studio spaces was performed. The analysis accounts for discomfort glare probability, monitor contrast, direct visibility of the sun and direct sunlight on the workplane. The space is a five story terraced open plan arrangement that houses over 500 graduate students.<sup>16</sup> It features clerestory windows and fully glazed north and south facing walls. The studio space is known to have localized visual comfort problems, because each term students located in the most offending areas erect their own shading devices. An online survey was administered in which 67 occupants participated who were either comfortable or experienced discomfort from daylight while also correctly identifying their desk location in the space.

Occupants' reported visual comfort assessments are compared against detailed simulations of their workspaces. The resulting visual comfort analysis detects when occupants will be uncomfortable. It also relates to the spatiality of a place, the time of occurrence and the potentially many causes of discomfort. Therefore, the analysis constitutes helpful clues to avoid discomfort problems during the design of a building.

## 5.1 Discomfort Metrics

In daylight spaces, there are several possible causes of discomfort: discomfort glare, reduced monitor contrast ratios from reflected daylight, direct visibility of the sun, and the presence of direct sunlight on the workplane. Discomfort due to electric lighting is not considered in this study, although it was reported by some students. In Chapter 3 it is shown that DGP is the most reliable metric for the assessment of discomfort glare, so it is used in this study because DGP accounts for contrast and brightness whereas other glare metrics only account for contrast (Wienold & Christoffersen 2006). DGP is described in more detail in Section 2.2.6. Monitor contrast ratio is calculated and evaluated based on the metric described in Section 2.3. Finally direct sunlight falling on the eye or on the workplane are calculated, described in Section 2.4.

## 5.2 Methodology

### 5.2.1 Survey on Visual Comfort

A survey was conducted of the students seated in the studio spaces of the Harvard University Graduate School of Design's Gund Hall at the end of the Spring 2011 academic term accounting for the time from January 24 until April 15. The survey was administered digitally, and participants were solicited to complete the survey via email and on their own time. Students were asked to identify their desk using a numbered seating plan of the school or the label affixed to their desk and to describe in detail their long-term visual satisfaction with the space. They rated their comfort during the semester for three specific periods of the day: morning, from 8:00–12:00; midday, from 12:00–14:00; and afternoon, from 14:00–18:00. For each of these intervals, students ranked their typical degree of discomfort in one of four categories: imperceptible, perceptible, disturbing or intolerable. Students were also given the opportunity to describe the cause or causes of their discomfort and what actions they took in response. The survey covered more topics than visual comfort alone, but the relevant questions and answer choices (in *italics*) are presented on the following page.

---

<sup>16</sup> Gund Hall was also highlighted in Chapter 3; see Figure 3.2.

1. Indicate the typical degree of discomfort glare you experienced at your desk during this semester.

Three time periods: Mornings (8:00 – 12:00), Midday (12:00 – 14:00), and Afternoon (14:00 – 18:00)

*Imperceptible / Perceptible / Disturbing / Intolerable*

2. If you are experiencing glare, what is its cause? (Choose all that apply.)

*I am not experiencing glare / Direct view of the sun / Electric lighting conditions / Reflections from the monitor (veiling glare) / Excessive brightness or contrast / Other (free response)*

3. If you experienced visual discomfort over the course of the semester, which strategies did you employ to increase your comfort? (Choose all that apply.)

*Nothing. Discomfort was **not** experienced /*

*Nothing. Discomfort was experienced /*

*Moved to another position in front of the desk /*

*Built a shading device not originally a part of the workspace /*

*Temporarily rotated my chair to avoid bright light or contrast /*

*Temporarily moved to a completely different location in the building /*

*Other. Describe the actions you took to avoid discomfort. (free response)*

### 5.2.2 Visual Comfort Simulations

A calibrated daylight simulation model was constructed of Gund Hall using the Radiance simulation engine.<sup>17</sup> The model is geometrically accurate including urban context and the glazing of nearby buildings. The simulation model accounts for measured visible window transmissivity (Voit et al. 2007) and measured diffuse reflectance values for opaque surfaces in the space, described in Table 5.1. The ceiling was modeled using a standard 80% reflectance, as it was inaccessible for measurement purposes. Electric lighting is supplied by louvered fluorescent fixtures, which are on for most hours of the day; however, discomfort from electric lighting is not considered.

---

<sup>17</sup> See Section 2.7.1.

**Table 5.1** Measured material properties.

Surface Description	Transmissivity
Clerestory glazing	0.142
North and south glazing	0.185
Dining hall glazing	0.948
	Reflectance
Concrete walls and floors	0.243
Desk surfaces	0.541
Desk backs	0.776
Floor	0.070
Mullions	0.100
(Painted) Cinder block walls	0.759
Handrails	0.048
Ceiling	0.800

The studio space of Gund Hall, portrayed in Figure 5.1 as a rendering of the simulation model, provides desks for approximately 500 students of architecture and urban design. It is a five story tiered space with plentiful daylight, which comes from clerestory windows and large floor-to-ceiling glazing at the north and south ends of the space. Student desks are either directly underneath the clerestory windows or sheltered by the level above. Figure 5.2 portrays the surrounding context of Gund Hall, notably the CGIS building, which has highly specular solar control glazing.

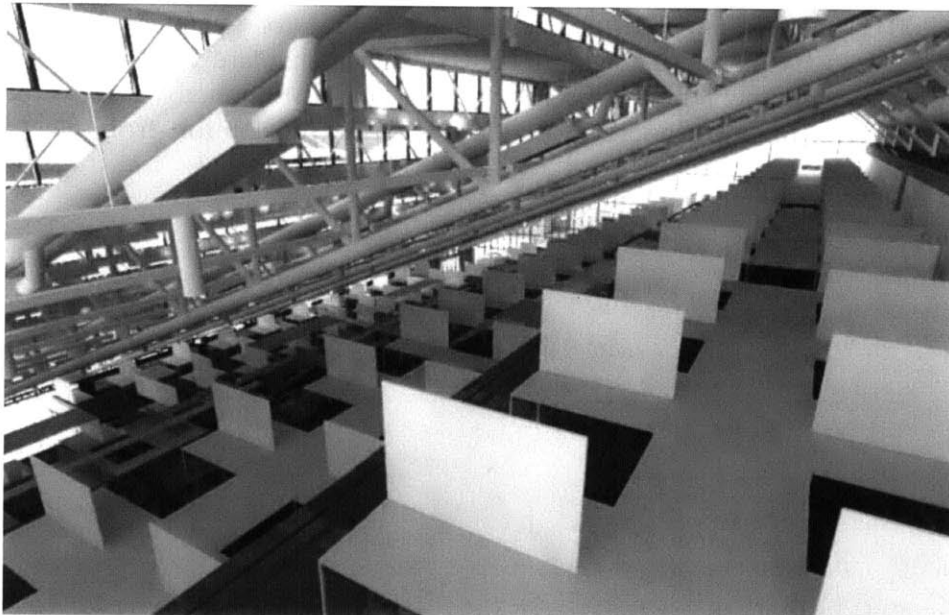


**Figure 5.1** A rendered image of the simulation model looking South from the fourth level corner.



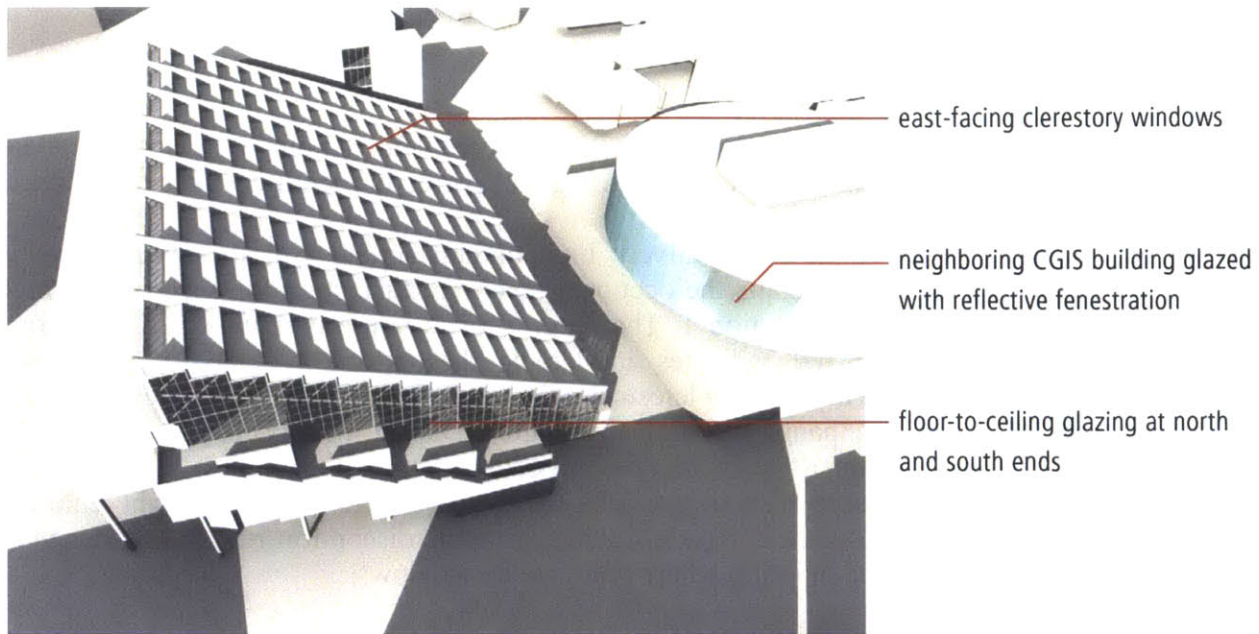


**Figure 5.2** Exterior rendering of Gund Hall showing key context.

In accordance with the proposed discomfort metrics (Section 5.1), each survey respondent's work area was the subject of discomfort glare, monitor contrast and direct sunlight simulations. Because of the many small clerestory windows relative to the size of the space, the presence of visual discomfort is highly transient in Gund Hall for those not seated near the large North or South windows. Therefore, all of the discomfort predictions performed in this study were simulated using a six-minute time interval from January 24 until April 15, from the start of the semester until the time when the survey was administered.

DGP predictions were made using the enhanced simplified DGP (eDGPs) method (Wienold 2009). Ordinarily, the eDGPs method substantially decreases calculation time by using Daysim (Reinhart & Walkenhorst 2001) to calculate vertical eye illuminance and rendered images of direct sunlight to determine contrast. However, in the case of this study, vertical eye illuminance was calculated using standard Radiance tools (gendaylit and rtrace) in order to avoid direct solar interpolation errors from Daysim's direct daylight coefficient methodology that may be exacerbated in deep spaces.

Monitor contrast ratios were predicted based on illuminance calculations as well. In this study, monitor reflectance was standardized based on the average measurement of three monitor screens (a Dell U2412Mb LCD monitor, a Lenovo Thinkpad T520 laptop LCD screen, and a Lenovo desktop LCD monitor) at 5.4% diffuse reflectance.  $L_H$  and  $L_L$  are fixed at realistic assumptions of 80 and 10  $\text{cd}/\text{m}^2$  respectively (Moghbell 2012), yielding a default contrast ratio of eight without the presence of reflected light when used with Equation 2.8. Specular reflections were not considered.

Weather data was acquired from a weather station approximately one kilometer (0.62 mi) away from the site for the period of the study (Keneli.org 2012). Measured global horizontal solar irradiation was converted into direct and diffuse components using the Reindl method (Reindl et al. 1990) and used as input information to the Perez all weather sky model (Perez et al. 1993).

## 5.3 Results

### 5.3.1 Survey Results

The survey received 194 responses of which 90 were complete, but only 67 respondents did not experience discomfort caused by electric lighting and correctly identified their desk space. Those 67 respondents are studied henceforth.

Overall, the survey results suggest a relatively high dissatisfaction with the space. This is represented in Figure 5.3, which details the occupant-reported satisfaction for each of the three intervals; this is the response to Question 1. The severity of response is represented by colors: green indicates comfort, and red indicates intolerable discomfort, a standard maintained throughout this chapter. As the building's clerestories face east, the morning hours yield the most discomfort with 52.3% of occupants reporting discomfort. During midday, fewer users report discomfort (36.9%), but the intensity of reported dissatisfaction is the highest with 9.2% of respondents reporting intolerable discomfort. This is likely due to direct sunlight entering through the full glazing of the southern façade. In the afternoon, discomfort is further reduced as the sun moves to the west of the building where there are no windows.

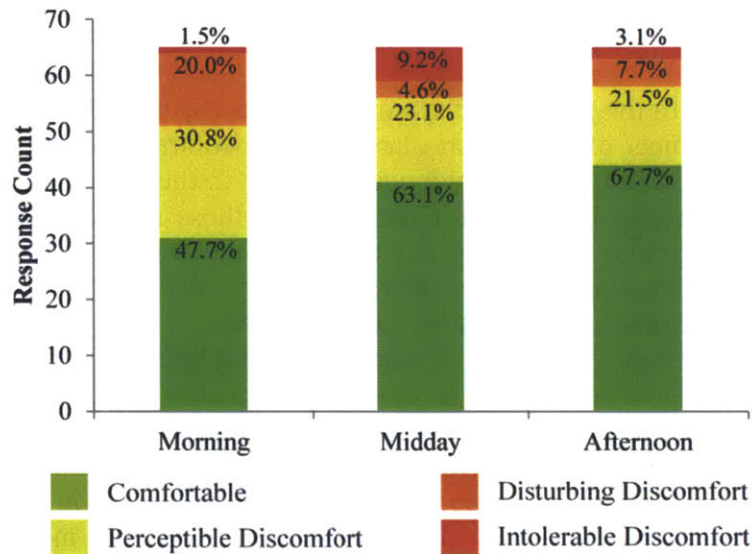


**Figure 5.3** Histogram of occupant-reported satisfaction (Question 1) by time of day.

Question number 2, asking about the causes of visual dissatisfaction found the following for all 90 complete survey responses,

- 28.8% (26) did not experience any discomfort.
- 30.0% (27) had a direct view of the sun.
- 17.8% (16) were made uncomfortable from the electric lighting.
- 27.8% (25) could not see their computer monitor due to reflections.
- 14.4% (13) experienced extreme brightness or contrast (discomfort glare).

The free response answers are documented in Appendix A. The answers shared in response to Question 2 clearly show that the choice to test for multiple visual discomfort metrics is a reasonable one. The answers to question 3 are shared in Section 5.4.3.

### 5.3.2 Predicting Long-Term Occupant Evaluations

With a complete set of discomfort glare, monitor contrast and direct sunlight (visible and workplane) simulation results for each desk location in Gund Hall, it is possible to analyze the intensity and frequency of discomfort from multiple causes. A logical question to ask is, how much discomfort glare, reduction of monitor contrast or direct sunlight must be experienced in order for an occupant to deem the space uncomfortable?

A strong correlation was found between the percentage of occupied hours above certain visual comfort thresholds with reported satisfaction values. Any time with a DGP value above 0.4, classified during a moment in time as ‘disturbing’ (Wienold 2009), predicted monitor contrast ratio below four (International Standards Organization 2008) or with direct sunlight on the eye or desk greater than 1000 lx (see Section 2.4) is considered uncomfortable for this purpose. Students in Gund Hall tended to be more sensitive to discomfort glare and direct sunlight than contrast ratio in their evaluations of the space. It was found that on average occupants experiencing discomfort glare (DGP  $\geq 0.4$ ) for more than 3.5% of occupied hours would evaluate the space as ‘intolerable.’ On average direct sunlight (vertical eye illuminance or illuminance on the workplane  $\geq 1000$  lx) needed to be experienced for 5.25% of occupied hours to evaluate the space as ‘intolerable.’ Finally, predicted low monitor contrast (CR  $< 4$ ) needed to be experienced 24% of the time, on average, to account for an ‘intolerable’ evaluation. In this model, multiple types of discomfort contribute to the overall evaluation of visual satisfaction in a space by accounting for partial contributions from multiple analysis types and a linear scale from imperceptible (0% occupied hours) to intolerable. For example, if discomfort glare is experienced for 1.7% of occupied time and direct sunlight is experienced for 3% of occupied time, the model prediction is still ‘intolerable.’

It is important to note that this result is specific to the students, space and culture of Gund Hall. For example, in an office space with fixed computer monitors and adjustable window blinds, occupants might be more sensitive to contrast ratio and less sensitive to discomfort glare or direct sunlight. The model described above can be represented by way of Equation 5.1 below,

$$VS = 28.6 * \%hrsDGP_{0.40} + 19.05 * \%hrsDirectSun_{1000} + 4.2 * \%hrsCR_4 \quad (5.1)$$

Where the equation evaluates such that,

- imperceptible  $< 0.5$ ,
- $0.5 \leq$  perceptible  $< 0.75$ ,
- $0.75 \leq$  disturbing  $< 1.0$ ,
- and  $1.0 \leq$  intolerable.

### 5.3.3 Spatial Display of Results

Predictions using simulation results are compared to the survey responses gathered from occupants in Figure 5.4. Results are overlaid on a plan of the Gund Hall studio spaces showing all four levels simultaneously. Shaded areas indicate desks that are covered by the floor above or shaded by a custom, student-built shading device. A small rectangle is located at each desk, representing the model-predicted visual satisfaction. These rectangles are color coded from imperceptible green (■) to intolerable red (■). Contained within squares where students who responded to the survey are seated, a small circle is placed representing occupant-reported visual satisfaction, and color coded in the same way (●, ●). The goal of this exercise was to match



model predictions (squares) to reported satisfaction (circles). Perfectly matched predictions will appear as one solid color with a thin line separating the two; however, over and under-predictions will be apparent by the color difference between the interior circle and the enclosing square.

During the morning (Figure 5.4a), the southern and eastern side of the building and clerestory windows are exposed to direct sunlight, causing discomfort predictions deep inside the space. Midday (Figure 5.4b), from 12:00 to 14:00, is when the altitude of the sun is at its peak. Thus, predicted discomfort is primarily localized to the southern side of the space. In the afternoon (Figure 5.4c), predicted discomfort is primarily concentrated near the south façade and on the east side of the building. This is because of reflections from the glazing of the neighboring building (Figure 5.2) and afternoon sun penetrating from west to east across the space.

#### 5.3.4 Ability to Predict Occupant Visual Satisfaction

Table 5.2 documents the predictive ability of the model for each time interval when compared to the survey results. Exact matching to actual occupant evaluations ranges from 53.7% in the morning to 70.1% for the midday period during the semester. This may seem low; however, the percentage of matching within one comfort threshold is relatively high, from 77.6% to 88.1%. This suggests that simulations are capable of tracking occupant visual satisfaction trends within a space; however, occupant assessments vary based upon personal luminous preferences.

**Table 5.2** Discomfort predicted by analysis.

<b>Matching Criteria</b>	<b>Morning</b>	<b>Midday</b>	<b>Afternoon</b>
Exact match	53.7%	70.1%	64.2%
Within one	77.6%	88.1%	83.6%
Over-prediction	22.4%	4.5%	9.0%
Under-prediction	23.9%	25.4%	26.9%

Most importantly, spatial agreement between the survey results and comfort predictions are overall high. The morning visual satisfaction predictions (Figure 5.4a) illustrate discomfort throughout the space with the notable exception of desks that are shaded. The occupant reported results seem to corroborate this analysis. Midday discomfort (Figure 5.4b) is localized to the south and east sides of the building. This result is also close to the occupant survey's results. During the afternoon many occupants report comfort near the southern glazing although the model predictions indicate the opposite due to the presence of direct sunlight. Potential reasons for this discrepancy are discussed in the following section.



(a) Predicted morning visual satisfaction from 8:00 – 12:00.



(b) Predicted midday visual satisfaction from 12:00 – 14:00.





(c) Predicted afternoon visual satisfaction from 14:00 – 18:00.

**Figure 5.4** Predicted semester-long visual satisfaction categorized by cause compared to actual response.

## 5.4 Discussion

What does the ability for simulation to predict occupant visual satisfaction in spaces mean for architecture, the building simulation community and design? One impact is that designers may probe a space for the potential appearance of discomfort resulting from several causes. The process proposed in this chapter can hence be used to assess designs of daylit spaces for maximum comfort without the use of operable shading devices. When discomfort is identified, it is possible to discover and address the causes by typology (discomfort glare, monitor contrast, direct sunlight) and time of occurrence. This same methodology can be applied to furniture and seating layouts. Space layout has a large impact on visual satisfaction, as visual discomfort is dependent on the viewing direction. Building simulationists currently have a large role to play in this analytical design process, as there is not an established method to determine view position and direction. There is also no fully automated method to produce and evaluate such metrics.

The comfort maps shown in Figure 5.4 and the accuracy of predicted occupant responses presented in Table 5.2 show that there is a reasonable correlation between the model predictions of visual satisfaction and occupant-reported visual satisfaction; however, deeper understanding of the significance of this result is probably warranted.

### 5.4.1 Using Multiple Visual Comfort Criterion

Occupant behaviour models such as Lightswitch (Reinhart 2004), DGP-based shading control in Daysim (Reinhart & Walkenhorst 2001), the Adaptive Zone (Chapter 4) and IES standard LM-83-12 (IESNA 2012) all utilize predictions of visual comfort.<sup>18</sup> However, until now, they have all looked at visual comfort through a narrow lens. Lightswitch lowers a shade when greater than 50 W/m<sup>2</sup> direct normal irradiation falls on the workplane. DGP-based shading control implemented in Daysim closes the blinds when a DGP probability of at least 0.40 is observed. The Adaptive Zone proposes a modification of the Daysim DGP control method, but occupants have the ability to adapt by looking in directions where the least discomfort is experienced. IES LM-83-12 suggests that window shades should be lowered when greater than 2% of the space receives direct sunlight.

The results in predicting visual discomfort allow important reflection on the assumptions made by the aforementioned models. Foremost, the use of a single metric for determining comfort is challenged. Results at each workspace were tallied separately for each time interval and for each type of predicted discomfort that occurs for greater than one percent of occupied time. During the morning interval, only 28.6% of workspaces with predicted discomfort originated from one type of discomfort analysis. During the midday interval when the sun is higher, this percentage increases to 47.4%. Finally, during the afternoon period only 37.5% of desks with predicted discomfort are affected by a single type of discomfort. This suggests that predicting visual discomfort with a single metric is inadequate, because in reality several measures (known and unknown) contribute to the assessment of visual comfort. It is reasonable to infer that occupant behavior models and comfort prediction methods analyzing only direct sunlight or discomfort glare will necessarily miss some periods of discomfort. Figure 5.5 shows how much visual comfort predictions can vary when using only direct sunlight or only discomfort glare by the resulting predictions of window shading closure using the two methods.

---

<sup>18</sup> See Sections 2.4.1 and 2.6.3.



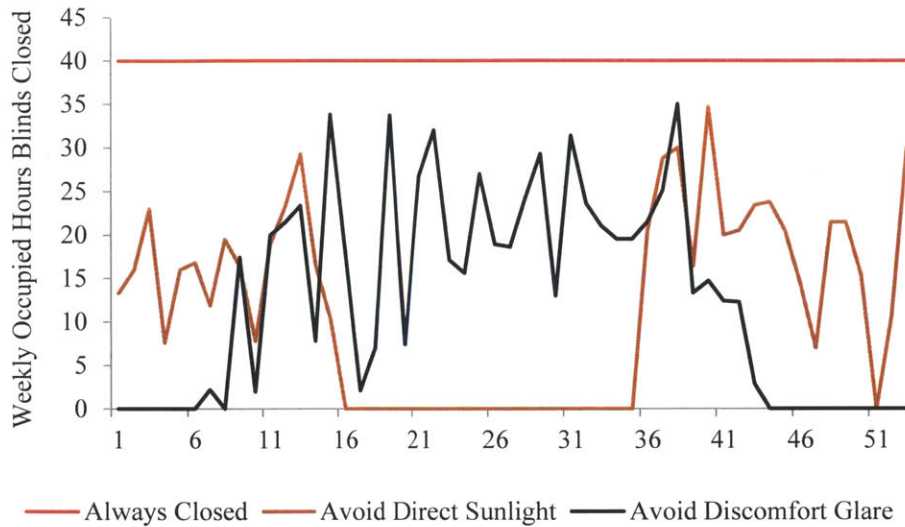


**Figure 5.5** Predicted weekly hours of shading closure for an office space in Boston using avoidance of direct sunlight or discomfort glare as the control scheme (Jakubiec & Reinhart 2011).

That single-metric models do not adequately quantify discomfort in daylight spaces is further reinforced by Figure 5.6, which compares hourly discomfort metrics using temporal maps for two desks labeled '1' and '2' in the plans of Figure 5.4. Discomfort glare probability, monitor contrast ratio, direct visible sunlight, and direct sunlight on the desk are displayed graphically with the horizontal axis indicating the day within the survey period and the vertical axis indicating time of day. The color scale for each metric is calibrated such that dark red (■) indicates a threshold at which discomfort would be predicted by a typical occupant behavior model. In these examples, all four causes of discomfort are observed. Furthermore, for both example 1 and 2, visible direct sunlight and direct sunlight on the desk have morning and afternoon periods of discomfort. These periods of direct sunlight are not entirely correlated with monitor contrast ratio or discomfort glare in example 1 and 2 respectively. Overall, the students at both desks experience discomfort, especially during morning and midday periods but from disparate causes, suggesting occupant comfort models that consider multiple sources of discomfort are necessary.

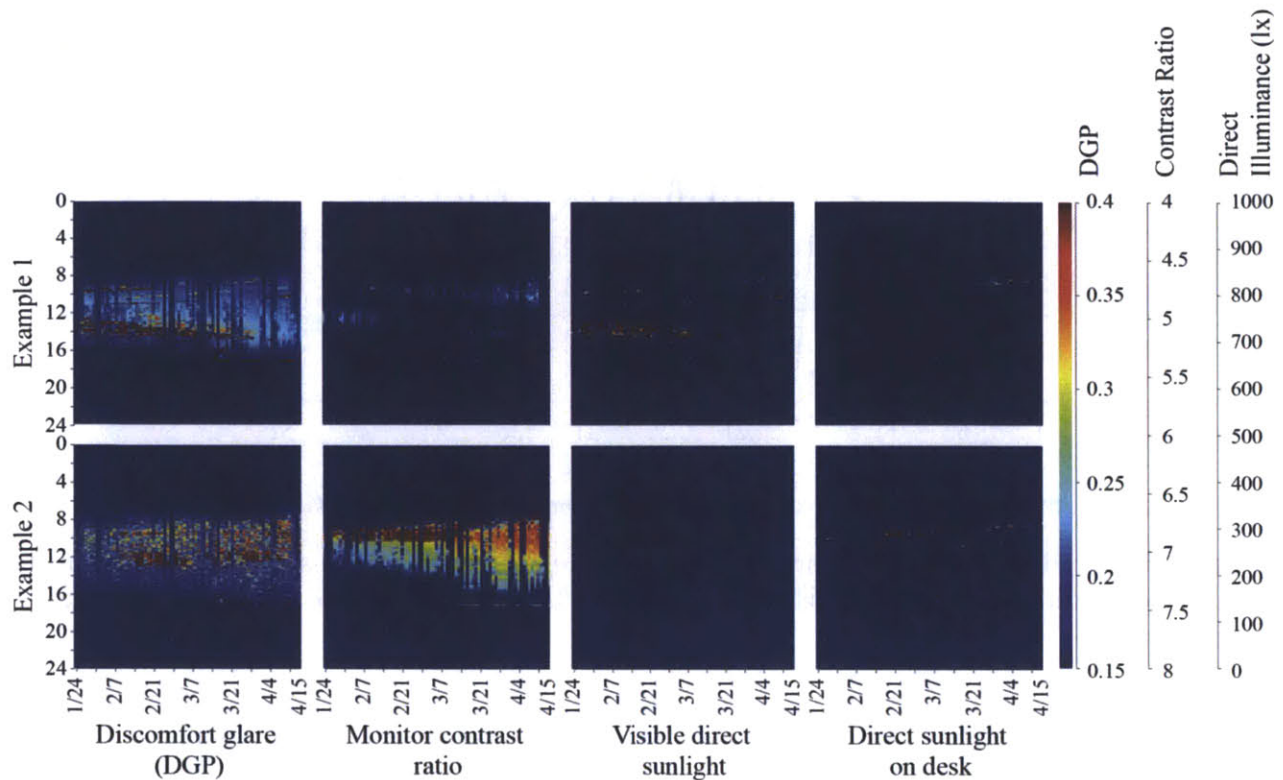


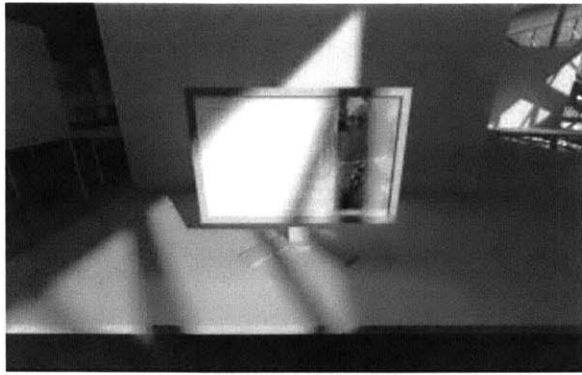
**Figure 5.6** Comparison of predicted discomfort for two desks. Values that might be associated with the closing of blinds are colored dark red (■).

#### 5.4.2 Occupant Variability

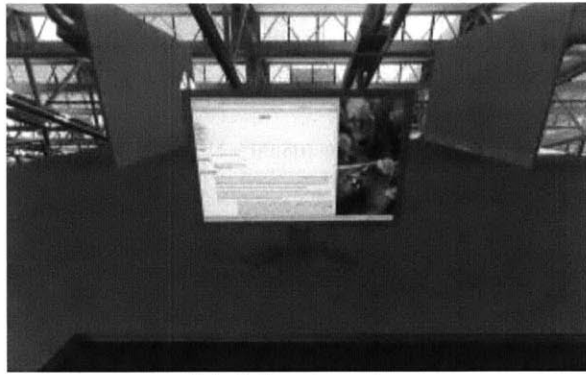
Occupants are highly variable in their assessments under similar conditions. For example, the student labeled ‘3’ in Figure 5.4 reports disturbing or intolerable visual discomfort for all three intervals despite that during midday and afternoon his or her neighbors are all relatively comfortable.

#### 5.4.3 Adaptation

The student indicated by ‘4’ in Figure 5.4 constantly feels more comfortable than our method predicts with the primary cause of discomfort being a reduction in monitor contrast. The view directions of each student in the study were modeled as observed during the start of the semester; however, over time some students opted to use their side tables as the main workspace. In the case of example 4, this means that the student would face east rather than north. Simulated images of monitor visibility and direct sunlight for the two seating scenarios on January 31<sup>st</sup> at 10:30, during the morning measurement period, are displayed in Figure 5.7. By turning 90-degrees, the student is able to avoid direct light falling on his or her monitor.



(a) Original view



(b) Adaptive view

**Figure 5.7** Example 4 monitor visibility at January 31st, 10:30 during morning survey period.

Students also adapted the environment to their comfort needs. Student-built horizontal shading devices were accounted for in the simulation; however, some students additionally erected vertical shades during the semester, which were not considered. Predictions of visual satisfaction for students who built their own shading devices were accordingly more prone to error. 33.3% (5) of the morning, 50.0% (4) of the midday and 27.3% (3) of the afternoon predictions varying from the survey by more than one comfort threshold are accounted for by students who built their own shading devices.

Finally, the survey results themselves lend credence to the concept of adaptation, at least in spaces such as Gund Hall where daylight qualities are highly dynamic and there is no user-controllable window shading system. Harkening back to Question 3, of the 90 students who answered (students could pick multiple responses),

- 25.6% (23) did not experience any discomfort.
- 21.1% (19) experienced some discomfort, but did nothing.
- 21.1% (19) changed position in front of the desk.
- 20.0% (18) built their own shading device.
- 30.0% (27) changed their orientation or view at their desk.
- 12.2% (11) moved to a completely different location (could not adapt).

In other words, in the lighting and space culture of Gund Hall, it is commonplace to adapt to the specific luminous environment.

#### 5.4.4 Survey Bias

One question raised by this study is, can people actually assess how they feel about a space long term, or are their impressions strongly biased by recent events? This question is especially important to the relevance of this chapter, as the questions asked of students (Section 5.2.1) are specifically targeted to ask about their long-term impressions of the space, and most other studies of this type look only at instantaneous visual comfort (Painter et al. 2009; Van Den Wymelenberg et al. 2010; Hirning et al. 2013; Van Den Wymelenberg & Inanici 2014). One way to address this line of thinking is simply to see if students who report negative feelings about the space did so during times where discomfort was likely to be experienced. Figure 5.8 illustrates this by plotting the number of predicted discomfort incidents for each student in a certain time interval preceding their survey response (4 hours, 24 hours and 1 week) against their reported visual satisfaction. In the case where bias is present, one would expect to find large quantities of

predicted discomfort incidents in the 4 and 24 hour period for those who rank the space ‘disturbing’ or ‘intolerable;’ however, this is not the case.

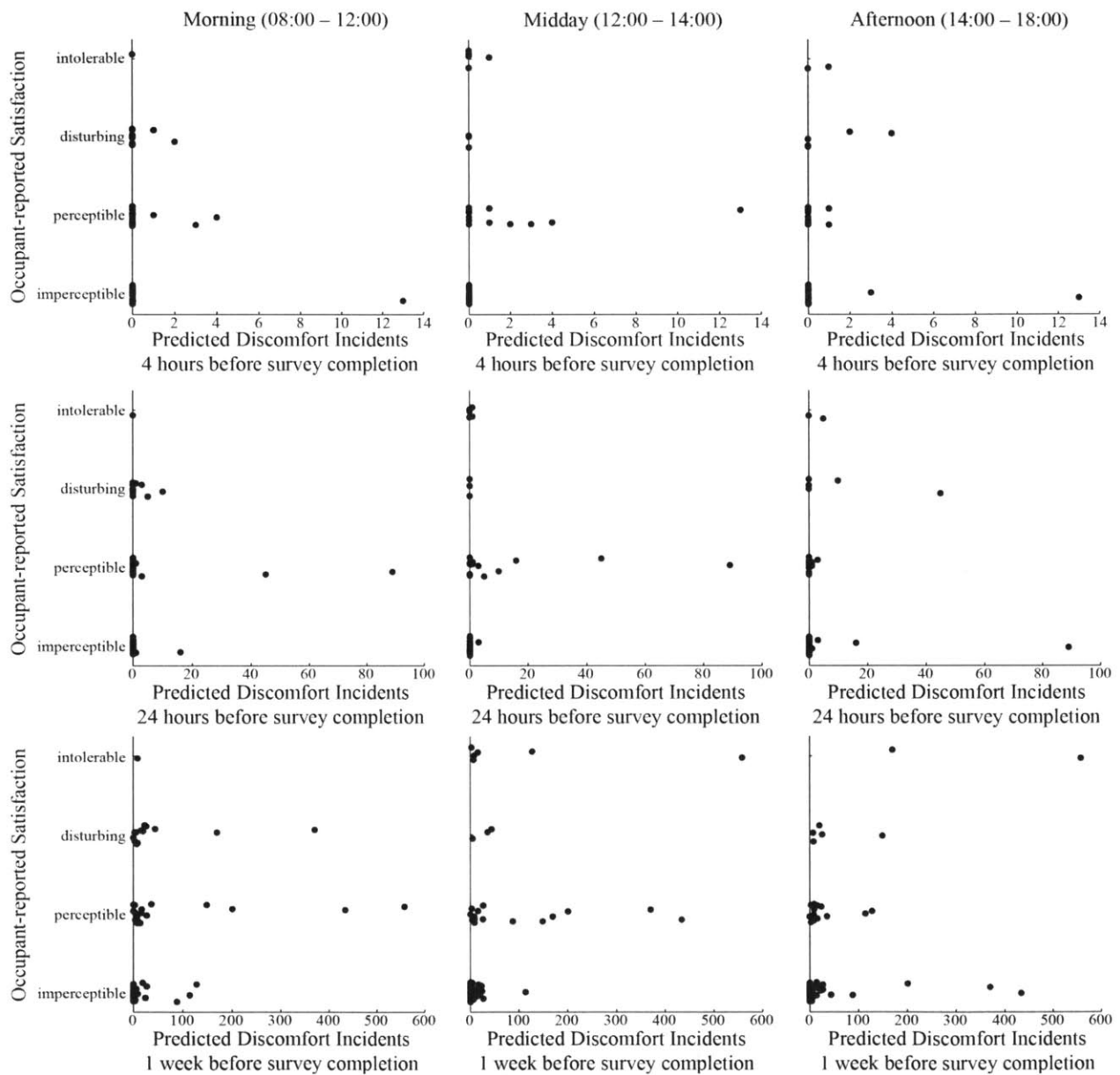


**Figure 5.8** Plots showing the number of predicted discomfort incidents during the time before answering the survey for each user.

Beyond the findings shown in Figure 5.8, in the free response sections of the survey, students are extremely eloquent when discussing the source of visual discomfort. Students were able to differentiate visual discomfort by time and location in the space and did not seem to be reacting to current conditions. A full accounting of these survey free responses can be found in the Appendix A.

#### 5.4.5 *Limitations of Study*

The survey data that is used to calibrate the semester-long visual satisfaction model is the same data by which the analysis is evaluated. An independent data set is desirable for evaluation; however, the visual comfort metrics used to evaluate each hourly or six-minute time step are based on a wealth of research and experimental data. Therefore, the trends observed in this chapter are probably already applicable to the design of comfortable, daylit spaces.

### 5.5 Conclusion

This chapter shows that it is possible to use current visual comfort metrics to predict occupants' long-term assessments of visual satisfaction in a complex daylit space. The model presented in this chapter explains, within one comfort threshold, between 77.6% and 88.6% percent of polled occupant responses depending on the time of day. Spatial trends of discomfort (Figure 5.4) show good agreement with reported occupant values. In this study, using a single cause of discomfort would have resulted in missing significant periods and areas of discomfort within the space. Depending on the time interval analyzed, between 28.6% and 47.4% of seating positions that experience discomfort are affected by a single type of discomfort. It is plausible that this is the case in other spaces as well, because discomfort glare, monitor contrast and the visibility of direct sunlight may occur independently in any space. Chapter 6 expands upon these findings with a study of luminance-calibrated high dynamic range photographs and associated subjective occupant survey data using similar metrics. This second human subjective comfort survey aims to support the findings of the current chapter.



## Chapter 6

# Integrated Luminance-based Analysis for the Prediction of Visual Discomfort

Chapter 5 noted that by utilizing multiple visual comfort metrics, it is possible to resolve between 53.7% and 70.1% of long-term visual satisfaction assessments, and only 28.6% to 47.4% of views with predicted discomfort have the discomfort originate from a solitary metric type such as discomfort glare alone. In Chapter 5, the metrics investigated were: visible direct sunlight, direct sunlight on the workplane, monitor contrast ratio and discomfort glare. This chapter follows up on Chapter 5's analysis by testing the same type of comfort metrics against instantaneous assessments using a high quality dataset including luminance-calibrated HDR photographs, measured illuminance data and detailed subjective occupant evaluations.<sup>19</sup> A standardized set of methods is then proposed for deriving the metrics using calibrated HDR photographs or simulated renderings. For the former type, the issue of luminous overflow, a condition where measurements cannot accurately resolve extreme peak luminances, is considered, and a process for correcting such photographs is proposed. In the results section, individual metrics are compared in their ability to identify subjective evaluations. Finally, subjective thresholds are identified where discomfort is highly likely. Going forward, these thresholds can be used in evaluating HDR renderings during the design of daylit spaces or in post-occupancy evaluations of real spaces.

---

<sup>19</sup> The work presented in this chapter has been submitted for publication as,

Jakubiec, J.A., Reinhart, C.F. & Van Den Wymelenberg, K., 2014. Towards an integrated framework for predicting visual comfort conditions from luminance-based metrics in daylit spaces. In *2014 ASHRAE/IBPSA-USA Building Simulation Conference*. Atlanta.



## 6.1 Methodology

### 6.1.1 Data Source and Subject Evaluations

A series of luminance-calibrated HDR photographs previously collected by Van Den Wymelenberg and Inanici (2014) are reanalyzed in this chapter. Two nearly identical side-by-side office spaces located in Boise, Idaho were used for this experiment. One test room was set up for occupant surveys, while the adjacent space contained instrumentation for capturing HDR photos, illuminance and luminance measurements from the point of view of the occupant in the first test room. Each HDR photograph was calibrated using a luminance measurement taken from a neutral grey card in the scene and has an accompanying measurement of vertical eye illuminance from an independent sensor. The photographs were taken using a 180 degree fisheye camera lens. Vignetting correction was applied to each photograph in accordance with best practice (Inanici 2006). More discussion on HDR photography techniques can be found in Section 2.7.3.

48 individuals participated in the experiment, which took place from June to December, 2011. Each participant spent one day in summer and one day during fall evaluating 16 separate daylight conditions. This chapter specifically analyzes two conditions where participants were asked to adjust a venetian blind system with electric lighting turned off in all but two cases to find their 'most preferred' and 'just uncomfortable' luminous environments during a time where direct sunlight could enter the space. While experiencing each lighting condition, the participants were asked to rate statements about their current comfort (Van Den Wymelenberg & Inanici 2014). For this chapter, the following three statements were focused on (1, 2 and 6 in the original research),

1. This is a visually comfortable environment for office work.
2. I am pleased with the visual appearance of the office.
3. The computer screen is legible and does not have reflections.

These three statements were selected because they are directly related to visual comfort (1 and 2) as well as the ability to perform work (1 and 3). The research presented in Chapter 5 suggested that the ability to perform tasks as well as general subjective measures of visual comfort were important to occupants when asked to evaluate a daylight space. Each of these statements was rated on a seven point Likert scale where, 7 means Very Strongly Agree, 6 means Strongly Agree, 5 means Agree, 4 means Neither Agree nor Disagree, 3 means Disagree, 2 means Strongly Disagree, and finally 1 means Very Strongly Disagree. In this case, the sum of question responses range between 3 and 21. 21 is a response from a very comfortable individual capable of performing office tasks and using the computer. 3 is the opposite, a response from an individual whose lighting conditions are uncomfortable enough to cause displeasure and negatively impact the ability to perform tasks. Combined Likert responses between 3 and 21 indicate various intermediate subjective ratings of comfort for each individual.

### 6.1.2. Luminous Overflow and Correction

When capturing HDR photographs in daylight areas, it is likely for small but highly intense luminous peaks to occur caused by direct capture of the sun or strong specular reflections. These peaks may be orders of magnitude higher than typical values for interior surfaces ( $\sim 1\text{--}1000\text{ cd/m}^2$ ) or large light sources such as diffuse portions of sky and luminaires ( $\sim 3,500\text{ cd/m}^2$ ). Considering that the sun has a luminance of over a billion  $\text{cd/m}^2$  (Grondzik et al. 2006), it is easy to imagine a condition where camera exposures cannot be taken quickly enough to accurately



resolve these peak brightnesses. When this occurs, it can be referred to as luminous overflow – a condition where the range of the HDR photograph is not great enough to capture the true luminous range of the visual reality.

Stumpfel, et al. (2006) propose a measurement methodology using a neutral density filter and two lens apertures that allows HDR photography to resolve the luminance of very bright sources such as the sun. It seems sensible to use such a method in future work for daylit interiors where the sun could be seen directly; however, in this study and in typical indoor HDR methodologies, luminous overflow does occur. In order to account for the resulting errors of HDR photographs, the authors propose a method of identifying and correcting images that exhibit luminous overflow using an illuminance measurement taken at the same time as the photograph. Then pixels above an overflow threshold are adjusted to be brighter such that the calculated illuminance from the photograph ( $E_{v,image}$ ) becomes equal to the measured illuminance ( $E_v$ ). To do so, illuminance is calculated from the calibrated fisheye HDR photograph as in Equation 6.1,

$$E_{v,image} = \sum \cos \theta * L * \omega \quad (6.1)$$

where  $\theta$  is the incident angle of light arriving at the camera,  $L$  is the pixel luminance in  $\text{cd}/\text{m}^2$ , and  $\omega$  is the solid angle of the pixel in steradian. In this case, the incident angle and solid angle values for each pixel were determined using a Radiance angular fisheye view type (Ward, 1994). For a photograph to be a candidate for luminous overflow correction, the image-derived vertical eye illuminance must be less than the measured value. This procedure is described in Appendix B.2.

As pixels in a HDR photograph increase in luminance, the likelihood they indicate a luminous overflow increases in tandem. Each image is also analyzed to find its brightest pixels. This value is proposed to be at least  $10000 \text{ cd}/\text{m}^2$ , a value one order of magnitude above a diffuse portion of sky or typical indoor surface luminances, in order to suggest potential luminous overflow (see Appendix B.3).

Luminances greater than 95% of the observed maximum constitute an overflow threshold – the highest luminance at which the measurement was able to effectively resolve luminances. If pixels brighter than the overflow threshold identify an image area with a solid angle of 0.0002 str or greater in the field of view, then the image is likely to exhibit an overflow and is a candidate for correction (see Appendix B.4). For a 400 pixel radius fisheye HDR image, 0.0002 str is approximately 15 pixels. Figure 6.1 illustrates two cases of overflow analysis. In the case of 6.1a, the sun is directly captured and takes up a large amount of the visible area (0.001 str); it identifies a luminous overflow. In the case of 6.1b, a small specular highlight from a car across the street causes a single pixel to be at the overflow threshold (0.00001 str); it does not identify a luminous overflow. The 0.0002 str threshold allows the separation of larger areas of near-peak brightness (6.1a) and very small reflections (6.1b).

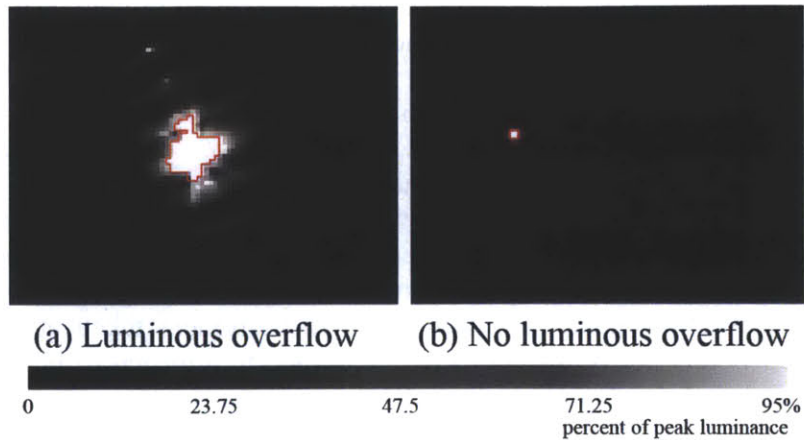


**Figure 6.1** Visual analysis of potential luminous overflows.  
 Pixels above the 95% luminance threshold are outlined in red.

Figure 6.2 plots the three factors used in identifying images exhibiting luminous overflow. The horizontal axis chronicles maximum pixel luminance while the vertical axis is the difference in percent between measured and calculated illuminance. Finally the size of the dots is relative to the solid angle of the overflow threshold. Images that were corrected for luminous overflow are colored in red. A general method for these corrections is outlined in Appendix B.5.

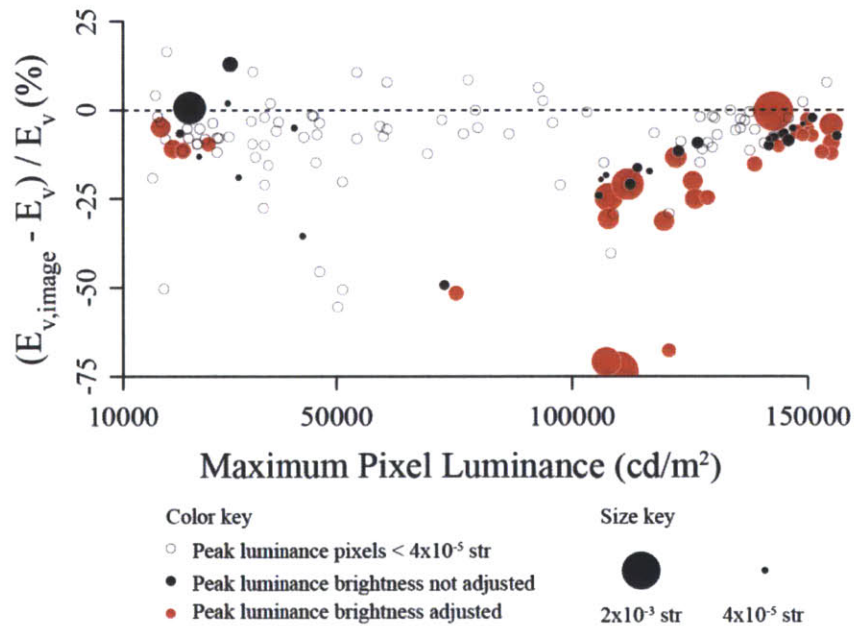


**Figure 6.2** Luminous overflow identifying factors.

## 6.2 Calculation of Image-based Analysis Metrics

Once the relevant images were corrected for luminous overflow, measured vertical eye illuminance ( $E_v$ , lx), discomfort glare calculations (DGP), the brightness of direct sunlight on the eye (maximum window luminance,  $\text{cd}/\text{m}^2$ ), the brightness of reflections from horizontal working planes (maximum workplane luminance,  $\text{cd}/\text{m}^2$ ), and monitor contrast ratio were collected. All

images were cropped to a 180 degree hemispherical view boundary and have a corresponding circular image mask applied. A method of implementing such masks is included in Appendix B.1.

### 6.1.1 Vertical Eye Illuminance

As mentioned previously, vertical eye illuminance is measured directly from an independent sensor, registering the sum luminous flux falling upon the sensor per area. The assumption in utilizing vertical eye illuminance is that with more light reaching the eye, the probability of experiencing discomfort is increased. As in the previous section, vertical eye illuminance can also be calculated from a fisheye HDR photograph.

### 6.1.2 Discomfort Glare

Discomfort glare is physical discomfort caused by extreme brightness, contrast or both. As previously in this research, the DGP metric is used to represent discomfort glare.<sup>20</sup>

### 6.1.3 Direct Sunlight

Direct sunlight falling on the workplane or the eye directly is likely to cause discomfort. IES standard LM-83-12 states that horizontal illuminance from direct solar exposure over 1000 lx, as derived using specific simulation parameters, is a good indicator for visual discomfort (IESNA 2012). Experience also shows that viewing the sun directly is uncomfortable. Using HDR photographs luminance, and therefore the intensity of direct light, can be directly measured. For this purpose, image masks are employed (see Appendix B.1) to account for maximum luminances originating from either the window (6.3b) or a horizontal working plane (6.3b).

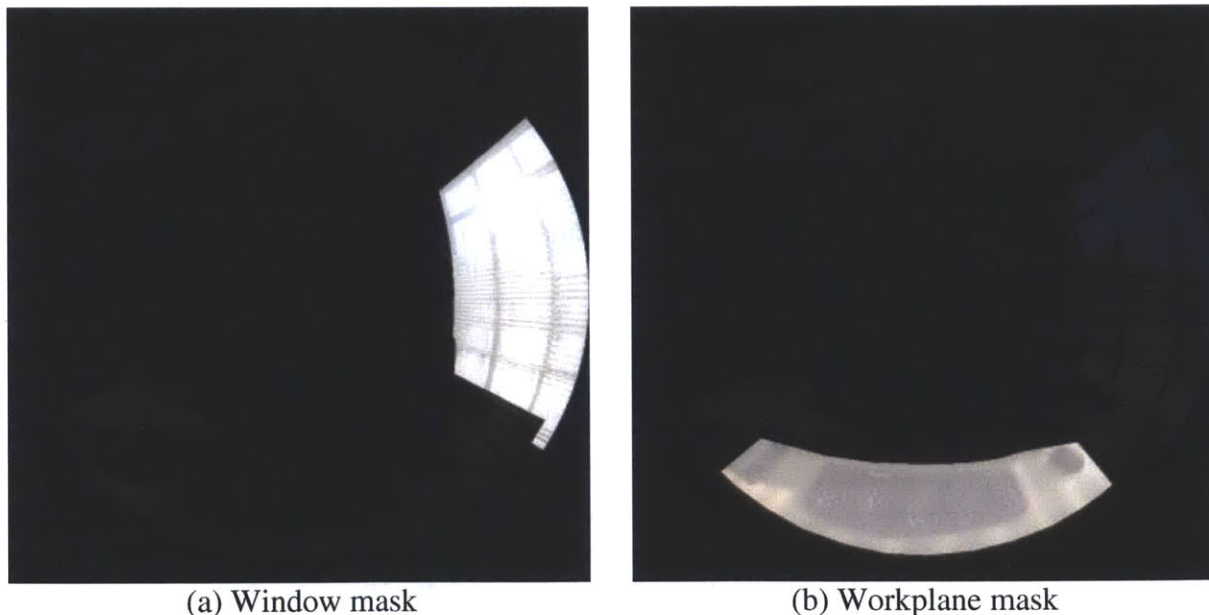


**Figure 6.3** Image masks employed for direct sunlight analysis.

---

<sup>20</sup> See Section 2.2.6.



### 6.1.4 Monitor Screen Visibility

Monitor contrast ratios are also calculated as described in Section 2.3. In this study,  $L_H$  and  $L_L$  were measured from a HDR photograph taken in the otherwise dark test room with the monitor turned on and a screen of text displayed, shown in Figure 4a.  $L_r$  was estimated for each HDR image by subtracting  $L_H$  from the maximum observed pixel brightness within the monitor mask (4b). It is noteworthy that there are some difficulties measuring monitor luminance using HDR photography. LCD pixels do not flicker during their refresh process as a CRT monitor does, which alleviates one traditional problem; however, even slight variations in viewing angle between the camera and the actual viewer can change the perceived and reflected luminance dramatically.

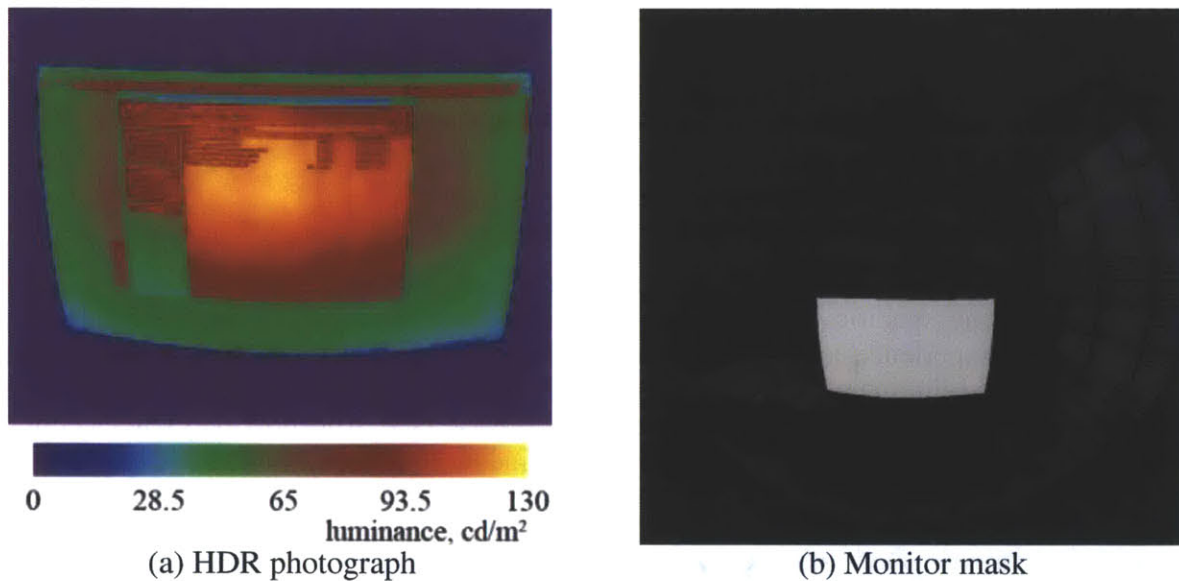


**Figure 6.4** Luminance data and image mask used in contrast ratio calculation.

## 6.3 Results

Figure 6.5 compares each of the individual analysis methods to the sum of the subjective questionnaire responses. High subjective responses (21) indicate comfort and the capability of performing office tasks. Low subjective responses (3) indicate uncomfortable lighting conditions that cause displeasure and negatively influence the ability to perform tasks. Green points represent times where participants adjusted the blinds to achieve ‘most preferable’ conditions. Red dots represent times where blinds were adjusted to achieve ‘just uncomfortable’ conditions. Black lines on the maximum window luminance and DGP plots indicate changes in values that occurred in photographs adjusted for luminous overflow using the proposed method.

The correlation between monitor contrast ratio and subjective comfort is very weak in this study ( $R^2 = 0.021$ ). This may be because the layout of the space is such that direct sunlight never falls on the monitor screen during the specific study conditions. Therefore contrast ratio may not correlate well with subjective measures in this particular study. Higher values of vertical eye illuminance contribute to a greater likelihood of discomfort ( $R^2 = 0.228$ ). Maximum luminance on the workplane, a proxy for direct sunlight, correlates noticeably with subjective discomfort ( $R^2 = 0.242$ ). Especially when reflected light from the desk entering the eye is  $1000 \text{ cd/m}^2$  or greater, discomfort is observed. Maximum window luminance, once accounting for luminous

overflow adjustments, suggests that a direct view of the sun would cause discomfort ( $R^2 = 0.199$ ). Without adjusting for luminous overflow, the  $R^2$  is only 0.082. Note that the horizontal axes of luminance are plotted logarithmically to correspond more readily with human perception. DGP, an evaluation of discomfort glare, has a correlation with subjective comfort nearly identical to maximum luminance on the workplane ( $R^2 = 0.242$ ). Without adjusting for luminous overflow, the  $R^2$  is 0.185. It is important to reiterate that DGP results should be evaluated within a very narrow range of values. Anything below 0.35 is likely to be ‘imperceptible’ to the average occupant, and anything above 0.45 is likely to be ‘intolerable’ (Wienold 2009).

A multiple linear least squares regression was performed using vertical eye illuminance,  $\log_{10}$ (maximum workplane luminance),  $\log_{10}$ (maximum window luminance) and DGP. Monitor contrast ratio was not included in the model due to the aforementioned lack of direct lighting on the monitor during the analyzed most preferred and just uncomfortable conditions used in the study. Table 6.1 shows the regression outcome with  $\log_{10}$ (maximum workplane luminance) being the most critical factor. The  $R^2$  value of the regression model is 0.322, and the model predictions are compared to the survey data in Figure 6.6.

**Table 6.1** Regression coefficients.

<b>Name</b>	<b>Estimate</b>	<b>Pr(&gt; t )</b>
Intercept	23.5781347	< 2e-16
DGP	-5.9043087	0.4156
$\log_{10}$ (Max. Window)	-0.5185797	0.4363
$\log_{10}$ (Max Workplane)	-2.0821229	0.0004
$E_v$	-0.0006597	0.3198

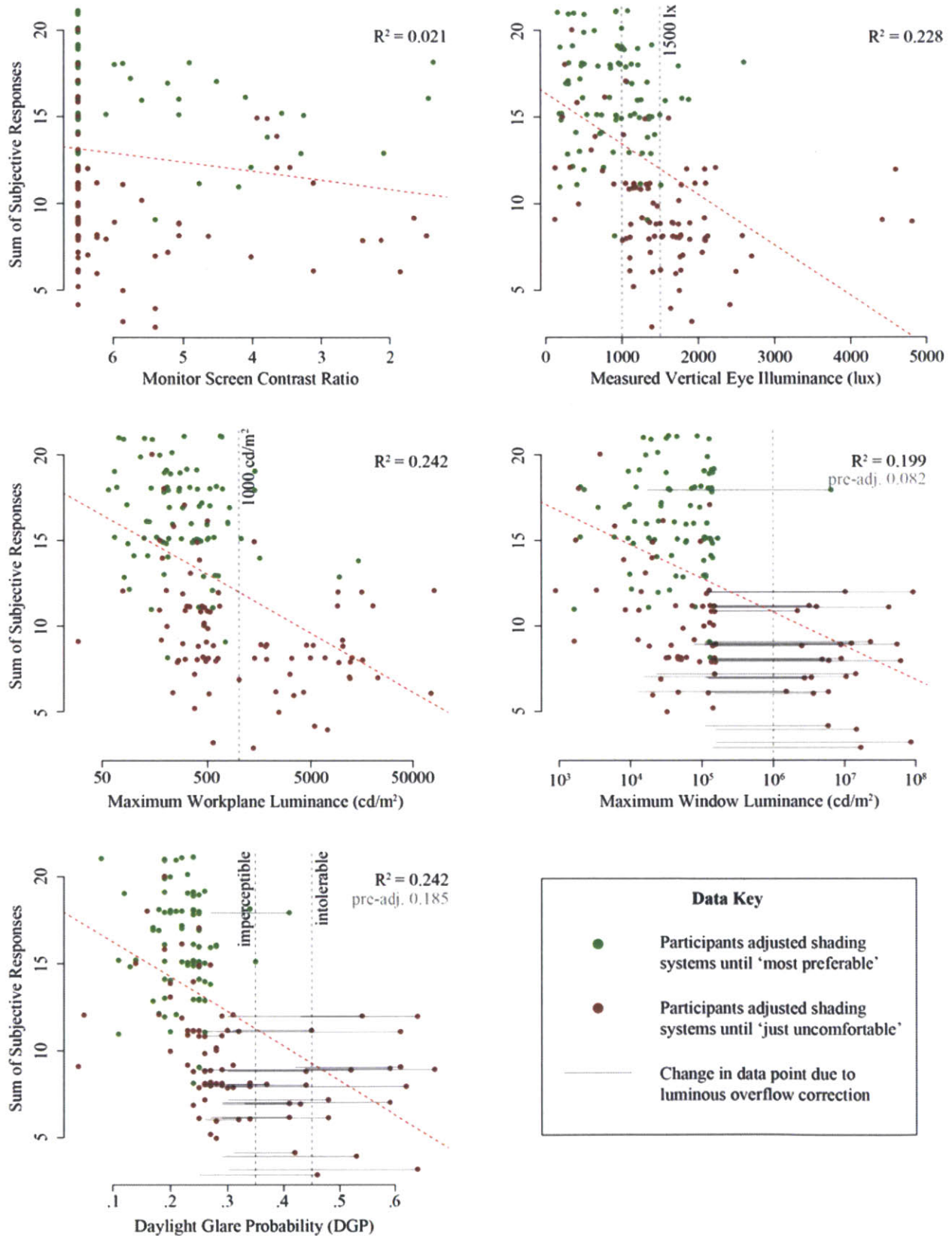


**Figure 6.5** Single analysis metrics related to participant comfort evaluations



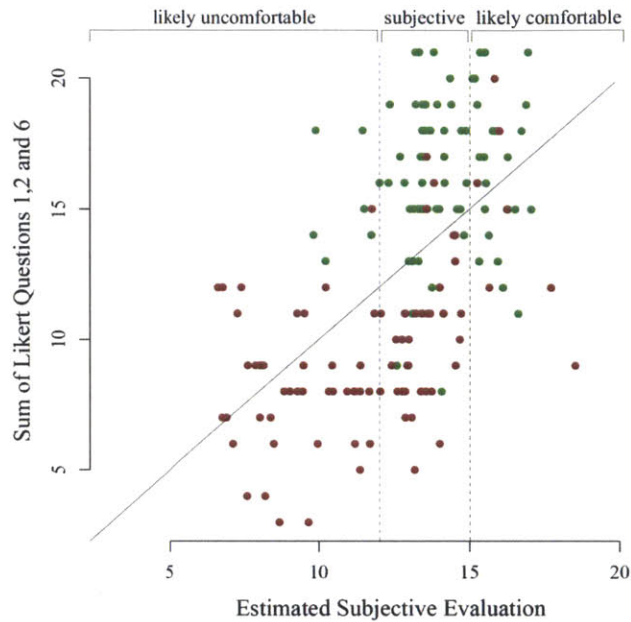


**Figure 6.6** Regression model predictions plotted against actual subjective responses.

## 6.4 Discussion

### 6.4.1 Identifying Subjective Discomfort Thresholds

Overall, Figure 6.5 illustrates that no individual measure is likely to fully explain subjective human comfort. Van Den Wymelenberg and Inanici (2014) noticed, in an independent analysis of the dataset, that vertical eye illuminances below 1000 lx correspond with comfortable subjective evaluations, while subjective responses at illuminances greater than 1500 lx grow increasingly uncomfortable. This study notices the same, and illuminances between these two thresholds contain the entire subjective range of discomfort reported by occupants. This suggests a relationship between increased mean brightness in the field of view and comfort but leaves a subjective range where some participants feel comfortable or uncomfortable at similar measured values. It seems likely that specific measures occurring within this range of vertical eye illuminance such as task visibility, contrast or the presence of direct sunlight may aid the identification of uncomfortable scenes. These other measures are portrayed in Figure 6.5 such as maximum task and window luminances (direct sunlight) and DGP (discomfort glare, contrast) clearly suggest threshold values that when exceeded are nearly certain to cause discomfort. For example, DGP values greater than 0.4, maximum window luminances above  $10^6$  cd/m<sup>2</sup>, and maximum workplane luminances above 1000 cd/m<sup>2</sup> are primarily observed in cases where the sum of subjective evaluations are less than 12. Such thresholds can be used as inputs to long-term visual satisfaction predictions such as those proposed in Chapter 5.

The intriguing thing about these measures is that they do not necessarily occur at the same time. For example, direct sunlight on the workplane can occur when an occupant may not see the sun directly through the window. In the same manner, strong contrast in the scene that leads to an uncomfortably high DGP calculation can occur separately from a low monitor contrast ratio depending on whether glaring sources are located in front of or behind the occupant as the solar position changes over time.

The low  $R^2$  value from the multiple linear regression model (Table 6.1, Figure 6.6) might be expected since the model attempts to quantify highly subjective human phenomena. Still, Figure 6.6 illustrates that there are thresholds where the regression model predictions could be considered 'likely comfortable', 'subjective' or 'likely uncomfortable,' similar to the bounded borderline between comfort and discomfort concept (Luckiesh & Guth 1949; Van Den Wymelenberg & Inanici 2014). However, if we consider that a subjective answer of 12 – an average equating to 'neither agree nor disagree' – is at the borderline of discomfort and answers above 12 are at least moderately positive, the previously identified subjective thresholds can be tested against whether they identify scores which are uncertain to uncomfortable (score  $\leq 12$ ) or comfortable (score  $> 12$ ). Using this set of criteria, 74.4% of scenes are correctly identified.

#### *6.4.2 Application to Design*

Associating occupant's subjective impressions of spaces with objective measures has a broader application than to HDR photographic documentation of existing spaces. Many software platforms are capable of accurately simulating renderings with associated luminance information, and some can produce annual sets of physically-based luminance renderings (McNeil 2013). The renderings from such programs are functionally identical to the calibrated HDR photographs used in this study, and they can be analyzed in the same manner; however, many realistic (and reflective) details of the physical world such as puddles, cars, and snow are omitted in typical simulation processes. By applying the earlier discussed subjective thresholds to simulated spaces, it is possible to identify likely uncomfortable conditions in daylit spaces throughout the year and to address them before construction and potentially without the use of operable shading devices.

#### *6.4.3 Research Limitations*

Chapter 5 found that occupants in daylit spaces describe a number of sources of discomfort when asked, including reflections from the monitor. From the survey of 90 students in a sidelit, toplit and electrically lit space, 25 (27.8%) identified an inability to see the content on their monitor screens as a significant cause of dissatisfaction. Because the qualities of the space in this study do not allow direct light to fall upon the monitor during the evaluation conditions of interest, the authors suggest that similar studies in varied space types may prove useful. Furthermore, Van Den Wymelenberg and Inanici (2014) note that, of the established metrics that can be calculated from an occupant's view, vertical eye illuminance correlates most strongly with the subjective evaluation that the monitor is legible. It is therefore plausible that both larger amounts of light in the scene and the amount of light reaching the eye contribute in part to this evaluation.

This study is based on data from a sidelit space with the view direction parallel to the window. DGP was derived in sidelit spaces with view directions perpendicular to the window. Keeping with the comments in the preceding paragraph, it is likely the case that full applicability for certain visual comfort measures may not be understood until a broader variety of space types are investigated.



#### 6.4.4 Luminous Overflow Methodology

The luminous overflow methodology utilized in this paper is reasonable, but necessarily spreads out the solar or specular brightness across all pixels above the overflow threshold. Further research is warranted in order to check its reliability compared to more accurate but onerous capture methods such as using multiple apertures (Stumpf et al. 2006). Still, its effect upon the results in terms of increased correlation shows the method has promise; the  $R^2$  for maximum window luminance predicting subjective responses increases from 0.082 to 0.199, and for DGP increases from 0.185 to 0.242. 10.1% of photographs were corrected for luminous overflow (17/168). In order to investigate the uncertainty of this method, a small experiment was performed. Three HDR photographs were taken in an office space with direct sunlight incident upon the exterior façade; these photographs are compared in Figure 6.6. The first photograph (6.6a) uses a multiple-aperture capture method (Stumpf et al. 2006; Inanici 2010) where fast exposures were taken at f4 and f16 apertures in order to resolve the high luminance of the sun. The second photograph (6.6b) was taken using a more normative capture methodology using only a f4 aperture. Finally, the third photograph (6.6c) was also taken using a f4 aperture, but with the blinds down such that no direct sunlight enters the space. None of these photographs use a neutral density filter as proposed by Stumpf and colleagues, under the assumption that the window's attenuation of light and low-emissivity coatings would suffice to protect the camera sensor. Measured illuminance at the front of the camera lens was also collected at the time each photograph was taken.

The photograph of the room with shades drawn (6.6c) has a HDR-calculated vertical eye illuminance value of 676 lx, 97.1% of the 696 lx measured value. This image functions as a sort of control and assurance against errors in the HDR capture methodology. The shaded image is a good indication of accuracy at non-extreme luminance values and that pixel luminances do not reach an overflow threshold. The single-aperture capture (6.6b) has a maximum luminance of 262,013  $\text{cd}/\text{m}^2$  and only resolves 52.2% of measured illuminance. The multi-aperture capture (6.6a) identifies a peak luminance of 3,489,626  $\text{cd}/\text{m}^2$  and resolves 64.1% of measured illuminance. Comparing the two photographs capturing the visible sun, it is clear that the multi-aperture method measures more, but not all, of the solar brightness. Also, while the camera was not damaged by the direct sunlight, the large amount of lens flare and inability to capture the solar luminance even using a f16 aperture and exposure time of 1/8000 s suggests that a neutral density filter could be appropriate even in an indoor setting.



(a) Multi-aperture capture method (f4 + f16)      (b) Single-aperture capture method (f4)      (c) Single-aperture shaded capture (f4)

<i>Measured Ev</i>	19000 lx	18960 lx	696 lx
<i>Calculated Ev</i>	12183 lx	9901 lx	676 lx
<i>DGP</i>	0.96	0.82	0.34
<i>Max. Lum.</i>	3,489,626 cd/m <sup>2</sup>	262,013 cd/m <sup>2</sup>	10,002 cd/m <sup>2</sup>

**Figure 6.6** Series of high dynamic range photographs taken to investigate the efficacy of the luminous overflow method.

The luminous overflow methodology was applied to the single-aperture photo (6.6b) in order to increase the luminance of pixels brighter than the overflow threshold in order to achieve calculated vertical eye illuminances of 12183 lx as in 6.6a and 18960 lx as measured. This is presented visually in Figure 6.7. As noted previously, the pixels greater than the overflow threshold constitute a larger solid angle than the actual solar disk; therefore, correcting the single-aperture photo to an illuminance of 12183 lx, increases a larger area to a less bright luminance (6.7c), 663,106 compared to 3,489,626 cd/m<sup>2</sup>. Even still, this luminance is clearly bright enough to cause visual discomfort, and DGP values calculated for the multi-aperture method and the single-aperture method corrected to 12183 lx are very similar, 0.96 compared to 0.97. The photograph corrected to the measured illuminance (6.7d) simply has its brightness increased further, resulting in greater maximum luminance and DGP values.

The concern with images corrected for luminous overflow is a lack of certainty about the distribution and intensity of extreme luminances surrounding the sun and bright specular reflections such as those from the desk seen in 6.7a. The spread of solar luminance can have a large effect, because the DGP equation uses the square of luminance multiplied by the solid angle.<sup>21</sup> It is likely that the single-aperture correction (6.7c) agrees with the multi-aperture value because specular reflections from the desk were also above the overflow threshold. Still, an increase in DGP of 0.18 (from the original single-aperture method to its corrected value) is enough to move from imperceptible glare to intolerable (a difference of 0.10), and it is probably warranted to account for this potential difference when possible rather than ignoring potential glare sources. With regards to future HDR photography, it is prudent to use a lens filter in order to avoid lens flare and to enable a fuller range of luminous capture by attenuating the light entering the camera lens.

<sup>21</sup> See Section 2.2.6.

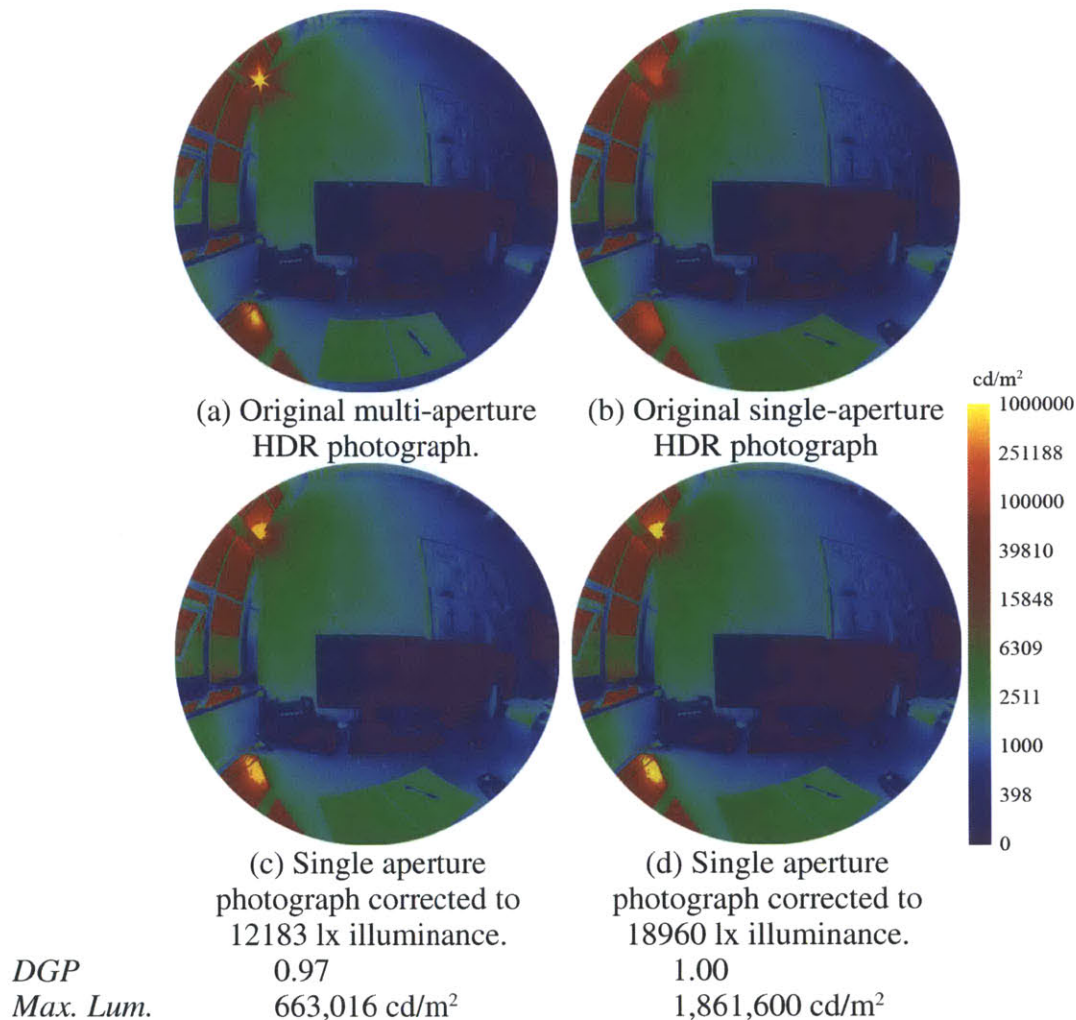


**Figure 6.7** Falsecolor luminance visualizations of the original multi and single-aperture images and two corrected single-aperture images using the proposed overflow correction methodology.

## 6.5 Conclusion

This chapter uses a set of plausible metrics from practice and research to analyze a set of 168 HDR photographs of daylit interior office scenes with associated subjective user survey data on visual comfort. A method for the standardized identification and correction of ‘luminous overflow,’ which can occur when very bright light sources or reflections exceed the capacity of measurement equipment to capture them, is proposed and implemented. The results identify several subjective thresholds that indicate discomfort in the participant study:

- vertical eye illuminances greater than 1500 lx,
- DGP values greater than 0.4,
- window luminances greater than  $10^6$  cd/m<sup>2</sup>,
- and workplane luminances greater than 1000 cd/m<sup>2</sup>

Monitor contrast ratio weakly correlates with subjective evaluations in this study, potentially due to the spatial qualities of the test rooms. Combined, the four thresholds correctly

identify 74.4% of subjective evaluations when classified as neutral to negative (subjective score  $\leq 12$ ) or positive (score  $> 12$ ). This result supports Chapter 5's long-term analysis of visual satisfaction in a complex daylight space, which found good agreement using similar metrics. The establishment of the above thresholds and proposed methods of image processing for HDR photographs and renderings will help to evaluate instantaneous subjective visual comfort as well as to analyze annual discomfort from luminance simulations.

### *6.5.1 Future Outlook*

Beyond the desire to apply similar research methods to a variety of spatial typologies expressed in the research limitations section, consideration of view in visual comfort analysis is another important factor. Chapters 3 and 4 showed that within a space, even small changes in view can have a large effect on various visual comfort metrics. Sarey Khanie and colleagues (2013) note that space occupants focus on different areas depending on task and lighting quality in a space, which influences discomfort glare metrics such as DGP. Using the same dataset as this chapter, Van Den Wymelenberg and Inanici (2014) found that the perceived brightness of a view towards the window rather than parallel to it correlated better with other subjective measures, leading them to propose an 'inverse adaptive zone' where the least comfortable view might be the most useful to consider when evaluating a design. In light of this study and these other emerging research projects, it seems necessary to consider view in both future research and future simulation of visual environments.





## Chapter 7

# Disability Glare

Chapters 3 through 6 describe studies of discomfort glare in various settings. However, only Chapter 5 is an analysis of a real discomfort condition as Chapter 6 describes a laboratory study. And in Chapter 5, no design recommendations are made as the intent was purely to document the conditions of the space. In contrast, Chapter 7 intends to take the ideas of luminance-based analysis from the previous chapters and apply them to the study and design remediation of a real disability glare situation.<sup>22</sup>

New constructions such as photovoltaic (PV) panels or buildings can cause glare due to intense reflections of sunlight from their surfaces. Such reflections can literally occur in blinding quantities, preventing occupants from performing tasks. This effect is known as disability glare.<sup>23</sup> To remedy such issues after construction is expensive, and those affected must tolerate the glare until the problem is remedied. In order to address the issue of glare hazards from new constructions, this chapter presents a general method for analyzing glare potential based on three-dimensional (3D) models produced during the design phase, measured material properties and physically accurate lighting simulations.

The new method is presented through a case study analysis of glare at an airport caused by intense reflections from a PV array consisting of 2,478 panels located between the airport's air traffic control tower (ATCT) and an airplane taxiway. Specular reflections from the PV array are

---

<sup>22</sup> The work presented in this chapter was originally presented as,

Jakubiec, J.A. & Reinhart, C.F., 2014. Assessing disability glare potential due to reflections from new constructions: A case study analysis and recommendations for the future. In *Proceedings of the Transportation Research Board 93rd Annual Meeting*. Washington DC.

and has subsequently been accepted for publication in the 2014 series of the *Transportation Research Record: Journal of the Transportation Research Board*. The material from the paper is reproduced here with the permission of the Transportation Research Board.

<sup>23</sup> See a complete discussion in Section 2.5.



so extreme that they prevent the visibility of aircraft on the taxiway and cause temporary after images that impede the viewing of computer monitors inside the ATCT. As such, the reflections at the case-study airport meet the qualifications to be considered disabling.

The PV array was analyzed according to Federal Aviation Administration (FAA) best practice guidelines for the installation of solar technologies prior to its construction; however, the original analysis did not detect the glare hazard. Thus, there is a need to define a clear process through which to conduct glare prediction analysis that is useful during the design of new constructions that have the potential to reflect large quantities of daylight. A case study approach is taken to address this need through an analysis of the airport's glare problem. First, a review of existing methods for analyzing glare from specular surfaces is conducted. Following that, the problem is reproduced in a physically-based daylighting simulation software capable of predicting reflections from new designs before they are constructed. The simulations use physically accurate material models that account for specular and diffuse reflective surface properties of PV panels. Side-by-side comparisons of high dynamic range (HDR) photographs and physically-based renderings confirm the accuracy of these models. Next, an annual analysis is conducted using a ten-minute simulation interval for every daylit hour in the year. Following this, the likelihood of experiencing disability glare is displayed spatially and temporally in order to understand the time, location and intensity of potential glaring reflections. Finally, the new method is used to analyze proposed remediation strategies of the disability glare problem at the case-study airport.

## 7.1 Qualifying Disability Glare due to Specular Reflections

### 7.1.1 Disability Glare at the Case-study Airport

To document the disability glare problem, HDR photographs calibrated to physical light levels were taken from the case-study airport's ATCT. Calibrated HDR photographs record the brightness of each pixel in a photograph, and can be used to calculate the likelihood of discomfort or disability glare at the time the photograph was taken. Figure 7.1 illustrates one such photograph with spot brightness values measured at the red squares and indicated in units of luminance (candela per square meter,  $\text{cd}/\text{m}^2$ ). The method used to create such images relies upon capturing several exposures with known shutter speeds and lens apertures. Afterwards the photos are composited and calibrated to physical values using a camera-specific calibration function based on measured luminance data. Inanici found this method to have an average error of 5.8% for outdoor scenes and 10.1% for daylit interior scenes (2006). The resulting HDR photograph is stored in the Radiance RGBE image format, a lossless format where each pixel corresponds to a physical value.<sup>24</sup> A Konica Minolta Ls-110 spot luminance meter was used to calibrate the HDR images and to verify that values above  $250,000 \text{ cd}/\text{m}^2$  were observed reflected from the PV panel installation.

---

<sup>24</sup> See Section 2.7.3.





**Figure 7.1** High dynamic range photograph of glare problem taken on August 30<sup>th</sup>, 2013 at 7:22 solar time.

These ultra-bright reflections cause disability glare, preventing air traffic controllers from seeing aircraft on the taxiway. During glaring periods, controllers report an inability to see the taxiway and experience after-images subsequent to looking at the portion of the taxiway obscured by the reflections. Of the taxiway's 2900 m length, 900 m have the potential to be obscured by glare from the PV array, illustrated in Figure 7.2. The potentially obscured area therefore accounts for a centrally located 31% of the taxiway.



**Figure 7.2** Potential areas of obscured runway.

Most indoor surfaces, with the exception of areas illuminated by direct sunlight, shown in Figure 7.1, have luminances below  $300 \text{ cd/m}^2$ . Outdoor objects are often brighter than these reference interior surfaces. At the time of observation, outdoor surface luminances were between  $2,475$  and  $10,900 \text{ cd/m}^2$ . The sun, even partially obscured by the shading system, is very bright and over  $6,000,000 \text{ cd/m}^2$ ; however, it is not directly in the field of view when looking toward the taxiway. The very bright ( $> 250,000 \text{ cd/m}^2$ ) reflections from the PV panels are located in the field of view when looking toward the taxiway and take up a much larger perceived size in the field of vision than the sun. The growth in size compared to that of the sun is due to an effect known as forward scattering. Forward scattering is when a reflected direct light source is spread out in an angular opening area due to roughness and sub-surface scattering properties of the reflecting material. When an extremely bright light source such as the sun is spread across a large surface area due to forward scattering, extreme discomfort or visual disability is likely to occur.

### 7.1.2 Dynamic Range of Human Vision

To assess the impact bright specular reflections have on perception, considering the physiology of human vision is useful. The eye is a logarithmic sensor capable of perceiving 12 log units of luminance; however, human vision is only capable of resolving a small portion of the luminous scale at any given time based on the visible luminous environment (Boyce 2003). Specifically, the adaptation luminance is the brightness level the eye is adapted to that determines what luminous range is perceivable.

Ferwerda and colleagues suggest that the adaptation luminance should be half of the brightest visible object (1996); however, this works primarily for normal viewing conditions where glaring reflections are not present. In the case of disability glare analysis, it makes sense to choose the adaptation luminance relative to the desired tasks. From Figure 7.1, the monitor ( $255 \text{ cd/m}^2$ ) is the lowest task luminance level; however, the darker portions of the monitor are as dim as  $30 \text{ cd/m}^2$ . The highest task luminance level is the taxiway ( $8,901 \text{ cd/m}^2$ ). In this case the adaptation luminance would be roughly  $4,500 \text{ cd/m}^2$ . Considering this adaptation luminance, between two and three orders of magnitude of luminous difference can be visualized (Boyce 2003; Hopkinson & Collins 1970) – enough to see the darkest portions of the monitor and the bright taxiway.<sup>25</sup>

What happens when the PV panels reflect the sun? If one begins with the darker portions of the monitor ( $30 \text{ cd/m}^2$ ), between two and three orders of magnitude place the extreme upper limit of vision somewhere below  $30,000 \text{ cd/m}^2$ . Therefore a brightness of  $30,000 \text{ cd/m}^2$  is proposed as a threshold at which the probability of experiencing disability glare is likely. It should be noted that the proposed value of  $30,000 \text{ cd/m}^2$  is not an absolute threshold as vision varies from person to person, but it is a useful value that will cause discomfort for the majority of humans. The measured value of  $250,000 \text{ cd/m}^2$  from the PV panels in Figure 7.1 is also well above this threshold. Although the sky is very bright and often above  $30,000 \text{ cd/m}^2$ , the operable shades present in the ATCT can be used to block the brightness of the sky; however, they cannot be lowered to obstruct the PV array without also blocking the taxiway (see the label, useful range of shade from Figure 7.1). Until the glare problem is remedied, the airport is covering the PV array with tarps, which prevents disability glare but has the side effect of also preventing the generation of electricity.

---

<sup>25</sup> See Figure 2.1.

### 7.1.3 Existing Disability Glare Metrics from Specular Reflections

The FAA defines interference from solar panels concerning airspace penetration, reflectivity, and communication systems interference (Federal Aviation Administration, Office of Airports & (APP-400) 2010). As this analysis relates to visual disability, the regulations dealing with reflectivity are of interest. All solar installations at airports must include an “assessment of reflectivity including time periods when reflection may contact [the ATCT] and aircraft.” The FAA provides three methods of analyzing potential glare problems:

1. A qualitative analysis of potential impact in consultation with [air traffic control staff], pilots, and airport officials,
2. a demonstration field test with solar panels at the proposed site in coordination with FAA Tower personnel or,
3. a geometric analysis to determine days and times when an impact is predicted.

Method 1 is potentially inadequate as the involved parties may not have the experience or the ability to assess the potential glare hazards involved with the proposed PV system. Method 2 is inadequate as the field test is performed during a single moment; however, the sun changes position in the sky throughout the entire year. A test at a single time may miss glare hazards during other parts of the year. Method 3, geometric analysis, could analyze potential glare hazards throughout the year; however, there is currently no guidance on its implementation beyond two example figures that portray a perfectly specular reflection at four times during the year as if from a mirror. Such an analysis ignores potential glaring reflections during other times of the year. More importantly, a purely specular geometric analysis neglects the true behavior of reflected light from PV panels. Such an analysis could miss identifying potential glare hazards where an analysis that considers forward-scattering when daylight is reflected would not.

Ho et. al propose a geometric analysis method that accounts for forward-scattering as well as the form of a reflecting surface in order to assess glare hazards (2011). The result of their geometric calculation is evaluated using irradiance at the retina and the size of the glaring source. It is based on previous research on the physiology of the human eye to experience after images and retinal burning. The method is useful for detecting problems and quickly iterating through solutions; however, it does not provide spatial feedback regarding the origin of glare at any given time.

## 7.2 Methodology

In order to analyze the current glare situation at the airport, the authors created a high-quality daylight simulation model of the ATCT, PV array, taxiway and surrounding buildings. The simulation environment used is the physically-based backward raytracer Radiance, developed at Lawrence Berkeley National Laboratory (Ward 1994). Radiance is a reasonable choice as it allows users to set up custom materials based on optical measurements (Reinhart & Andersen 2006) and has been validated by numerous studies.<sup>26</sup>

Unfortunately, detailed measured reflection data for PV panels is largely unavailable. The best practice method for resolving the complex, angular-dependent reflections from objects such as PV panels would be to use costly goniophotometer measurements (Apian-Bennewitz 1998). Goniophotometer measurements have been used to show that measured reflections can differ from standard material models by over two orders of magnitude, especially at shallow incident

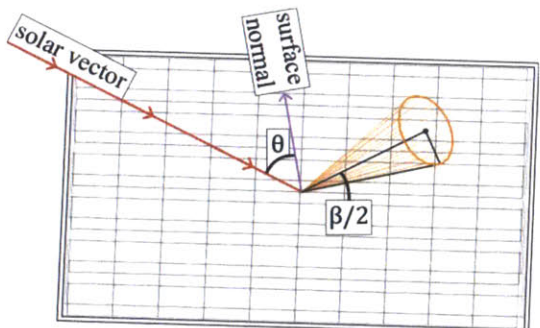
---

<sup>26</sup> See Section 2.7.1.



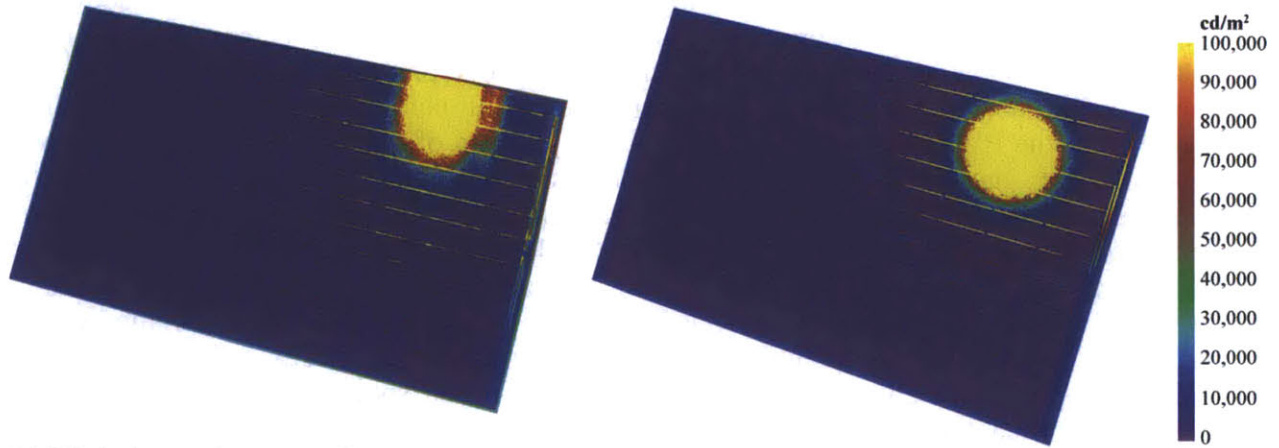
angles of sunlight (PAB Advanced Technologies Ltd. n.d.). As such measurement devices were not available for this study, measurements were taken of the installed PV panels using a Konica Minolta 2600d portable spectrophotometer and HDR photography as documented in Table 7.1. The spectrophotometer measurements characterize the overall percentage of diffuse and specular reflection from the PV panel surface sampled at every 10 nm of the visible spectrum; however, the instrument is unable to resolve information about the amount of forward-scattering of specular reflections from the panel at differing incident angles of sunlight. Therefore forward-scattering properties were quantified based on HDR photography taken with the sun at a near-normal incidence (12 degrees) to the panel and at an oblique angle (76 degrees). This results in beam spread angles described in Table 7.1, which were translated into the Ashikhmin-Shirley material type in Radiance (Ashikhmin & Shirley 2000; Ward 2013). The Ashikhman-Shirley material description is useful as it allows separate diffuse and specular reflection parameters, which vary significantly in the measured PV panel data. The measurements found a total beam spread angle of between 2.0 and 9.2 degrees depending on the incident angle and area-weighted diffuse and specular reflectances of 8.67 and 5.58 % respectively.

**Table 7.1** Measured properties of PV Panel



Angle from normal solar incidence ( $\theta$ )	Half beam spread angle ( $\beta/2$ )	Ashikhman-Shirley specular exponent
12 deg.	1.0 deg.	3500
76 deg.	4.6 deg.	175
Measured area and type	Reflectance	Relative area
PV Cells Diffuse	2.56%	84.80%
PV Cells Specular	4.12%	
White Areas Diffuse	45.13%	5.62%
White Areas Specular	4.52%	
Silver Strips Diffuse	18.63%	4.47%
Silver Strips Specular	36.40%	
Frame Diffuse	61.23%	5.11%
Frame Specular	3.97%	
<b>Area-Weighted Diffuse</b>	<b>8.67%</b>	
<b>Area-Weighted Specular</b>	<b>5.58%</b>	

Figure 7.3 portrays an example HDR photograph of the PV panel (7.3a) and a rendering using the Radiance software and the author’s custom materials (7.3b) displayed in falsecolor. In a falsecolor rendering, the color of each pixel corresponds to a physical luminance value in  $\text{cd}/\text{m}^2$  as indicated by the colorbar scale. Such falsecolor imagery constitutes a way to assess large luminous ranges visually as they vary across a calibrated photograph or physically-based rendering. For example, yellow areas in Figure 7.3 reflect greater than or equal to  $100,000 \text{ cd}/\text{m}^2$  while dark blue areas reflect approximately  $10,000 \text{ cd}/\text{m}^2$ . The photograph and the rendering were captured and rendered under similar clear sky conditions. Visually, the behavior of the simulation closely mimics that of the actual panel.



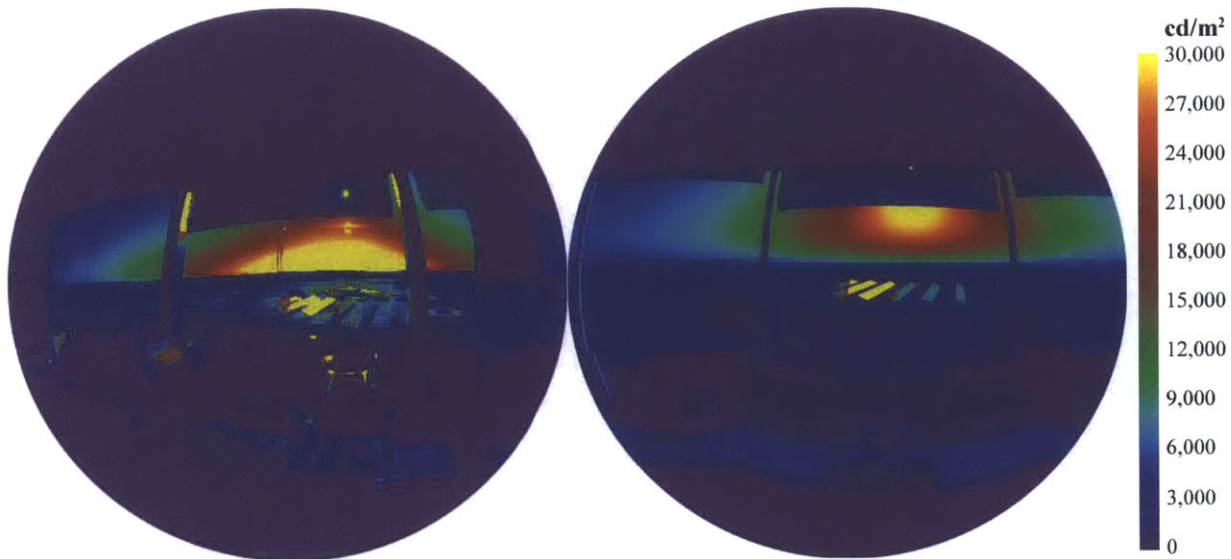
(a) High dynamic range photograph taken on August 31st, 2012.

(b) Physically-based rendering under ideal CIE clear sky conditions with sun.

**Figure 7.3** Photographed and rendered falsecolor images of a single PV panel with the sun at near-normal incidence.

Apart from appropriate material descriptions, a geometrically precise 3D model is necessary to accurately reproduce the observed glaring conditions in the Radiance simulation environment. A 3D model was provided by the US Department of Transportation's (DOT) Volpe center and was translated by the authors into the Radiance format. Using the 3D model and the detailed material definitions described previously, it is possible to predict the probability of disability glare for every daylight hour in the year. As a proof of concept, a HDR photograph and a Radiance rendering using the same daylight condition are compared in Figure 7.4. 7.4a is a HDR luminance photograph taken at 7:22 solar time on the morning of August 30<sup>th</sup>, 2012 from the ATCT viewing the taxiway. The image is displayed such that yellow areas correspond to brightnesses greater than 30,000 cd/m<sup>2</sup>. A rendering simulated at the same time is shown in 3b. Careful comparison of Figures 7.4a and 7.4b shows a very good agreement of areas greater than 30,000 cd/m<sup>2</sup>. There are some differences between the luminance distribution of the measured sky and idealized CIE clear sky, but from the point of view of observers in the control tower, bright skies can be reduced utilizing movable shades (Figure 7.1). Using this calibrated model, it is possible to simulate the intense solar reflections from the PV panels at any time during the year in a few seconds.





(a) HDR photograph taken on 8-30-2012 at 7:22 solar time. (b) Physically-based rendering simulated for 8-30-2012 at 7:22 solar time.

**Figure 7.4** Imagery of glare issues seen from the ATCT.

The glare potential for every ten minutes in the year was analyzed assuming a CIE clear sky (Commission Internationale de l’Eclairage 1996) distribution as a ‘worst case’ scenario when the sun is present and the sky is free of clouds. The analysis therefore yields the times in the year during which glare could be caused by direct sunlight being reflected from the PV panels and does not account for overcast or cloudy days.

### 7.3 Results

In order for glare analysis to be meaningful, it is necessary to know when the glare occurs and from where it originates. To accomplish this, the analysis results are displayed temporally and spatially. This dual display is useful to assess the extent, location, and time of occurrence of disability glare. Figure 7.5 illustrates a falsecolor plot showing the perceived size of glaring reflections over 30,000 cd/m<sup>2</sup> for every ten minutes in the year. The horizontal axis contains one column for every day, the vertical axis a row for each ten minute interval, and the colors correspond to the perceived size of the glare source in solid angle steradian (str). Figure 7.5 suggests that significant, disability glare producing reflections will occur in the control tower on clear days from mid-February to mid-October between about 6 to 8 AM solar time. In order to assess this chart, it is useful to note that the solid angle of an idealized viewing hemisphere is  $2\pi$  str, and the solid angle of the sun viewed from Earth is roughly  $6 \times 10^{-5}$  str. Annually there are 3.57 str-hrs of glaring area caused by the PV panels in the line of sight to the taxiway. This can be compared to the visibility of the sun from the ATCT of 0.18 str-hrs annually. The reflections account for a nearly 20-fold increase. The photo and rendering in Figure 7.4 portray a solid angle of  $9 \times 10^{-3}$  str, roughly 15 times larger than that of the sun, but located in the line of sight to the taxiway.



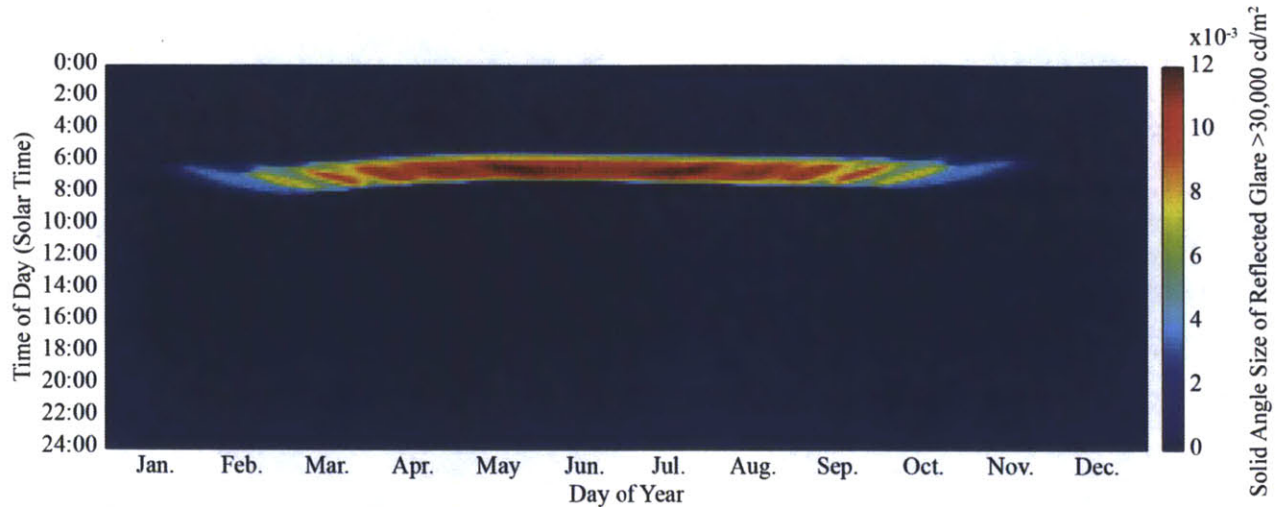


**Figure 7.5** Annual temporal map showing the perceived size of reflections greater than 30,000 cd/m<sup>2</sup>.

The metrics of Ho, et al. (2011) can also be calculated using input from rendered images. The benefit of rendering physically-based images rather than using geometric results is that images provide spatial feedback that reveals the causes of disability glare while geometric calculations alone do not. For example in Figure 7.4, it is evident that disabling glare originates from the center of the PV array; however, a geometric method would only report that there is glare, not its location or intensity. To calculate Ho and colleagues' metric, the size of the glaring source in rendered images must be converted from a three-dimensional solid angle to a two-dimensional angle in radians. This is achieved using Equation 7.1 where  $\Omega$  is the solid angle of the glaring reflection and  $\omega$  is its equivalent in radians. The diameter of the image projected on the retina ( $d_r$ , m) can be calculated using Equation 7.2. Finally, the retinal irradiance ( $E_r$ ) is a function of a 0.5 transmission factor, the irradiance at the cornea ( $E_c$ , W/m<sup>2</sup>) and the diameter of the pupil when exposed to daylight (0.002 m) as shown in Equation 7.3. Using the visual conditions of Figure 7.4 as an example, there is a solid angle of  $9.5 \times 10^{-3}$  str brighter than 30,000 cd/m<sup>2</sup>. Using Equation 7.1 renders an angle of  $1.1 \times 10^{-1}$  rad, which equates to a  $1.9 \times 10^{-3}$  m diameter projection onto the retina. Finally, the mean irradiance at the cornea is 940 W/m<sup>2</sup> as derived from the simulations using Radiance's 179 lm/W luminous efficacy for ideal sky models. It is worth noting that real skies have varying luminous efficacies. Plugging these values into Equation 3 gives a retinal irradiance of 522.8 W/m<sup>2</sup>. Using Ho and colleagues' metric, this irradiance and retinal projection is likely to cause after-images (2011).<sup>27</sup>

$$\omega = 2 \cos^{-1} \left( 1 - \frac{\Omega}{2\pi} \right) \quad (7.1)$$

$$d_r = 0.017\omega \quad (7.2)$$

$$E_r = 0.5E_c \left( \frac{0.002^2}{d_r^2} \right) \quad (7.3)$$

<sup>27</sup> See Section 2.5.

Supplementing the temporal map of Figure 7.5, Figure 7.6 shows in falsecolor the location of glaring reflections throughout the year in hours above 30,000 cd/m<sup>2</sup> with the scale ranging between 0 and 60 hours. Purple-colored areas cause no glare, and yellow-colored areas cause 60 or greater hours of glare annually. As each rendered photograph in the Radiance RGBE image format has a physical luminance value associated with each pixel, by adding 1 for every timestep when a pixel is over 30,000 cd/m<sup>2</sup> and then dividing by 6 – the number of ten minute intervals within an hour – spatial representations of the glare problem are quickly and easily created. In the figure, labels for each row in the PV array are applied from A1 to C3. The bottom corner of row C2 and all of row C3 do not cause glare; therefore, it is likely that if the PV array was located further north, no glare problems would occur. Such an image would have provided valuable feedback during the design of the PV array.

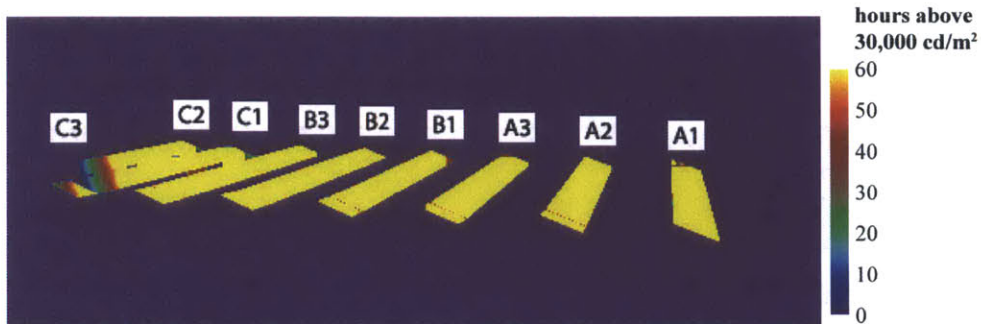


**Figure 7.6** Annual hours of predicted glare under CIE clear sky conditions with sun.

As discussed earlier, the airport is covering portions of the PV array with tarps in order to prevent disability glare from occurring. This method was used to plan when each row should be covered throughout the year until remediations can be implemented. Figure 7.7 illustrates monthly falsecolor hours of occurrence of glaring reflections for half of the year from July 1st to December 31st generated using an identical methodology to that of Figure 7.6 but using monthly intervals. For example, in July rows B2 – C2 should be covered with tarps; however, in November it is only necessary to cover row A1. In December all rows can be left uncovered in order to maximize PV electric production as there is no likelihood of glare from specular reflections. Figure 7.7 also clearly portrays that doing a spot field test of PV panels as possible in the FAA’s guidelines can be insufficient. For example, if a field test was done in July, no glare would be detected for panel rows A1-B1; however, those rows cause glaring reflections in September, October and November.



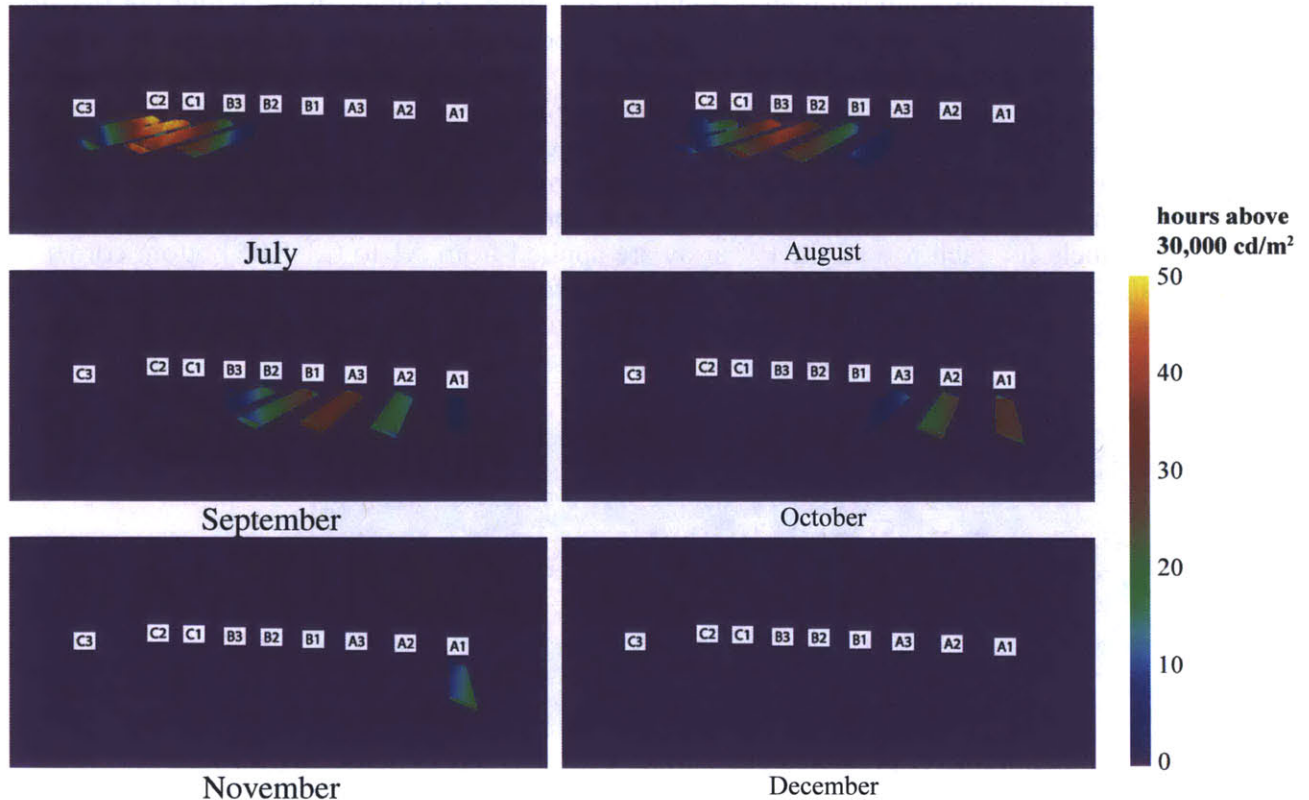


**Figure 7.7** Selected monthly images showing hours of predicted glare under CIE clear sky conditions with sun.

## 7.4 Discussion

In the results section, it is shown that the new image-based analysis method can identify glare problems during the design of a PV system based on sky models that accurately resolve the solar position, appropriate material representations and a complete 3D model. Furthermore, the occurrence of glare can be displayed temporally and spatially. It is therefore useful to employ the method to detect potential new glare hazards in proposed remediation strategies. Two remediation options that were developed in concert with the airport staff were analyzed. Option 1 was to replace the PV panel with a less-reflective panel. Option 2 was to rotate the entire array 90 degrees towards the east such that it faces away from the ATCT. These two options constitute typical material and formal changes that may occur during a PV array design process. Other options, including constructing exterior shading systems on the ATCT or the parking structure, were not considered due to regulatory pressures and their potential size (five stories tall in the case of a vertical shading device on the parking structure).

#### *7.4.1 Option 1: A Less Reflective PV Panel*

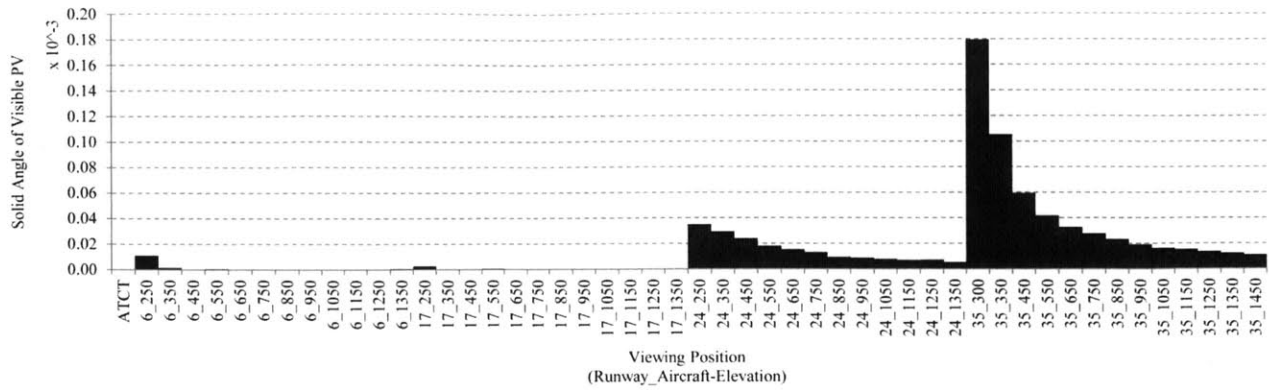
A potential replacement panel was measured using the same process as documented in Table 7.1, which resulted in an area-weighted diffuse reflectance value of 4.73% and an area-weighted specular reflectance value of 2.97%. This means the proposed panel reflects 45.3 and 46.8 percent less light than the installed panel. Is this substantial reflective reduction enough to solve the glare problem? Before describing the results, it is worthwhile to consider the case of the photograph in Figure 7.1, where the PV panels had a measured brightness of over 250,000 cd/m<sup>2</sup>. Half of this value is 125,000 cd/m<sup>2</sup>, a substantial reduction; however, it is still much higher than the defined visibility threshold of 30,000 cd/m<sup>2</sup>. Therefore, in the case of Figure 7.1, a less-reflective panel will not correct the glaring situation unless the panel is substantially less forward-scattering.

The less reflective PV panels do cause a perceptible glare decrease. The reflections would always be less bright as noted above; however, the annual glaring area decreases only 8.0% to 3.29 str-hrs. This is because the reduced specular reflections of the improved panel are still above 30,000 cd/m<sup>2</sup>, causing disability glare.

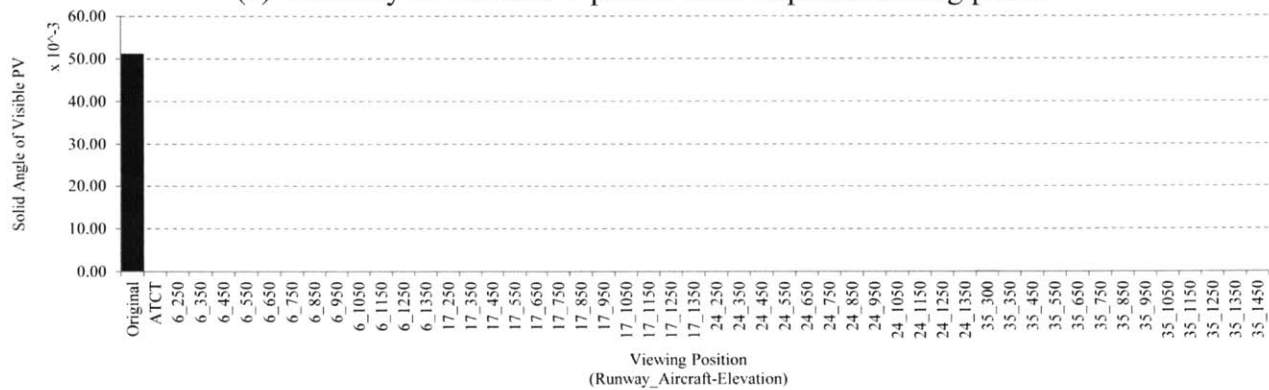
#### *7.4.2 Option 2: Rotate the Panels 90-degrees to the East, Away from the ATCT*

A geometric solution to rotate the panels such that they face away from the ATCT was explored. By rotating the panels 90 degrees counter-clockwise, they will face southeast and away from air traffic operators. In this way, air traffic controllers can no longer see the reflective face of the PV panels. This was confirmed using annual simulations identical to those exemplified by Figure 7.5 and by creating renderings similar to Figure 7.4b. One concern was that by rotating the PV panels to face away from the ATCT, a new glare hazard may be created for pilots.

Before assessing disability glare potential for each position along the landing paths, it is worthwhile to investigate the potential for glare. The visible size of the PV panels can be determined, which is exactly the maximum potential perceived size of specularly reflected glare. The case-study airport has four landing paths (two runways) which were analyzed at every 100 vertical feet of descent. The maximum visibility of the solar panels occurs on landing path 35 at 300 feet above sea level (just before landing) with a visible solid angle of  $1.8 \times 10^{-4}$  sr or 0.0029% of the visual hemisphere. For reference this is 2% of the glare size observed on August 30th 2012, depicted in Figures 7.1 and 7.4. The visible solid angle sizes of the proposed redesign of the PV array are shown in Figure 7.8a from the ATCT and along the various landing paths. To reinforce what this 2% means, Figure 7.8b adds an extra data point, the current visibility of the PV array from the ATCT ( $5 \times 10^{-2}$  sr). When comparing PV visibility, the maximum possible glaring reflection, from the aircraft landing paths to the existing visibility of PVs from the ATCT, there is very little potential for pilots to experience glare. Further, the potential for air traffic controllers to experience glare in option 2 is zero as only the back sides of the PV panels are seen.



(a) Visibility of rotated PV panels from airplane landing paths.



(b) Visibility of rotated PV panels from airplane landing paths compared against the original visibility of PV panels from the ATCT.

**Figure 7.8** Solid angle of visible area of PV in steradian as viewed from the ATCT and landing paths.

## 7.5 Conclusions

This case study illustrates the potential for physically-based renderings to analyze proposed new constructions that use specular materials in critical situations such as at airports. The new method of analysis is appropriate to analyze the specular surfaces of PV panels; however, it is also appropriate to use for other cases such as buildings with a large amount of glazing or bodies of water. The authors have shown that simulations closely mimic the behavior of physical reflections when using appropriately calibrated material models. A new maximum visible luminance value of 30,000 cd/m<sup>2</sup> in the line of sight has been proposed based on the physical ability of the eye to resolve items beyond that threshold while also viewing a typical computer screen. This upper luminance limit was applied to the analysis of an airport with a known disability glare problem.

It is important to consider the required effort of the new method. Assuming in the future measured or typical PV panel reflection data becomes easily accessible, the 3D model and simulation setup will take no longer than for any other standard daylighting consulting project. In this study, a single laptop computer was able to perform an evaluation every 10 minutes for an entire year in about 18 hours. This would take 3 hours for an hourly calculation, and the required time can be further shortened by parallelizing the simulation processes, already common in architecture and consulting firms. With this in mind, an accurate annual calculation investigating

specular glare takes significantly less time to perform than other annual calculations common in the field of daylighting such as interior illuminance and discomfort glare, which can take up to several days each for a complex 3D model. Therefore it is reasonable to assume that as such analysis becomes standard, costs will be similar to those already involved in standard daylighting and PV engineering consulting.

An issue identified in this study is that the analysis guidelines proposed in the FAA's "Technical Guidance for Evaluating Selected Solar Technologies on Airports" document are vague and allow analysis that does not account for the physical reality of reflections from PV panels or that does not account for differing solar positions throughout the year. Had the analysis method proposed in this study or that of Ho and colleagues been utilized, the glare problem likely would have been identified before construction.

A significant barrier to such analysis is that measured material data from PV panels is largely not available in practice. This makes it nearly impossible to compare the benefits of choosing between different PV panels or specular materials. In order for meaningful analysis to be made in the future, detailed angular-dependent material measurements (Apian-Bennowitz 1998) need to be performed and made available for a wide variety of potential construction materials that may be used in critical situations.

After using a HDR photographic method to derive angle-dependent reflection data, the authors undertook an annual analysis of the case-study airport with a known occurrence of disability glare. The new method produces charts (Figure 7.5) that illustrate the time and intensity of glaring reflections and images (Figures 7.6 and 7.7) that show the location of glaring reflections. Such results allow intuitive design changes based on observations. For example, Figure 7.6 suggests that a more northern site for the PV array would have been beneficial. The authors' new method was used to analyze two proposed remediation strategies. This analysis found that a material solution using a less-reflective PV panel was not viable in this case, but that a geometric solution to rotate the PV panels would remedy the glare hazard.





## Chapter 8

# Conclusions: A Framework for Design Analysis

This thesis presents several studies analyzing visual comfort using building performance simulation and physical measurement technologies in Chapters 3 through 7. Chapter 3 identifies DGP as the most plausible existing discomfort glare metric and introduces new spatial glare analysis images. Chapter 4 builds upon the spatial analysis data of Chapter 3, and proposes a new adaptive visual comfort model – similar to the concept of adaptive thermal comfort – that allows integrated modeling of occupant behavior regarding window shades with adaptive views in daylit spaces. Chapters 5 and 6 introduce detailed human subject research to support the ideas presented in Chapters 3 and 4. Chapter 5 presents a study that was able to successfully resolve between 53.7% and 70.1% of long-term visual satisfaction in a large daylit space. Chapter 6 utilizes an independently collected dataset, and found, using similar measures to those in Chapter 5, that 74.4% of neutral to uncomfortable or comfortable scenes as reported by occupants could be identified. Chapter 7 is concerned with the appearance of disability glare from exterior reflections and constitutes a case study for how luminance-based visual metrics can be used in a design process. Finally, Chapter 8 aims to bring the work of the previous chapters together in order to propose a framework for evaluating visual comfort in daylit spaces.

### 8.1 Implementation into Design Processes

The results presented in Chapters 3 through 7 contain methodologies that can be directly implemented into architectural building performance analysis during the design process in order to avoid visual discomfort in daylit spaces.

#### *8.1.1 Visual Comfort Metrics*

Chapter 3 identified Daylight Glare Probability (DGP) as the discomfort glare metric most likely to avoid false indications of comfort and to work in the most numerous variety of daylit conditions and spaces. In that sense, DGP appears to be a reasonable metric for use in the

analysis of unbuilt spaces. The work presented in Chapter 5 found that only 28.6% to 47.4% of occupants with predicted discomfort could be explained by one type of discomfort analysis; however, in combination with other visual comfort metrics from the literature between 53.7% and 70.1% of visual satisfaction can be explained. These additional metrics are: monitor contrast ratio, direct sunlight on the horizontal task plane, and direct sunlight falling on the eye. The accompanying survey results in Chapter 5 also support the transition to multiple metric analysis in visual comfort and visual satisfaction work. 14.4% of students found the space visually unsatisfying due to contrast or brightness, 30.0% due to direct sunlight, and 27.8% due to monitor visibility. Chapter 6 also lends credence to this choice of metrics. In that chapter, vertical eye illuminance ( $E_v$ ), DGP, the maximum luminance reflected from the working plane, and the maximum luminance originating from the window were all found to correlate well with reported subjective comfort ( $R^2$  between 0.199 and 0.242), although in that study direct light did not fall onto computer monitors, which would reduce contrast. Furthermore, clear thresholds of those measures were found that indicate discomfort. A model that combined the aforementioned metrics was able to correctly identify 74.4% of neutral to uncomfortable scenes. While clearly not knowing everything about human visual comfort and acknowledging that human luminous preferences differ from person to person (Van Den Wymelenberg et al. 2010), there is a comfortable amount of evidence to suggest that the following measures are appropriate for detecting visual discomfort in daylit spaces,

- vertical eye illuminances greater than 1500 lx
- DGP values greater than 0.4
- maximum workplane luminances greater than 1000 cd/m<sup>2</sup>
- maximum window luminances greater than 10<sup>6</sup> cd/m<sup>2</sup>
- monitor contrast ratios below 4.0

### 8.1.2 Simulations, Process and Time

Some annualized simulations necessary to calculate the metrics above take radically different amounts of time. The time information presented below is simulated using a single-core of a 1.8 GHz processor and high quality (-ab 6 -ad 2000 -as 100 -ar 500 -aa 0.1) Radiance parameters unless otherwise noted. Using the scene shown in Figure 8.1 as an example, the time required to calculate an annual hourly vertical eye illuminance simulation is 71m56.7s. The time required to generate an annual eDGPs<sup>28</sup> calculation is 327m11.6s. Measures such as the maximum luminance from the window can be resolved in a mere 3.4s at a single time by using simple (0 ambient bounce) image calculations; however, the ideal case is to have a full set of hourly annual high quality luminance images for every daylit hour in the year. Using standard Radiance tools, such a simulation is predicted to take 4399 hours.<sup>29</sup>

---

<sup>28</sup> See section 2.7.1.

<sup>29</sup> Careful calibration of Radiance parameters can reduce this time significantly.



**Figure 8.1** Visualization of scene used in time comparisons.

A significant amount of time can be saved by calculating the simplest measures first, such as vertical eye illuminance. Of the 4465 daylight hours in the Boston, MA TMY3 weather data file (USDOE 2014) and using the scene portrayed in Figure 8.1, 1179 hours (26.4%) identify visual discomfort from vertical eye illuminance alone. This already reduces the hours remaining necessary to check visual discomfort to 3286. Using the eDGPs method, DGP, maximum window luminance and first order luminances from workplane reflections can be checked simultaneously. Finally, only 2486 hours remain where high quality luminance renderings are necessary to check contrast ratio on the monitor or detailed DGP calculations using standard Radiance tools. In this case, the entire analysis process takes much less time by simulating the faster measures first. By defining the question which simulation is designed to interrogate to be, “Will occupants be comfortable or not?” for each hour, the least time-consuming simulations can be run first, and only the necessary high quality luminance renderings can be run later. However, this can still take a large amount of time. A benefit of this approach is that identifying a large amount of discomfort quickly from direct sunlight already establishes a problem to be solved without having spent many days running simulations.

There are exciting new developments in the daylight simulation world that enable reasonably fast generation of high-quality luminance images for an entire year (McNeil 2013). This is the so-called ‘five-phase’ method in Radiance, called as such because its daylight-coefficient based rendering methodology uses five calculation phases: (1) luminous transfer from the sky to the exterior façade, (2) transmission through fenestration, (3) distribution of light to

interior surfaces, (4) the removal of dispersed direct light from the first three phases, (5) the addition of direct light using direct solar positions. McNeil (2013) suggests that an annual set of renderings using the five-phase method may take as little as 15 hours. Using such a method, the metrics proposed in Section 8.1.1 can be calculated directly from each resulting HDR image. There is some concern that such methods may make it difficult to visualize actual fenestration geometry such as fixed shading devices or window blinds.

### *8.1.3 Visualization and Communication*

Overall, the consideration of view in the prediction of visual comfort considerably complicates issues of analysis and communication. For example, operative temperature can be plotted spatially simply by knowledge of the mean air temperature and surrounding surface temperatures (Webb 2012); however, when considering visual comfort at any point in the space, an occupant could look in any direction, adding an additional dimension of both simulation and display complexity. Throughout this thesis, the issues of visualization and therefore communication have been tackled in several ways.

When considering a single location in a space, such as for a prototypical single office or shoebox façade model (Reinhart et al. 2013), the new visualizations proposed in Chapter 3 are appropriate. At specific points in time, the spatial qualities of discomfort in a space can help to identify potential issues with visual comfort in a space. Such images can be generated for key points in the year, such as on the solstices and an equinox, in order to understand visual comfort issues over time. Figure 8.2 illustrates how such visualizations might be presented by a designer or building engineer.

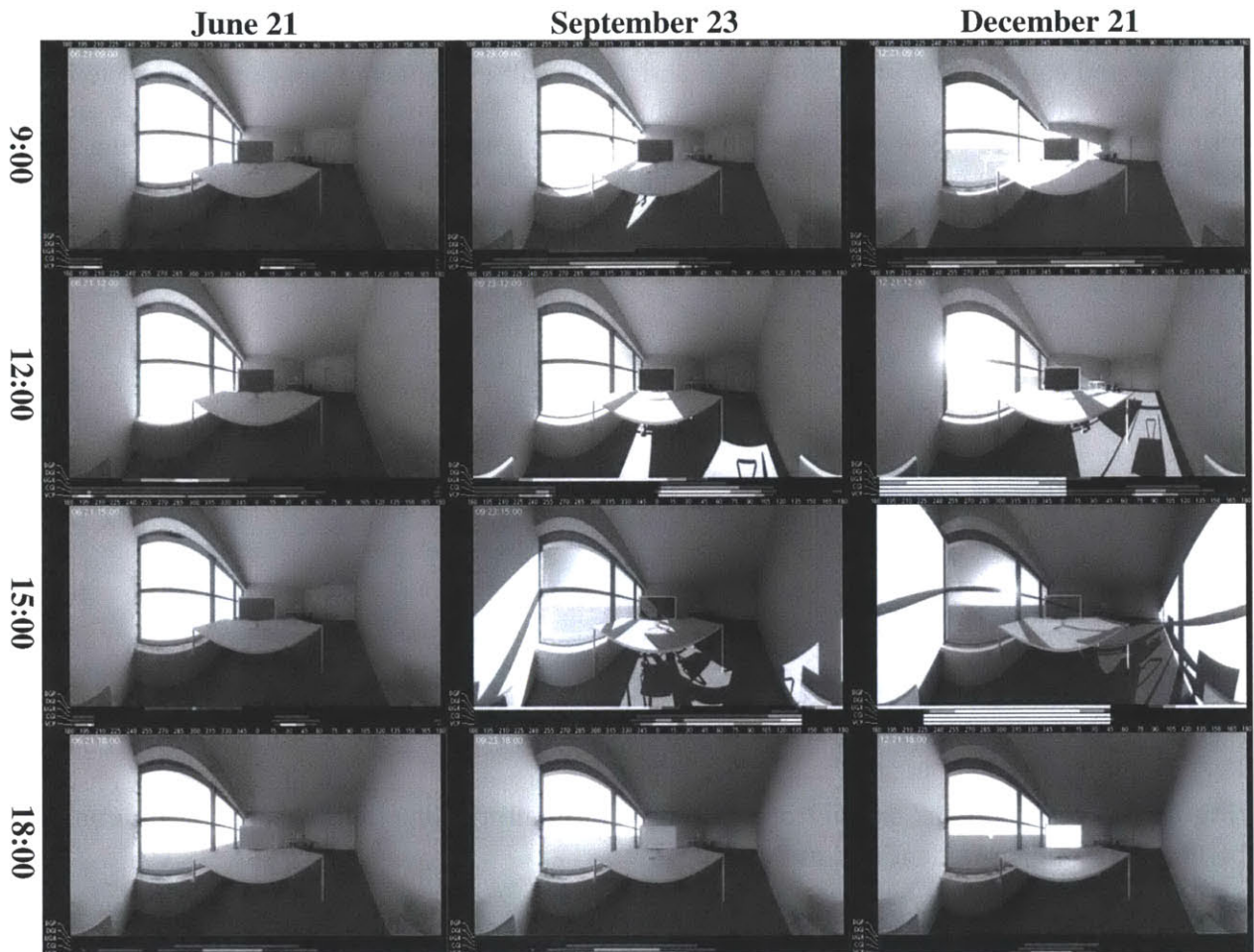
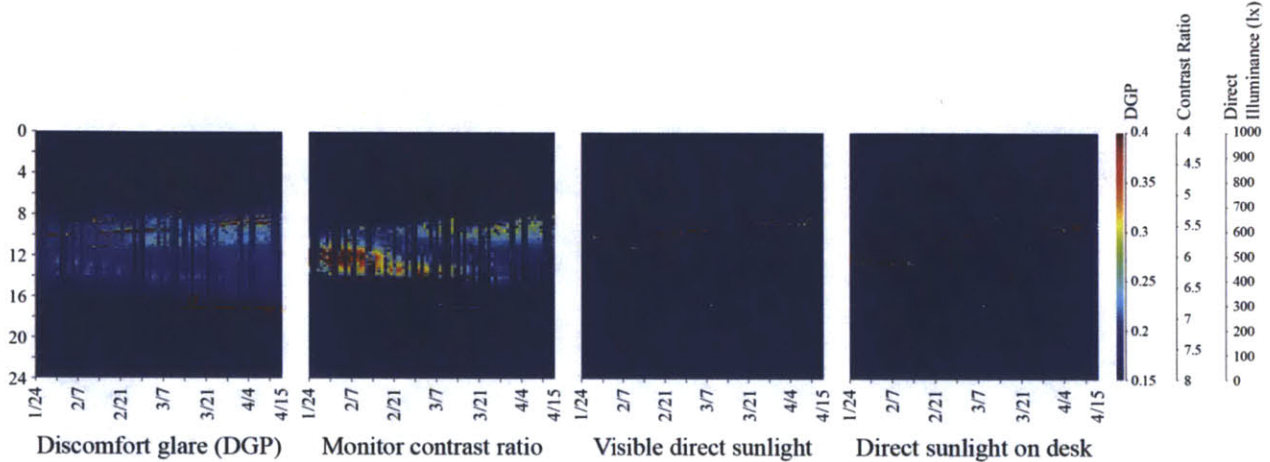


Figure 8.2 Spatial investigations of discomfort glare at key times during the year.



While general temporal trends are visible from such image series, it is also useful to present temporal and causal data. Figures 4.3, 5.6 and 7.5 are all examples of presentations of temporal visual discomfort data for each simulation timestep (1 hour, 6 minutes and 10 minutes respectively). Figure 8.3 is another example for the purposes of this discussion. Viewing Figure 8.3, it is clear that an occupant under such luminous conditions will experience discomfort due to direct sunlight for a short period each morning, have difficulty reading their monitor screen due to low contrast in the early afternoons of January and February and experience discomfort glare in the afternoons of March and April.



**Figure 8.3** Temporal and causal trends of visual discomfort using the measures, or illuminance-based proxies thereof, identified in Section 8.1.

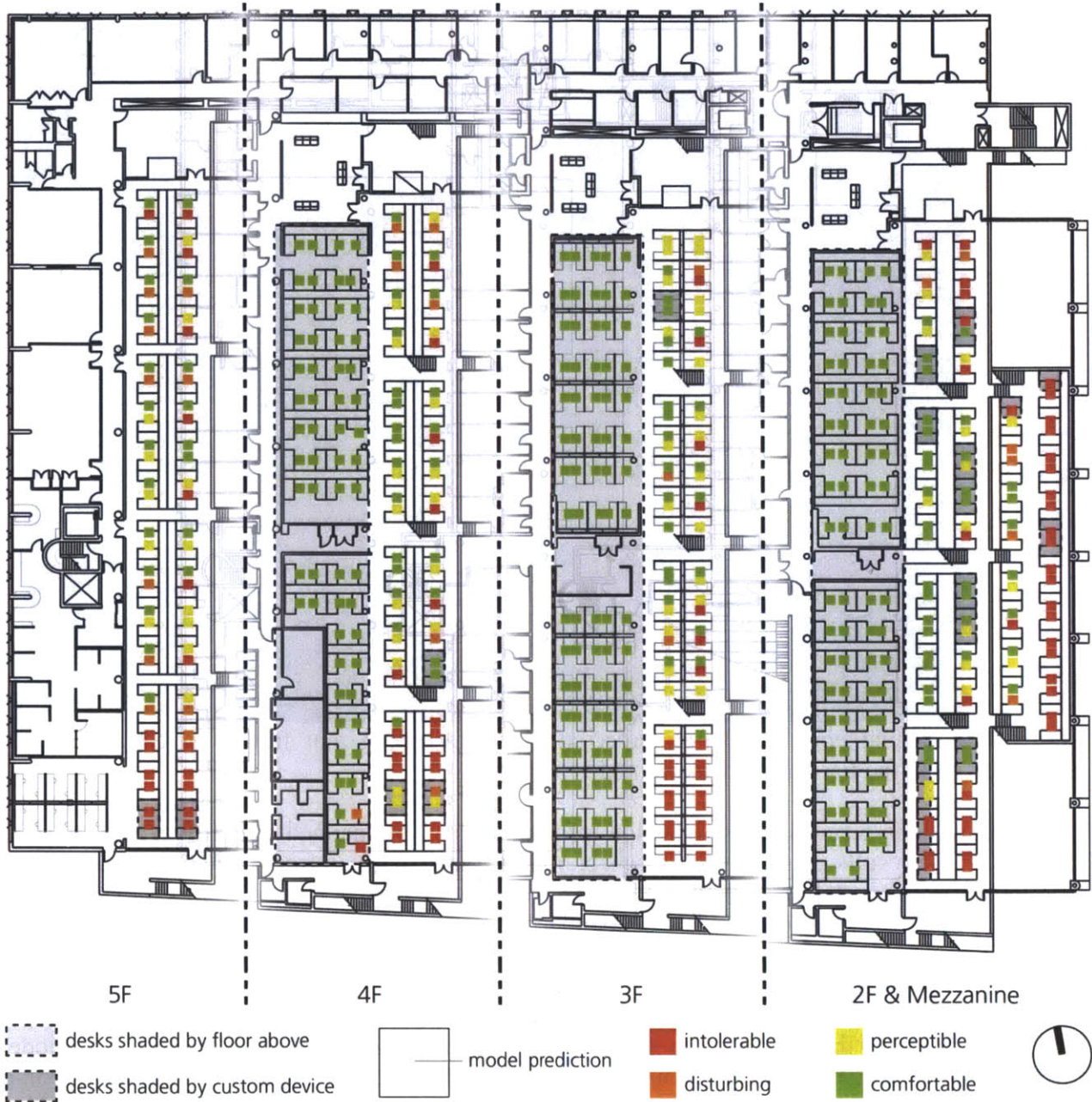
Visualizations can also aid in determining the cause of glaring situations. Figures 7.6 and 7.7 from the previous chapter, clearly illustrate where glaring reflections from a photovoltaic array occur from. Such imagery can be used to identify sources of visual discomfort and inform designers about how to correct any identified problems, such as in Section 7.4. Figure 8.4 below follows from the spatial interest of the referenced figures from Chapter 7 by proposing a fast method for checking the contribution of direct solar specular reflections in daylight scenes. Thanachareonkit et al. (2014) have also proposed several visualization types that map the intensity and location of discomfort glare sources experienced over time on top of a hemispherical fisheye visualization of a view in a space.





**Figure 8.4** Annual contribution of direct sunlight illustrating that further investigation into reflections from the PV array are warranted.

Finally, long-term visual satisfaction information can be mapped spatially as presented in Chapter 5. The results presented in that chapter used a scale derived from one study in one space type; however, any arbitrary mapping could be useful in the case of design. For example, the oft-cited (Reinhart & Wienold 2011) 5% avoidance threshold could also be applied to spatial dissatisfaction mapping. Beyond that, such maps can be used to display important information about view direction related to comfort. For example, using the simulation data from Chapter 5, it is possible to imagine alternative seating and space layouts that could improve the comfort in Gund Hall, such as the ones presented in Figure 8.5 for the morning visual satisfaction model predictions. Of the 196 views with some level of discomfort (8.5a), 52 (26.5%) of students could adjust their view by sitting at a side table to increase their visual satisfaction. These views are marked with pink arrows in 8.5b.



(a) Original seating position.





(b) Seating position based on side table orientation potential to increase predicted comfort.  
**Figure 8.5** Comparison of morning predicted satisfaction for two seating layouts in Gund Hall.

## 8.2 Summary of Contributions

At the outset of this thesis, in Chapter 1, three research goals were proposed: (1) to develop and test methods of predicting visual discomfort with regards to their plausibility, (2) to investigate behavioral reactions to visual discomfort, and (3) propose useful ways to integrate goals 1 and 2 into design processes through analysis frameworks and communication methods.

### 8.2.1 *Plausibility of Predicting Visual Discomfort*

Chapter 3 shows that the DGP metric is useful in many daylight conditions and space types and identified shortcomings in other popular measures of discomfort glare. Furthermore, Chapters 5 and 6 partially validated and identified several key metrics listed in Section 8.1.1 through detailed human subject studies. Using these identified metrics, it was found that between 53.7% and 70.1% of long-term visual satisfaction and 74.4% of instantaneous subjective comfort could be resolved in two separate studies. Therefore, the work presented in this thesis strongly suggests that visual comfort analysis is plausible, and measures have been identified and tested that give good results when compared to reported visual comfort collected using occupant surveys. Before this thesis, it was not certain that visual comfort metrics had the capability to resolve reported comfort (Painter et al. 2009; Hirning et al. 2013; Van Den Wymelenberg & Inanici 2014). This is likely because using a single discomfort metric is only appropriate for a limited number of spaces, between 28.6% to 47.4% in the study presented in Chapter 5. The case study presented in Chapter 7 illustrates that visual metrics can be used in a design process and identifies a new luminous overflow correction methodology allows more reliable analysis of typical HDR photographs with regards to visual comfort.

### 8.2.2 *Behavioral Reactions to Visual Discomfort*

Chapter 4 proposes an adaptive visual comfort model, the ‘adaptive zone,’ which allows a consideration of spatiality and view direction in visual comfort analysis. A behavioral and analytical model combining a changing view in space had never been proposed before this thesis. The ‘adaptive zone’ model was implemented into Daysim, a popular annual daylighting software used by over 3,500 architecture and engineering firms and 1,000 research institutions (Reinhart 2010). In Chapter 5, survey results found that 53.3% of the students in Gund Hall adapted to increase their visual comfort, and the comparison in Figure 8.5 shows that an analysis of adaptive potential can provide useful design feedback.

### 8.2.3 *Frameworks and Communication*

Finally, Section 8.1 integrated the work of the previous chapters to propose methods for using visual comfort metrics in analysis processes that could occur during the design of buildings and spaces. New measures, visualization and communication methods for visual discomfort are referenced from the previous seven chapters. Innovative spatial and temporal multi-direction glare visualizations were developed that are useful in assessing the visual quality of a space for the purposes of design analysis. Temporal maps that detail multiple causes of visual discomfort over time are also proposed. Furthermore, methods of mapping long-term visual satisfaction throughout daylight spaces have been developed. These plan-based comfort maps are useful for identifying ‘hot spot’ locations of visual discomfort in daylight spaces that can be addressed during design. An order for performing visual comfort simulations in order to minimize computational time is also proposed that can reduce simulation time by as much as half while also looking

towards developing simulation methodologies that could further decrease analysis time in the future.

## 8.3 Future Work

### 8.3.1 Behavioral and Control System Models for Window Shades

Most existing behavioral models for the operation of window shades (Reinhart 2004; IESNA 2012) are based on human reactions to the presence of direct sunlight; however, strong evidence has been amassed in this thesis (Chapters 5 and 6) that direct sunlight is not the only potential cause of visual discomfort that might lead to the closure or adjustment of window shades.

It has been shown in Chapter 4 that designing flexible workspaces can allow occupants to adapt to relatively high amounts of discomfort glare, and in Chapter 5 survey results showed that 53.3% of the students in Gund Hall adapted to increase their visual comfort. An occupant behavioral model was also proposed in Chapter 4 using predicted discomfort glare, the ‘adaptive zone,’ which could be extended to use all of the visual discomfort measures identified in Section 8.1.1. Still, 12.2% of students found that at least some of the time, they were unable to adapt to visual discomfort. This is exactly when even the most daylight-loving occupant would ordinarily close window shades when that is an option, but currently there is not enough research available to make this distinction of the tradeoffs between adaptation, view and useful daylight versus comfort.

### 8.3.2 View

The cylindrical visualizations from Chapter 3 and the adaptive potential from Chapter 4 both illustrate that view is an important consideration when analyzing or predicting visual comfort. For example, when looking out the window an occupant could be irritated by direct sunlight, but looking away from the window there may be no visual comfort problems. View is also constantly changing, further complicating the notion of what a view in a space for an occupant should be defined as. Sarey Khanie and colleagues (2013) note that space occupants focus on different areas depending on task and lighting quality in a space, which influences discomfort glare metrics such as DGP. From Chapter 6, Van Den Wymelenberg and Inanici (2014) found that the perceived brightness of a view towards the window rather than parallel to it correlated better with other subjective measures, leading them to propose an ‘inverse adaptive zone’ where the least comfortable view might be the most useful to consider when evaluating a design. It seems necessary for future research to address the notion of view further when investigating visual comfort.





# Appendices



# Appendix A

## Free Response Survey Answers

**Table A.1** Free response replies to the question, “If you are experiencing glare, what is its cause?”

Response	My Comments
Note that my flat-screen monitor has a mat finish -- and thus no reflections of lighting are in my view.	No glare.
Reflections off of my pin-up board. reflections from CGIS	Bright reflections. CGIS is the neighboring building to the East of Gund Hall identified in Figure 5.2
rarely happens... not so much now in the spring, in winter mornings there is a point the sun shines directly at my face/ desk.	Illustrates the idea that occupants do recall comfort problems from the past.
I have noticed little or no glare in the corner.	No glare.
My problem is not the glare, but it is the sunlight projecting directly on my screen which is very hard for me to see my screen.	Monitor contrast ratio.
shiny macs.	Monitor contrast ratio.
There are a small, select number of hours I have noticed where the sun is shining in my eyes or through the glazing in the stepped area of Gund's roof (either early morning or late afternoon)- however these are very infrequent.	Direct sunlight.
a slight shift of the laptop screen quickly alleviates any/most glare issues	Adaptation to monitor contrast ratio.
my desk faces north so i get south sun reflected on my monitor in early afternoons	Monitor contrast ratio.
Late afternoon sun gets reflected from the CGIS façade into the studio space.	Bright reflections.
reflection off of building to east (only for a few minutes, only when the blinds are up, which is now a choice we have to make)	

**Table A.2** Free response replies to the question, “If you experienced visual discomfort over the course of the semester, which strategies did you employ to increase your comfort?”

<b>Response</b>	<b>My Comments</b>
Rotated my monitor	Adjusted monitor.
Used my desk lamp as a heating device -- and positioned it low enough to be about 4-5 inches away from my hands at my keyboard, to allow the heat from the lamp to be felt.	This user reported no visual discomfort.
In the past I've tried unscrewing the bulb and/or using my laser cut sheets as screens inside the fixture.	Built shading device.
worked from home	Could not adapt.
I use a lamp sometimes	
Tilted my monitor so that the glare was more in the upper left corner.	Adjusted monitor.
i would try to tilt my screen but it didn't really work. squint.	Adjusted monitor.
Tilted my monitor.	Adjusted monitor.
In [Desk Number], last semester, I would just avoid my desk during the afternoon.	Could not adapt.
moved from a desk in the "cave" to a desk out in the open to get more sunlight	
When the sun would hit my monitor, I would try to move the position of my laptop. When this is not possible, I stop working on my computer and wait until I can move my laptop to a position on my desk where the sun is not hitting it.	Adjusted monitor.
Rotated my monitor away from the glare	Adjusted monitor.
Used task lamps to augment adverse lighting conditions.	
changed task	
rotated monitors	Adjusted monitor.
Moved my monitor and laptop towards one end of the desk since the stairs provide some screen.	Adjusted monitor and position.
I didn't work in the trays during these times	Could not adapt.
Worked from home.	Could not adapt.
I rotate my screen to a level of less discomfort.	Adjusted monitor.
Started working from home.	Could not adapt.
In the evening if I'm the only one in studio I often turn off the lights	







## Appendix B

# Calculating Luminance-based Metrics from Radiance RGBE Format Images

The appendix contains a series of standard Radiance (Ward, 1994) commands useful in reproducing the methods of this paper.

### *B.1. Masking a HDR Image*

A monochromatic bitmap format image of the same dimension as the HDR photograph can be converted to the Radiance RGBE format using the below command,

```
ra_bmp -r mask.bmp > mask.hdr
```

and HDR images can have this mask applied by the following command,

```
pcomb -e "lo=mask*li(1); mask=if(li(2)-.1,1,0);" -o image.hdr -o mask.hdr > image_masked.hdr
```

One must append the view information to the resulting file header. In the case of a hemispheric image, this is,

```
VIEW= -vta -vh 180 -vv 180
```

### *B.2. Calculating Illuminance from a Masked Hemispherical Image*

Illuminance can be calculated from a circularly masked hemispherical fisheye image using the command,

```
pcomb -e "lo=L*Sang*cosCor; L=179*li(1); Sang=S(1); cosCor=Dy(1);" -o image.hdr  
| pvalue -d -b -h -H  
| total
```

### B.3. Finding the Maximum Pixel Luminance

The Radiance command,  
`pextrem image.hdr`

will return the location and RGB Radiance values of the extreme brightest and darkest pixels. The luminance of these pixels can be determined by Equation B.1.

$$L = 179 * (0.2651R + 0.6701G + 0.0648B) \quad (B.1)$$

### B.4. Determining the Solid Angle of Pixels Greater Than a Luminance Threshold

The solid angle size of pixels over a set luminance threshold can be determined using,  
`pcomb -e "lo=if(li(1)-L_threshold/179, Sang, 0); Sang=S(1);" -o image.hdr`  
| `pvalue -d -b -h -H`  
| `total`

### B.5. Increasing Select Pixel Luminances to Achieve a New Illuminance Value

In order to increase pixels over a certain luminance to match an image's calculated illuminance ( $E_{v,image}$ ) to an illuminance measurement ( $E_v$ ), first the current illuminance contribution ( $E_{contrib}$ ) of the pixels to be corrected should be determined using the command,

```
pcomb -e "lo=if(li(1)-L_threshold/179, illContrib, 0); illContrib=L*Sang*cosCor;
L=179*li(1); Sang=S(1); cosCor=Dy(1);" -o image.hdr
| pvalue -d -b -h -H
| total
```

The potential contribution ( $E_{potential}$ ) of the same group of pixels with regards to a new luminance value ( $\sum \omega \cos \theta$ ) can be determined by the following,

```
pcomb -e "lo=if(li(1)-L_threshold/179, illPoten, 0); illPoten=Sang*cosCor;
Sang=S(1); cosCor=Dy(1);" -o image.hdr
| pvalue -d -b -h -H
| total
```

It is then possible to select the new pixel luminance required to make the  $E_{v,image}$  equal to the measured value of  $E_v$  as in Equation B.2 below,

$$L_{new} = \frac{E_v - (E_{v,image} - E_{contrib})}{E_{potential}} \quad (B.2)$$

And finally this new luminance value ( $L_{new}$ ) can be used to replace pixels over the luminance threshold,

```
pcomb -e "lo=if(li(1)-L_threshold/179, L_new/179, li(1));" -o image.hdr >
image_corrected.hdr
```

It is once again necessary to append the original view information to the resulting file header,

```
VIEW= -vta -vh 180 -vv 180
```





## References

- Apian-Bennowitz, P., 1998. Enhancing and calibrating a goniophotometer. *Solar Energy Materials and Solar Cells*, 54, pp.309–322.
- Ashikhmin, M. & Shirley, P., 2000. An Anisotropic Phong BRDF Model. *Journal of Graphics Tools*, 5, pp.25–32.
- Bodart, M. & De Herde, A., 2002. Global energy savings in offices buildings by the use of daylighting. *Energy and Buildings*, 34, pp.421–29.
- Boyce, P.R., 2003. *Human factors in lighting* Second Ed., New York: Taylor & Francis Inc.
- Clarke, J.A. & Janak, M., 1998. Simulating the thermal effects of daylight-controlled lighting. *Building Performance*, 1, pp.21–23.
- Commission Internationale de l’Eclairage, 2002. *CIE collection on glare*, Vienna: CIE.
- Commission Internationale de l’Eclairage, 1996. *Spatial distribution of daylight - CIE standard overcast sky and clear sky*. *CIE Publication S003*, Vienna: CIE.
- Commission Internationale de l’Eclairage TC3-13, 1995. *Discomfort glare in interior lighting*, *CIE Publication 117*, Vienna: CIE.
- DiLaura, D. et al. eds., 2011. *IESNA lighting handbook* 9th Ed., New York City: Illuminating Engineering Society.
- Einhorn, H.D., 1979. Discomfort glare: a formula to bridge differences. *Lighting Research and Technology*, 11, pp.90–94.
- EnergyPlus Development Team, 2012. EnergyPlus input output reference: The encyclopedic reference to EnergyPlus input and output. *The Encyclopedic Reference to EnergyPlus Input*

and Output. Available at:

<http://apps1.eere.energy.gov/buildings/energyplus/pdfs/inputoutputreference.pdf>.

- Erhorn, H., De Boer, J. & Dirksmoller, M., 1997. ADELINe - An integrated approach to lighting simulation. In *Proceedings of IBPSA Building Simulation '97*. pp. 79–85.
- Fan, D., Painter, B. & Mardaljevic, J., 2009. A data collection method for long-term field studies of visual comfort in real-world daylight office environments. In *Proceedings of PLEA*. pp. 22–24. Available at: <http://www.plea2009.arc.ulaval.ca/papers/2.strategies/2.1/daylighting/oral/2-1-03-plea2009quebec.pdf> [Accessed March 13, 2014].
- Federal Aviation Administration, Office of Airports, O. of A.P. and P. & (APP-400), A.P. and E.D., 2010. Technical guidance for evaluating selected solar technologies on airports. Available at: [http://www.faa.gov/airports/environmental/policy\\_guidance/media/airport\\_solar\\_guide.pdf](http://www.faa.gov/airports/environmental/policy_guidance/media/airport_solar_guide.pdf).
- Ferwerda, J.A. et al., 1996. A model of visual adaptation for realistic image synthesis. In *Proceedings of the 23rd annual conference on Computer graphics and interactive techniques - SIGGRAPH '96*. pp. 249–258.
- Grondzik, W.T. et al., 2006. *Mechanical and electrical equipment for buildings* 10th Ed., Hoboken: John Wiley and Sons.
- Harrold, R. ed., 2003. *IESNA lighting ready reference: A compendium of materials from the IESNA*, New York: Illuminating Engineering Society of North America.
- Hirning, M.B. et al., 2013. Post occupancy evaluations relating to discomfort glare: A study of green buildings in Brisbane. *Building and Environment*, 59(January), pp.349–357. Available at: <http://linkinghub.elsevier.com/retrieve/pii/S0360132312002429> [Accessed February 23, 2014].
- Ho, C.K., Ghanbari, C.M. & Diver, R.B., 2011. Methodology to assess potential glint and glare hazards from concentrating solar power plants: Analytical models and experimental validation. *Journal of Solar Energy Engineering*, 133(3), p.031021.
- Holladay, L., 1926. The fundamentals of glare and visibility. *Journal of the Optical Society of America*, 12(4), pp.271–319.
- Hopkinson, R., 1940. Discomfort glare in lighted streets. *Transactions of the Illuminating Engineering Society*, 5, pp.1–29.
- Hopkinson, R., 1972. Glare from daylighting in buildings. *Applied Ergonomics*, (December), pp.206–215.
- Hopkinson, R. & Collins, J., 1970. *The ergonomics of lighting*, London: Macdonald & Co.



- Hopkinson, R.G., 1971. Glare from windows. *Construction Research and Development Journal*, 2-3, pp.2:98–105, 169–175; 3: 23–28.
- Hopkinson, R.G., Longmore, J. & Petherbridge, P., 1954. An empirical formula for the computation of the indirect component of the daylight factor. *Transactions of the Illuminating Engineering Society*, 19(7), pp.201–219.
- IESNA, 2012. *IES LM-83-12. IES spatial daylight autonomy (sDA) and annual sunlight exposure (ASE)*, New York: IESNA Lighting Measurement.
- Inanici, M.N., 2006. Evaluation of high dynamic range photography as a luminance data acquisition system. *Lighting Research and Technology*, 38, pp.123–134.
- Inanici, M.N., 2010. Evaluation of High Dynamic Range Image-Based Sky Models in Lighting Simulation. *Leukos*, 07, pp.60–84.
- International Standards Organization, 1992. ISO 9241-3. Ergonomic requirements for office work with display terminals (VDTs), Part 3: Visual display requirements.
- International Standards Organization, 2008. ISO 9241-303. Ergonomics of human-system interaction Part 303: Requirements for electronic visual displays.
- Jakubiec, J. & Reinhart, C., 2013. Predicting visual comfort conditions in a large daylit space based based on long-term occupant evaluations: a field study. In *13th International IBPSA Conference, Building Simulation*. pp. 3408–3415.
- Jakubiec, J. & Reinhart, C., 2012. The “adaptive zone” - A concept for assessing discomfort glare throughout daylit spaces. *Lighting Research and Technology*, 44(2), pp.149–170.
- Jakubiec, J.A. & Reinhart, C.F., 2014. Assessing disability glare potential due to reflections from new constructions: A case study analysis and recommendations for the future. In *Proceedings of the Transportation Research Board 93rd Annual Meeting*. Washington DC.
- Jakubiec, J.A. & Reinhart, C.F., 2011. DIVA 2.0: Integrating daylight and thermal simulations using Rhinoceros 3D, Daysim And EnergyPlus. In *12th International IBPSA Conference, Building Simulation 2011*. pp. 14–16.
- Jakubiec, J.A., Reinhart, C.F. & Van Den Wymelenberg, K., 2014. Towards an integrated framework for predicting visual comfort conditions from luminance-based metrics in daylit spaces. In *2014 ASHRAE/IBPSA-USA Building Simulation Conference*. Atlanta.
- Keneli.org, 2012. Cambridge, Massachusetts Weather. Available at: <http://weather.keneli.org/index.html> [Accessed July 21, 2012].
- Larson, G. & Shakespeare, R., 1998. *Rendering with Radiance: The art and science of lighting visualization*, San Francisco: Morgan Kaufmann Publishers.

- Lighting Analysts Inc., 2014. AGi32. Available at: <http://www.agi32.com/>.
- Lindsay, C. & Littlefair, P., 1992. *Occupant use of venetian blinds in offices*, Watford.
- Luckiesh, M., 1927. Defining glare and visibility. *Journal of the Franklin Institute*, 203(5), pp.715–6.
- Luckiesh, M. & Guth, S., 1949. Brightness in visual field at borderline between comfort and discomfort (BCD). *Illuminating Engineering*, 44, pp.650–670.
- Lynes, J.A., 1968. *Principles of natural lighting*, London: Applied Science Publishers Ltd.
- Mardaljevic, J. et al., 2012. Daylighting metrics: Is there a relationship between useful daylight illuminance and daylight glare probability? In *Building Simulation and Optimization Conference BSO12*. Available at: <http://www.ibpsa.org/proceedings/BSO2012/3B1.pdf> [Accessed March 13, 2014].
- Mardaljevic, J., 2000. Simulation of annual daylighting profiles for internal illuminance. *Lighting Research and Technology*, 32, pp.111–118.
- Mardaljevic, J., 1995. Validation of a lighting simulation program under real sky conditions. *Lighting Research and Technology*, 27, pp.181–188.
- McNeil, A., 2013. The five-phase method for simulating complex fenestration with Radiance. , (August). Available at: [http://radiance-online.org/learning/tutorials/fivephasetutorialfiles/Tutorial-FivePhaseMethod\\_v2.pdf](http://radiance-online.org/learning/tutorials/fivephasetutorialfiles/Tutorial-FivePhaseMethod_v2.pdf).
- Moghbell, N., 2012. *New model for VDT associated visual comfort in office spaces*. Karlsruhe Institute of Technology.
- Nabil, A. & Mardaljevic, J., 2006. Useful daylight illuminances: A replacement for daylight factors. *Energy and Buildings*, 38, pp.905–913.
- Nazzal, A., 2001. A new daylight glare evaluation method: Introduction of the monitoring protocol and calculation method. *Energy and Buildings*, 33, pp.257–265.
- Nazzal, A., Onaygil, S. & Guler, O., 2005. Subjective experience of discomfort glare in a daylit computerized office in Istanbul and its mathematical prediction with the DGIN method. *The Bulletin of the Istanbul Technical University, Interdisciplinary Journal of Physical and Engineering Science*, 54, pp.96–107.
- Ochoa, C.E. & Capeluto, I.G., 2006. Evaluating visual comfort and performance of three natural lighting systems for deep office buildings in highly luminous climates. *Building and Environment*, 41(8), pp.1128–1135.

- PAB Advanced Technologies Ltd., BME BSDF Data. Available at: [http://www.pab.eu/goniophotometer/demodata/bme/ward\\_metal\\_ps.anofol606.37.385/index.html](http://www.pab.eu/goniophotometer/demodata/bme/ward_metal_ps.anofol606.37.385/index.html) [Accessed July 1, 2013].
- Painter, B., Fan, D. & Mardaljevic, J., 2009. Evidence-based daylight research: development of a new visual comfort monitoring method. In *Proceedings of Lux Europa*. Istanbul.
- Perez, R., Seals, R. & Michalsky, J., 1993. All weather model for sky luminance distribution - preliminary configuration and validation (Erratum). *Solar Energy*, 5, p.1993.
- Pigg, S. et al., 1995. Behavioral aspects of lighting and occupancy sensors in private offices: A case study of a university office building. , pp.161–170.
- Reindl, D., Beckman, W. & Duffie, J., 1990. Diffuse fraction correlations. *Solar Energy*, 45(1), pp.1–7.
- Reinhart, C., 2010. Daysim. Available at: <http://daysim.com/download.html>.
- Reinhart, C. & Breton, P., 2009. Experimental validation of Autodesk 3ds Max Design 2009 and Daysim 3.0. *Leukos*, 6(1).
- Reinhart, C., Jakubiec, J. & Ibarra, D., 2013. Definition of a reference office for standardized evaluation of facade and lighting technologies. In *13th International IBPSA Conference, Building Simulation 2013*. pp. 3645–3652.
- Reinhart, C. & Voss, K., 2003. Monitoring manual control of electric lighting and blinds. *Lighting Research and Technology*, 35, pp.243–260.
- Reinhart, C. & Walkenhorst, O., 2001. Validation of dynamic RADIANCE-based daylight simulations for a test office with external blinds. *Energy and Buildings*, 33.
- Reinhart, C.F., 2004. Lightswitch-2002: A model for manual and automated control of electric lighting and blinds. *Solar Energy*, 77(1), pp.15–28.
- Reinhart, C.F. & Andersen, M., 2006. Development and validation of a Radiance model for a translucent panel. *Energy and Buildings*, 38(7), pp.890–904.
- Reinhart, C.F. & Herkel, S., 2000. The simulation of annual daylight illuminance distributions — a state-of-the-art comparison of six RADIANCE-based methods. *Energy and Buildings*, 32(2), pp.167–187.
- Reinhart, C.F., Mardaljevic, J. & Rogers, Z., 2006. Dynamic daylight performance metrics for sustainable building design. *Leukos*, 3, pp.7–31.
- Reinhart, C.F. & Wienold, J., 2011. The daylighting dashboard – A simulation-based design analysis for daylit spaces. *Building and Environment*, 46(2), pp.386–396.

- Rockcastle, S. & Andersen, M., 2012. Dynamic annual metrics for contrast in daylight architecture. In *Proceedings of the 2012 Symposium on Simulation for Architecture and Urban Design. Society for Computer Simulation International*. p. 12.
- Rubin, A., Collins, B. & Tibbott, R., 1978. *Window blinds as a potential energy saver: A case study*. NBS Building Science Series 112, Washington DC: National Bureau of Standards.
- Rubiño, M. et al., 1994. Discomfort glare indices: a comparative study. *Applied optics*, 33, pp.8001–8008.
- Sarey Khanie, M., 2013. Uncovering relationships between view direction patterns. In *LUXEUROPA*. Krakow.
- Stumpfel, J. et al., 2006. Direct HDR capture of the sun and sky. *ACM SIGGRAPH 2006*.
- Sutter, Y., Dumortier, D. & Fontoynt, M., 2006. The use of shading systems in VDU task offices: A pilot study. *Energy and Buildings*, 38, pp.780–789.
- Thanachareonkit, A., Lee, E.S. & Mcneil, A., 2014. Empirical assessment of a prismatic daylight- redirecting window film in a full-scale office testbed. *LEUKOS*, 10(1), pp.19–45.
- The Associated Press, 2004. New L.A. concert hall raises temperatures of neighbors. *USA Today*. Available at: [http://usatoday30.usatoday.com/news/nation/2004-02-24-concert-hall\\_x.htm](http://usatoday30.usatoday.com/news/nation/2004-02-24-concert-hall_x.htm).
- The Dallas Morning News, 2013. Editorial: Museum Tower needs to cut the glare. *The Dallas Morning News*. Available at: <http://www.dallasnews.com/opinion/editorials/20130721-editorial-museum-tower-needs-to-cut-the-glare.ece>.
- Tregenza, P.R., 1983. Daylight coefficients. *Lighting Research and Technology*, 15(2), pp.65–71.
- Tuaycharoen, N. & Tregenza, P., 2005. Discomfort glare from interesting images. *Lighting Research and Technology*, 37, pp.329–341.
- Tuaycharoen, N. & Tregenza, P.R., 2007. View and discomfort glare from windows. *Lighting Research and Technology*, 39, pp.185–200.
- USDOE, 2014. EnergyPlus Weather Data. Available at: [http://apps1.eere.energy.gov/buildings/energyplus/weatherdata\\_about.cfm?CFID=717368&CFTOKEN=52a80de4b685de0e-2B4D7FEA-9DCC-2862-D0843BBA4EE11CBD&jsessionid=C49766FC8E5D75C11271E865A75A6734.eere](http://apps1.eere.energy.gov/buildings/energyplus/weatherdata_about.cfm?CFID=717368&CFTOKEN=52a80de4b685de0e-2B4D7FEA-9DCC-2862-D0843BBA4EE11CBD&jsessionid=C49766FC8E5D75C11271E865A75A6734.eere).
- USGBC, 2009. *LEED 2009 for new construction and major renovations rating system*, US Green Building Council. Available at: <http://www.usgbc.org/ShowFile.aspx?DocumentID7244>.

- USGBC, 2001. *LEED Reference Guide*, US Green Building Council.
- USGBC, 2003. *LEED reference guide for new construction & major renovations, version 2.1*, US Green Building Council.
- Voit, P., White, D. & Bummele, A., 2007. Gund Hall: Analysis of envelope performance and thermal comfort. Transsolar Inc. report to Harvard University.
- Walkenhorst, O. et al., 2002. Dynamic annual daylight simulations based on one-hour and one-minute means of irradiance data. *Solar Energy*, 72(5), pp.385–395.
- Ward, G., 1994. The RADIANCE lighting simulation and rendering system. In *Proceedings of the 21st annual conference on Computer graphics and interactive techniques - SIGGRAPH '94*. pp. 459–472.
- Ward, G., 2013. What's new in Radiance for 2013. Available at: <http://www.radiance-online.org/community/workshops/2012-copenhagen/Day2/Ward/RadianceImprovements.pdf>.
- Webb, A.L., 2012. *Mapping comfort: An analysis method for understanding diversity in the thermal environment*. Massachusetts Institute of Technology.
- Wienold, J., 2009. Dynamic daylight glare evaluation. *Proceedings of Building Simulation*, pp.944–951. Available at: [https://www.ibpsa.org/proceedings/BS2009/BS09\\_0944\\_951.pdf](https://www.ibpsa.org/proceedings/BS2009/BS09_0944_951.pdf) [Accessed March 14, 2014].
- Wienold, J., 2007. Dynamic simulation of blind control strategies for visual comfort and energy balance analysis. *Building Simulation*, pp.1197–1204.
- Wienold, J., 2010. Evalglare. Available at: [www.ise.fraunhofer.de/radiance](http://www.ise.fraunhofer.de/radiance).
- Wienold, J., 2012. New features of Evalglare. *11th International Radiance Workshop*. Available at: [http://radiance-online.org/community/workshops/2012-copenhagen/Day3/Wienold/rad\\_ws\\_2012\\_evalglare\\_newfeatures.pdf](http://radiance-online.org/community/workshops/2012-copenhagen/Day3/Wienold/rad_ws_2012_evalglare_newfeatures.pdf).
- Wienold, J. & Christoffersen, J., 2006. Evaluation methods and development of a new glare prediction model for daylight environments with the use of CCD cameras. *Energy and Buildings*, 38(7), pp.743–757.
- Van Den Wymelenberg, K., 2012. *Evaluating human visual preference and performance in an office environment using luminance-based metrics*. University of Washington.
- Van Den Wymelenberg, K. & Inanici, M.N., 2014. A critical investigation of common lighting design metrics for predicting human visual comfort in offices with daylight. *LEUKOS*, 10(3), pp.145–164.

Van Den Wymelenberg, K., Inanici, M.N. & Johnson, P., 2010. The effect of luminance distribution patterns on occupant preference in a daylit office environment. *LEUKOS*, 7(2), pp.103–122.